Nearshore Optical Water Quality in the South Taranaki Bight

Prepared for Trans-Tasman Resources Ltd

Updated November 2015

Authors/Contributors:
Iain MacDonald
Mark Gall
Dave Bremner

For any information regarding this report please contact:

Iain MacDonald
Scientist
Coastal and Estuarine Processes Group
+64-7-859 1818
i.macdonald@niwa.co.nz

National Institute of Water & Atmospheric Research Ltd
Gate 10, Silverdale Road
Hillcrest, Hamilton 3216
PO Box 11115, Hillcrest
Hamilton 3251
New Zealand

Phone +64-7-856 7026
Fax +64-7-856 0151

NIWA Client Report No:	HAM2013-040
Report date:	May 2013
NIWA Project:	TTR13201

Contents

Executive summary **7**

1 Introduction **9**

1.1 Background 9

1.2 Project description 9

1.3 Nearshore optical water quality 10

1.4 This report 10

2 Methods **11**

2.1 Background 11

2.2 Moored deployment 15

2.3 Surf-zone water samples 20

2.4 Deployment considerations 21

3 Results **23**

3.1 Site selection and deployment information 23

3.2 Conditions experienced during the study period 27

3.3 Boat surveys 31

3.4 Moored deployment 42

3.5 Surf-zone water sampling 56

4 Summary **62**

5 Acknowledgement **63**

6 References **64**

Appendix A Additional information **65**

Appendix B Bio-Fish data plots **68**

Tables

Table 2-1: Summary of variables measured and instrumentation used during the boat surveys. 12

Table 2-2: Sieve sizes used in the analysis of the beach sediments. 19

Table 3-1: Summary information about the boat surveys. 24

Table 3-2: Locations of the water samples collected during the boat surveys. 25

Table 3-3: Summary information about the moored deployments. 26

Table 3-4: Summary information for the surf-zone water sampling. 27

Table 3-5: Rainfall in the South Taranaki Bight for the 4-month period from January to April 2013 29
Table 3-6: Summary of river flows at Paetawa and Whenuakura. 31
Table 3-7: Water sample results from boat survey 1 (S1). 37
Table 3-8: Water sample results from boat survey 2 (S2). 38
Table 3-9: Bed sediment grain size (from sieving). 56
Table 3-10: Water sample results from SZ1. 58
Table 3-11: Water sample results from SZ2. 58
Table 3-12: Water sample results from SZ3. 59

Table A-1: Additional information for the boat surveys. 65
Table A-2: Deployment information for the moored deployments. 67

Figures

Figure 1-1: Site map showing the proposed project location. 9
Figure 2-1: Example showing how k_d was estimated. 13
Figure 2-2: Laboratory calibration showing the relationship between T_n (turdidity) and the OBS output. 16
Figure 2-3: In-situ calibration of T_n versus SSC. 17
Figure 2-4: In-situ calibration of T_n versus c_{530} 18
Figure 2-5: In-situ calibration of T_n versus k_d. 19
Figure 2-6: Black disc equipment used for measuring visual water clarity (y_{BD}) from the surf-zone water samples. 20
Figure 2-7: Aerial photography of the nearshore region in the STB. 21
Figure 2-8: Site map showing the locations of environmental monitoring stations. 22
Figure 3-1: Site map showing profile locations from the first boat survey (S1). 23
Figure 3-2: Site map showing profile locations from the second boat survey (S2). 24
Figure 3-3: Site map, showing the locations of the moored instruments. 25
Figure 3-4: Site map showing the 11 sites selected for the surf-zone sampling. 27
Figure 3-5: Wind rose for winds measured at Wanganui over a period of 17-years (March 1996 to June 2013). 28
Figure 3-6: Wind rose for winds measured at Wanganui over the deployment period February 2013 to April 2013. 29
Figure 3-7: River flow and rainfall time series over the period 1/1/2013 to 2/5/2013. 30
Figure 3-8: Wind and flow conditions around the times of the boat surveys. 32
Figure 3-9: Cross-shore variability in SSC, y_{BD} and k_d at SP3. 33
Figure 3-10: Cross-shore variability in SSC, y_{BD} and k_d at SP8. 34
Figure 3-11: Cross-shore variability in SSC, y_{BD} and k_d at SP12. 35
Figure 3-12: Alongshore variability in SSC, y_{BD} and k_d. 36
Figure 3-13: Particle size distibution of the suspended sediments. 39
Figure 3-14: Absorption spectra. 40
Figure 3-15: Normalised absorption spectra. 41
Figure 3-16: Time series of wind speed, direction, rainfall, river flows and turbidity at Site 11. 43
Figure 3-17: Time series of SSC and optical variables at Site 11. 44

Figure 3-18: Time series of wind speed, direction, rainfall, river flows and turbidity at Site 12. 46
Figure 3-19: Time series of SSC and optical variables at Site 12. 47
Figure 3-20: Time series of wind speed, direction, rainfall, river flows and turbidity at Site 13. 48
Figure 3-21: Time series of SSC and optical variables at Site 13. 49
Figure 3-22: Time series of wind speed, direction, rainfall, river flows and turbidity at Site 14. 50
Figure 3-23: Time series of SSC and optical variables at Site 14. 51
Figure 3-24: Time series of wind speed, direction, rainfall, river flows and turbidity at Site 15. 52
Figure 3-25: Time series of SSC and optical variables at Site 15. 53
Figure 3-26: Time series of wind speed, direction, rainfall, river flows and turbidity at Site 16. 54
Figure 3-27: Time series of SSC and optical variables at Site 16. 55
Figure 3-28: Surf-zone estimates of SSC, Chl-a, g_{340} and y_{BD}. 60
Figure 3-29: Particle size distribution of sediments suspended in the surf-zone. 61

Figure B-1: Profiles of salinity, T_n, c_{530} and E_d (from which k_d is derived) for profiles 1 to 6. 68
Figure B-2: Profiles of salinity, T_n, c_{530} and E_d (from which k_d is derived) for profiles 7 to 12. 69
Figure B-3: Profiles of salinity, T_n, c_{530} and E_d (from which k_d is derived) for profiles 13 to 18. 70
Figure B-4: Profiles of salinity, T_n, c_{530} and E_d (from which k_d is derived) for profiles 19 to 24. 71
Figure B-5: Profiles of salinity, T_n, c_{530} and E_d (from which k_d is derived) for profiles 25 to 30. 72
Figure B-6: Profiles of salinity, T_n, c_{530} and E_d (from which k_d is derived) for profiles 31 to 36. 73
Figure B-7: Profiles of salinity, T_n, c_{530} and E_d (from which k_d is derived) for profiles 37 to 42. 74
Figure B-8: Profiles of salinity, T_n, c_{530} and E_d (from which k_d is derived) for profiles 43 to 48. 75
Figure B-9: Profiles of salinity, T_n, c_{530} and E_d (from which k_d is derived) for profiles 49 to 54. 76
Figure B-10: Profiles of salinity, T_n, c_{530} and E_d (from which k_d is derived) for profiles 55 to 60. 77
Figure B-11: Profiles of salinity, T_n, c_{530} and E_d (from which k_d is derived) for profiles 61 to 66. 78
Figure B-12: Profiles of salinity, T_n, c_{530} and E_d (from which k_d is derived) for profiles 67 to 72. 79
Figure B-13: Profiles of salinity, T_n, c_{530} and E_d (from which k_d is derived) for profiles 73 to 78. 80
Figure B-14: Profiles of salinity, T_n, c_{530} and E_d (from which k_d is derived) for profiles 79 to 84. 81
Figure B-15: Profiles of salinity, T_n, c_{530} and E_d (from which k_d is derived) for profiles 85 to 90. 82

Figure B-16: Profiles of salinity, T_n, c_{530} and E_d (from which k_d is derived) for profiles 91 to 96. 83
Figure B-17: Profiles of salinity, T_n, c_{530} and E_d (from which k_d is derived) for profiles 97 to 98. 84
Figure B-18: Cross-shore variability in SSC, y_{BD} and k_d at SP1. 84
Figure B-19: Cross-shore variability in SSC, y_{BD} and k_d at SP2. 85
Figure B-20: Cross-shore variability in SSC, y_{BD} and k_d at SP4. 85
Figure B-21: Cross-shore variability in SSC, y_{BD} and k_d at SP5. 86
Figure B-22: Cross-shore variability in SSC, y_{BD} and k_d at SP6. 86
Figure B-23: Cross-shore variability in SSC, y_{BD} and k_d at SP7. 87
Figure B-24: Cross-shore variability in SSC, y_{BD} and k_d at SP9. 87
Figure B-25: Cross-shore variability in SSC, y_{BD} and k_d at SP10. 88
Figure B-26: Cross-shore variability in SSC, y_{BD} and k_d at SP11. 88

Reviewed by

R. Davies-Colley

Approved for release by

M. Green

Formatting checked by

Executive summary

NIWA was commissioned by TTR to undertake a field programme to measure background optical water quality and suspended sediment concentrations (SSC) in the nearshore region (within 2.5 km of the shore) of the South Taranaki Bight (STB). The field studies were undertaken to provide background details to help assess the potential effects of offshore sand extraction on the surrounding environment, in particular the effect of sediment plume dispersal.

Specifically, NIWA was contracted to undertake a field measurement programme that consisted of:

1. Two boat surveys to measure vertical profiles of optical variables and SSC, in order to assess spatial variability.

2. A 6-week deployment of moored instruments at 6 nearshore sites (~10 m water depth) to access temporal variability and to establish relationships between measured near-surface optical backscatter and certain optical variables.

3. The collection of water samples from the surf-zone region at 11 sites along the STB. The water samples were analysed to determine variables relating to optical water quality and SSC.

This report presents a synthesis of the measurements. A summary of the key findings is as follows.

Measurements from both boat surveys (S1 and S2) showed that SSC and optical variables vary significantly with distance offshore, with SSC and diffuse light attenuation (k_d) being greatest closest to the shore, and visual clarity (as indexed by the horizontal black disc visibility) increasing rapidly with distance offshore. Both coloured dissolved organic matter (CDOM) and chlorophyll-a concentration also decrease with distance offshore.

Both boat surveys suggest a reduction in SSC (and hence an increase in visual clarity and a decrease in k_d) moving down the coast in a S SE direction. Measured SSC was greater during S2 than during S1, which was probably the result of higher river flows (and sediment loads). The maximum (averaged over the water column) SSC measured during S2 was 0.068 g/L near Hawera. During S2, in the waters ~500m offshore, the horizontal black disc visibility (y_{BD}) was less than 1 m along the entire length of the STB, which is a rather low visual clarity.

Using the boat survey data, statistically robust *in-situ* relationships were determined relating the nephelometric turbidity (T_n) as measured by an optical backscatter sensor to SSC, the beam attenuation coefficient (c) at 530 nm (from which y_{BD} is derived), and k_d. These relationships were applied to the optical backscatter data collected at the 6 moored instrument sites. The estimates of T_n, SSC, k_d, and y_{BD} from the 6 moored instrument sites all showed considerable temporal variability. During the last two weeks of the deployment period there was a significant increase in SSC, coinciding with increased river flows. At these times it is likely that the rivers were discharging fine sediments into the STB, which were then being transported in suspension through the measurement site. Some of the peaks in SSC also coincided with times of high wind speed but low river flows. These peaks in SSC are

most likely wave-driven. At these times, wave stirring is entraining fine sediments from the sea floor, which are subsequently mixed into the water column.

During river and wave events, the euphotic depth is less than the mean water depth at the instrument sites. This is significant, as it means that less than 1% of the ambient light is reaching the benthos at these times.

Rainfall data have shown that the deployment took place during a period of lower than expected rainfall for that time of year, and consequently during a period of low river flows. Since rivers are a major source of fine sediments into the STB, it is likely that the data are representative of conditions with clearer water.

Overall, the field dataset provides a comprehensive picture of the background optical water quality and SSC in the STB. These results can be used with confidence to help assess the potential effects of offshore sand extraction on the surrounding environment, and in particular the effect of sediment plume dispersal in the nearshore environment.

Information relating to TTR's additional scientific work undertaken since 2014 has been provided and the conclusions is this report remain valid.

1 Introduction

1.1 Background

Trans-Tasman Resources Ltd (TTR) has secured permits and is prospecting for iron sands on the seabed in the South Taranaki Bight (STB) of the West Coast, North Island. The prospecting licence areas lie within and seaward of the 12 nautical miles territorial sea. The proposed extraction area is in the Exclusive Economic Zone (EEZ) between 22 km and 35 km off the coast of Patea. A 10-year mining plan has been developed with the intention of applying for a 20-year mining permit for the area. TTR is applying for Crown Minerals Act mining permits and environmental marine consents under the new EEZ legislation in 2013.

NIWA is undertaking a range of biogeophysical studies in the South Taranaki Bight for TTR to help meet the likely consenting requirements for sand extraction from the seabed.

1.2 Project description

The iron sand extraction area will be 22 to 35 km offshore from Patea (Figure 1-1). Water depths in this region range between 25 to 55 m.

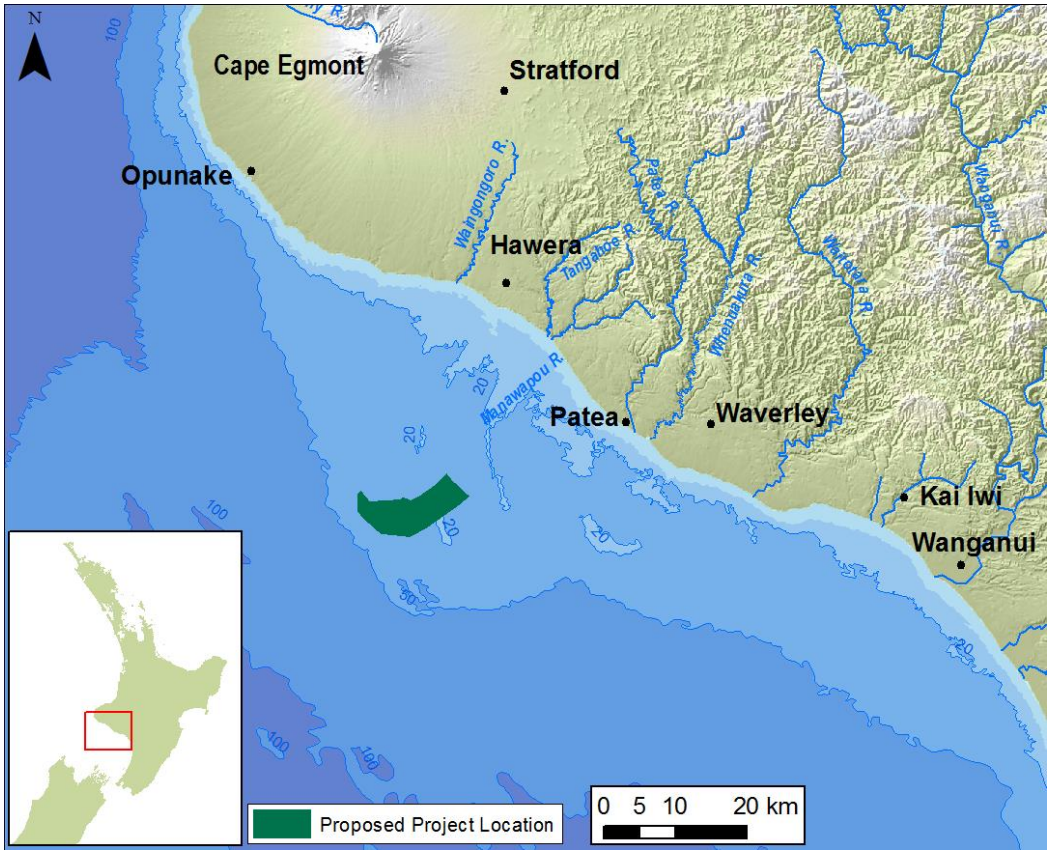

Figure 1-1: Site map showing the proposed project location.

Sand will be extracted by a Submerged Sediment Extraction Device (SSED) which is connected to a single FPSO (Floating Production Storage Offloading) vessel. The SSED, when located on the sea bed, is connected to the FPSO via an umbilical delivery pipe (power cable, hydraulic hose and delivery hose). The SSED operates under the stern of the FPSO at the base of the defined ore body and cuts to the full depth face (creating a 'lane' about 3 to

10 m deep and about 10 m wide) in a single operation, meaning there is no need to return. Sediment is pumped to the FPSO for processing. A winching system locates the FPSO relative to the SSED which will be working 300 m × 300 m blocks in a predetermined sequence. De-ored (remaining) sediment (about 90% of the total dredged volume) will be slurried by pipe from the bow of the FPSO to largely backfill the cut lanes as the FPSO follows the SSED.

The single FPSO vessel contains the extraction, processing and de-ored sediment management functions of the project. Sediment from the SSED is processed on board to separate iron ore concentrate from the rest of the sediment using magnetic separators and grinding mechanisms. The final iron ore concentrate is dewatered to ~10% moisture and stored temporarily on the FPSO before being slurried with fresh water to the FSO (Floating Storage Offloading). From the FSO the iron ore transhipts to ore carriers either at open sea or at a sheltered area depending on weather conditions. The ore carriers then deliver the iron ore concentrate to China and other export markets.

1.3 Nearshore optical water quality

Under Work Schedule C (Sediment Plume Modelling Phase 2) of the agreement between NIWA and TTR, NIWA has undertaken to “Estimate the concentrations and deposition rates of sediments released from the sand mining activities”. The results from Schedule C are reported in Hadfield (2011). The model results predict that, under certain conditions, a plume of fine sediments released from the sand extraction process extends to the southeast and can impinge on the nearshore coastal environment. In response to this, NIWA was commissioned by TTR to undertake a field programme to measure background optical water quality and suspended sediment concentrations in the nearshore region of the STB. Background SSC levels in the vicinity of the proposed project location have already been described by MacDonald et al. (2012).

The following three-stage approach was adopted:

1. Two boat surveys of optical variables and SSC to assess spatial variability.
2. A 6-week deployment of moored instruments at 6 nearshore sites (~10 m water depth) to access temporal variability and to establish relationships between measured near-surface optical backscatter and certain optical variables.
3. Measurements from the surfzone at 11 sites.

1.4 This report

This report provides TTR with a summary of the data.

2 Methods

2.1 Background

"Optical water quality" is a broad term used to encapsulate how changes in the colour and clarity of water are related to its "quality", which is a rather subjective term with potential social, economic, political and environmental significance (Davies-Colley et al. 2003).

In terms of the optical water quality, the key variables are light beam attenuation (c) and diffuse light attenuation coefficient (k_d).

Armed with c, which is an index of visual clarity, we can estimate the visual range of sighted animals. This parameter is of fundamental importance to many aquatic animals, as the maximum sighting distance, for example, is likely to be of great importance to visual predators such as fish, aquatic birds and other marine mammals. Specifically, the visual clarity is an upper bound to the "reactive distance" of a predator or prey animal.

The diffuse light attenuation coefficient (k_d) is a fundamental variable describing the attenuation of sunlight with depth, and therefore the light field of benthic plants. Light penetration into the water column and to the benthos is critical as sunlight is the driving energy source on which the vast majority of aquatic ecosystems depend (Davies-Colley et al. 2003).

The diffuse light attenuation coefficient (k_d) is referred to as an "apparent" optical parameter is it depends (weakly) on the incident light field. The light beam attenuation (c), on the other hand is referred to as an "inherent" optical parameter as it depends only on the composition of the water body (Kirk 2011; Davies-Colley et al. 2003).

The light beam attenuation (c) is the sum of two terms, the light scattering coefficient (b) and light absorption coefficient (a), i.e., $c = a + b$.

Several groups of light-attenuating elements are present in natural waters. Absorption and scattering by water molecules is low, and is only relevant in optically pure waters[1]. Suspended particulate matter strongly scatters light and may also significantly absorb light, depending on the organic content. Coloured dissolved organic matter (CDOM) has a negligible effect on scattering, but strongly absorbs light, especially at the blue end of the visual spectrum (Kirk 2011). Finally, phytoplankton scatters light strongly while also strongly absorbing both red and blue light (Kirk 2011).

In response to the above, the field measurement programme was designed to include measurements of light beam attenuation (c), light absorption (b), diffuse light attenuation coefficient (k_d), suspended sediment concentration (SSC), CDOM (indexed by g_{340}) and phytoplankton concentration (indexed by chlorophyll *a*).

2.1.1 Instrumentation

For the boat surveys, vertical profiles of various optical parameters were measured using a profiling instrument, Bio-Fish (ADM Electronik), which is a multiparameter system designed for the collection of various physical, chemical and biological variables (Table 2-1).

[1] The high salt content of sea water is also optically irrelevant.

Table 2-1: Summary of variables measured and instrumentation used during the boat surveys.

Optical variable	Symbol	Manufacturer/Instrument
Nephelometric turbidity	T_n	Seapoint./Optical Backscatter Sensor (OBS)
Light beam attenuation at 530 nm (green)	c_{530}	Wet labs/ C-Star transmissometer
Light beam attenuation at 650 nm (red)	c_{650}	Wet labs/ C-Star transmissometer
Downwelling irradiance	E_d	LI-COR/ PAR sensor
Conductivity, temperature, salinity	C, T and S	ADM Elektronik/Conductivity and Temperature sensor
Chlorophyll fluorescence	Chl-a	Wet labs/ Eco Triplet
Coloured dissolved organic matter fluorescence	CDOM	Wet labs/ Eco Triplet

From the list of variables shown in Table 2-1, we are particularly interested in c_{530} (light beam attenuation at 530 nm) and E_d (from which k_d is derived).

Estimating the diffuse light attenuation coefficient (k_d)

The diffuse light attenuation coefficient (k_d) is defined as (Kirk 2011):

$$k_d = -\frac{1}{E_d}\frac{dE_d}{dz} = -\frac{d(\mathrm{In}E_d)}{dz} \quad (1)$$

where z is the depth below the water surface and E_d is the downwelling irradiance. Equation (1) shows that the slope of the line, on a plot of z versus $\ln(E_d)$, is equal to negative k_d. Figure 2-1 shows an example of estimating k_d from data. Estimates of k_d were rejected when the R^2 for the fit of data to Equation (1) was less than 0.85. A poor fit usually resulted from boat interference that degraded the estimates of E_d.

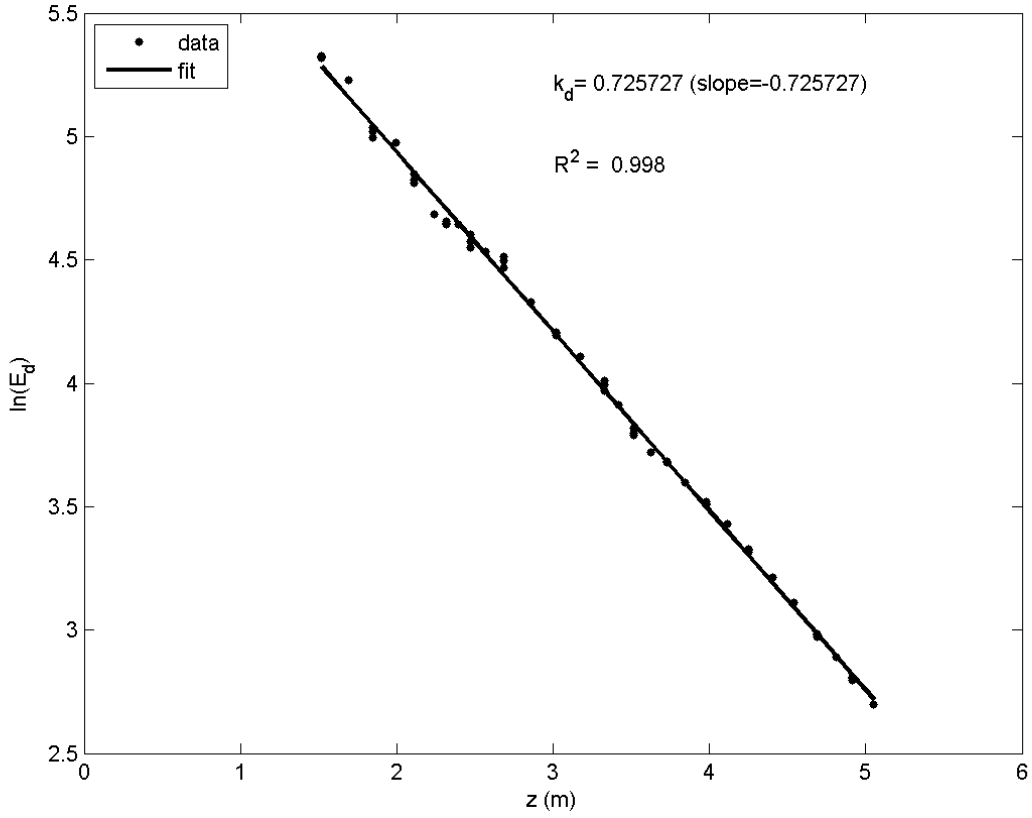

Figure 2-1: Example showing how k_d was estimated.

Visual clarity

The other fundamental variable of interest here is the visual clarity which we report in terms of the horizontal black disc visibility (y_{BD}), which is the distance in which objects can been seen through water. This is a more intuitive index than light beam attenuation (c), however, these two terms are easily inter-changeable, as the horizontal back disk visibility (y_{BD}) is related to c as (Zaneveld and Pegau 2003; Davies-Colley and Nagels 2008):

$$y_{BD} = \frac{4.8}{c_{550}}$$

where c_{550} is the beam attenuation at a wavelength of 550 nm. We measured c_{530} and not c_{530}, however as the ratio of c_{550} to c_{530} lies within the range of 0.9 to 0.985 (Zaneveld and Pegau 2003), we therefore assume that $c_{530} \approx c_{550}$.

Given the importance of k_d and y_{BD} in describing the optical properties of a water body, they are the primary variables of interest. However, the full set of variables measured during the boat surveys (Table 2-1) are shown in case such data are required in subsequent studies.

2.1.2 Water sampling and laboratory analysis

In addition to the Bio-Fish data collected during the boat surveys, water samples were also collected for laboratory analysis of: SSC, particulate absorption spectra (PABS), coloured dissolved organic matter (CDOM), chlorophyll a (Chl-a) and the particle size distribution (PSD).

The water samples were typically collected 1 m below the water surface and, when at mooring sites, at the depth of the deployed sensor (3 m). Water samples were kept on ice during transportation and processed at NIWA's Hamilton laboratory within 24 hours:

- SSC was estimated using Method # 2540D of the APHA Standard Methods for the Examination of Water and Wastewater, 21st Edition, 2005.
- PABS: Subsamples (50 ml) of water were filtered through a 25mm GF/F until colour was uniformly visible on the filter (noting volume filtered and in subdued light to avoid pigment degradation). In clear oceanic water about 1 L was sufficient; much less was required in turbid water (about 150 ml). Once filtration was complete, forceps were used to transfer the filter into a tissue-capsule. The capsule was then wrapped in a small square of aluminium foil and placed into liquid nitrogen for storage. PABS scans were made on the filter before and after pigment extraction by methanol extraction and then bleaching following the method of Tassan & Ferrari (1995). These methods provide the absorption (a) spectral (signatures) across a range of wavelengths (350-850 nm) for all particles (a_p), the non-algal particles remaining after pigment removal (a_{nap}), and therefore by difference the absorption of algal particles (a_{ap}). The absorption measurements were required for subsequent studies that are going to model the optical properties of the mining-derived sediment plume.
- CDOM is indexed by light absorption measurements made by a spectrophotometer on samples filtered through a 0.45 µm membrane filter at 340, 440 and 740 nm. The CDOM absorption coefficient at 340 nm was calculated as:

  $$g_{340} = \ln(10)\frac{[A_{340} - (740/340)A_{740}]}{0.04}$$

  where A_{340} and A_{740} is the spectrophotometer absorption at 340 and 740 nm, respectively, and the denominator (0.04) reflects the fact that 40 mm cuvettes were used in the analysis. Given the greater precision of absorption measurements at 340 nm in waters of low CDOM, we used g_{340} rather than g_{440} as the index of CDOM.
- Chla-a: The major pigment in algae is a robust measure of biomass concentration and was estimated using Method # 10200H of the APHA Standard Methods for the Examination of Water and Wastewater, 21st Edition, 2005.
- The particle size distribution (PSD) was measured using a Beckman Coulter LS 13 320 Dual Wavelength Laser Particle Sizer. The PSDs were collected to provide background information on the size of particles in suspension. Particle size also plays an important role in governing the optical properties of the suspend sediments: silt-sized particles, for example, have a pronounced effect on light attenuation, while sand-sized particles have a negligible effect.

2.2 Moored deployment

2.2.1 Instrumentation

For the 6-week moored deployments, a DOBIE gauge (NIWA LTD) was deployed at each of the 6 sites. The DOBIE gauges used in this study were equipped with a pressure sensor for measuring water level and an optical backscatter sensor (OBS, Seapoint Sensor Inc). The output from each OBS was first converted to an estimate of T_n (turbidity) by applying a laboratory calibration. T_n was then converted to estimates of SSC, c_{530} and k_d by applying an *in-situ* calibration determined from the deployment of the Bio-Fish during the boat surveys. An *in-situ* calibration was needed as the direct measurement of and c_{530} and k_d is not possible over long-term deployments: the beam transmissometers and LI-COR sensors used on the Bio-Fish are far too fragile to withstand long-term deployments in energetic conditions, such as those found in the STB. An OBS, on the other hand, is robust and can withstand such conditions.

The data conversion procedures are described in the following.

2.2.2 Laboratory calibration

For each OBS, the voltage output was related to nephelometric turbidity (T_n) by using a linear relationship:

$$T_n = GV + O \tag{2}$$

where G is the sensor gain (unit of NTU per volt) an O is the sensor offset (units of NTU).

Each sensor gain and offset were determined by calibration against a series of test suspensions in a large laboratory tank in which T_n was also measured using the turbidity sensor on the Bio-Fish. The sediment used in the calibration came from bed sediments collected near the mouth of the Wanganui River. The test sediment was sieved through a 63-micron sieve to remove sand, which is optically irrelevant. A regression was used to fit the linear relationship (Equation 2) to the calibration dataset (sensor output versus reference T_n) to the determine G and O for each sensor(Figure 2-2).

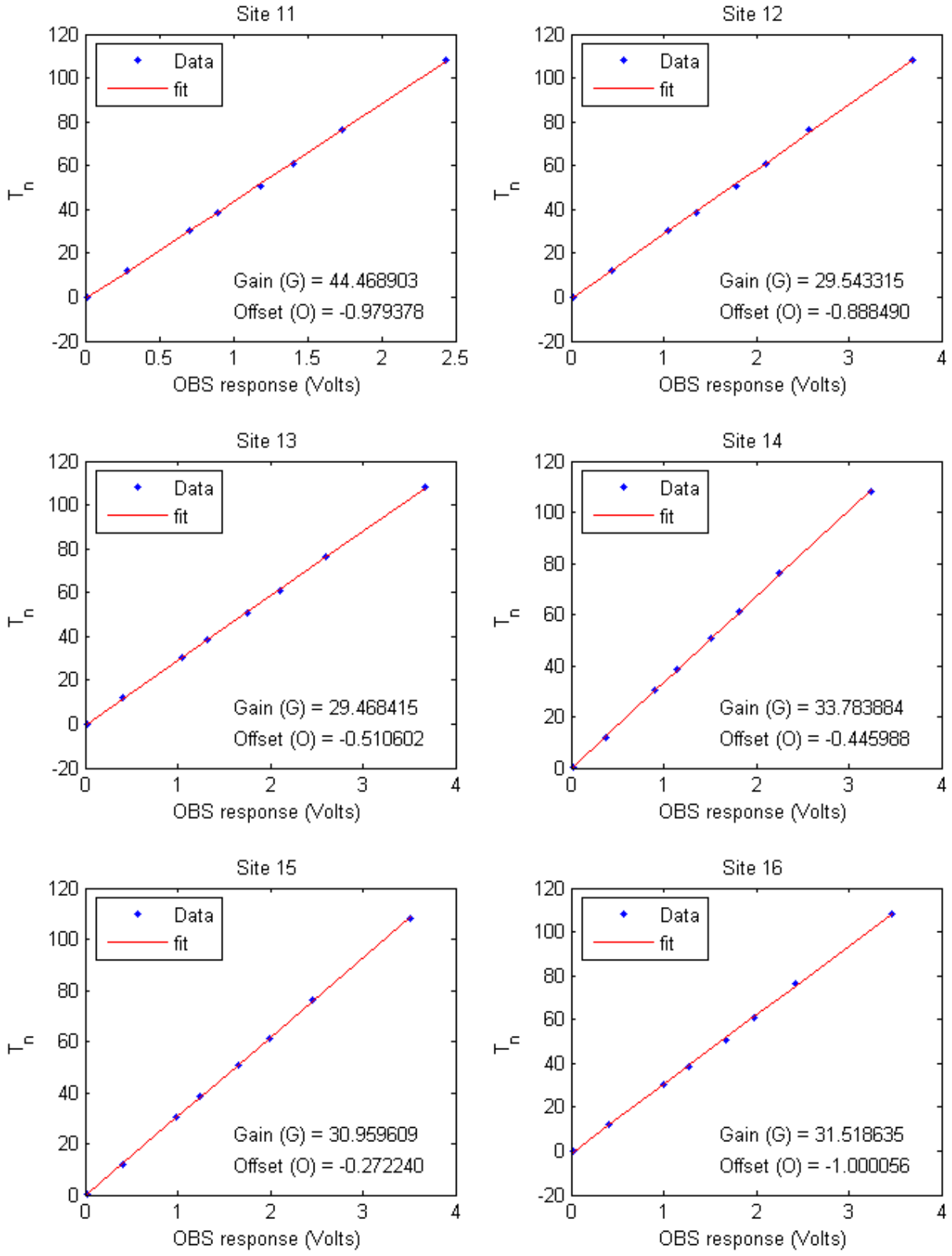

Figure 2-2: Laboratory calibration showing the relationship between T_n (turdidity) and the OBS output.

2.2.3 *In-situ* calibration

The *in-situ* relationships required to convert T_n into estimates of SSC, c_{530} and k_d were developed as follows.

Conversion of T_n into SSC.

T_n was related to SSC by using a linear relationship:

$$SSC = G_1 T_n + O_1 \quad (3)$$

where G_1 is the sensor gain (units of g/L per NTU) and O_1 is the sensor offset (units of g/L).

A regression was used to fit the linear relationship (Equation 3) to the calibration dataset (T_n versus SSC) to the determine G_1 and O_1(Figure 2-3). The estimates of SSC were obtained from analysis of the water samples collected during the Bio-Fish deployments, and T_n corresponds to the values measured at the times the water samples were collected.

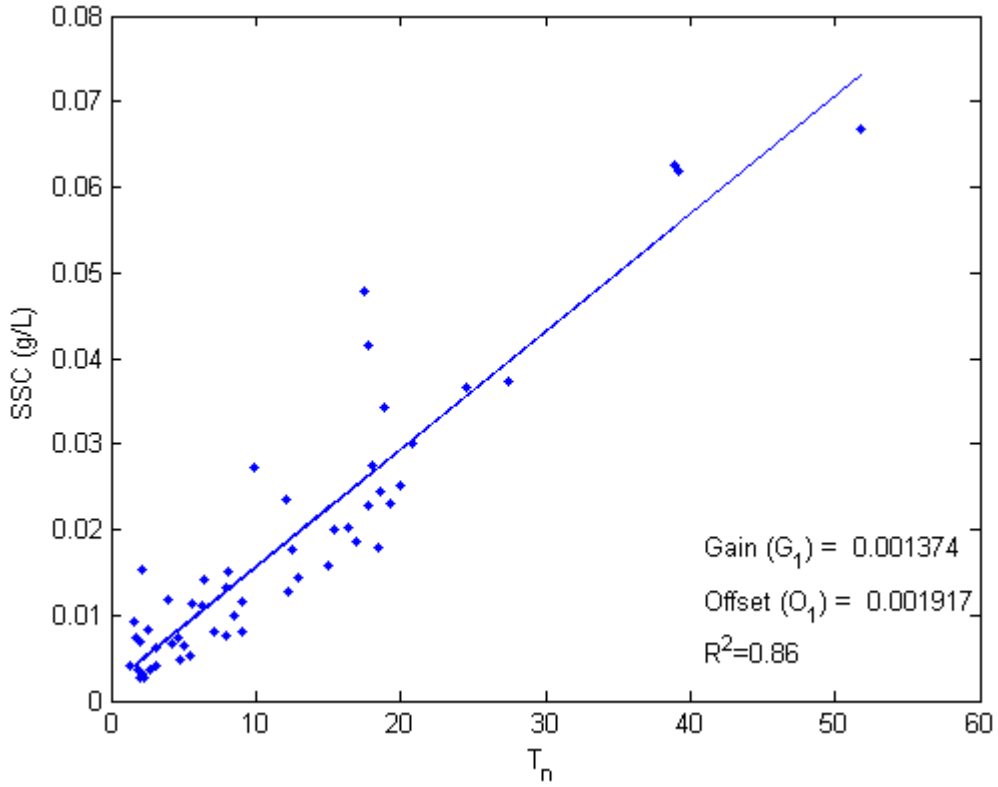

Figure 2-3: In-situ calibration of T_n versus SSC.

Conversion of T_n into c_{530}

T_n was related to c_{530} by using a linear relationship:

$$c_{530} = G_2 T_n + O_2 \quad (4)$$

where G_2 is the sensor gain (units of m^{-1} per NTU) and O_2 is the sensor offset (units of m^{-1}).

A regression was used to fit the linear relationship (Equation 4) to the calibration dataset (T_n versus c_{530}) to the determine G_2 and O_2(Figure 2-4). The estimates of c_{530} and T_n used in the calibration were measured concurrently by the Bio-Fish.

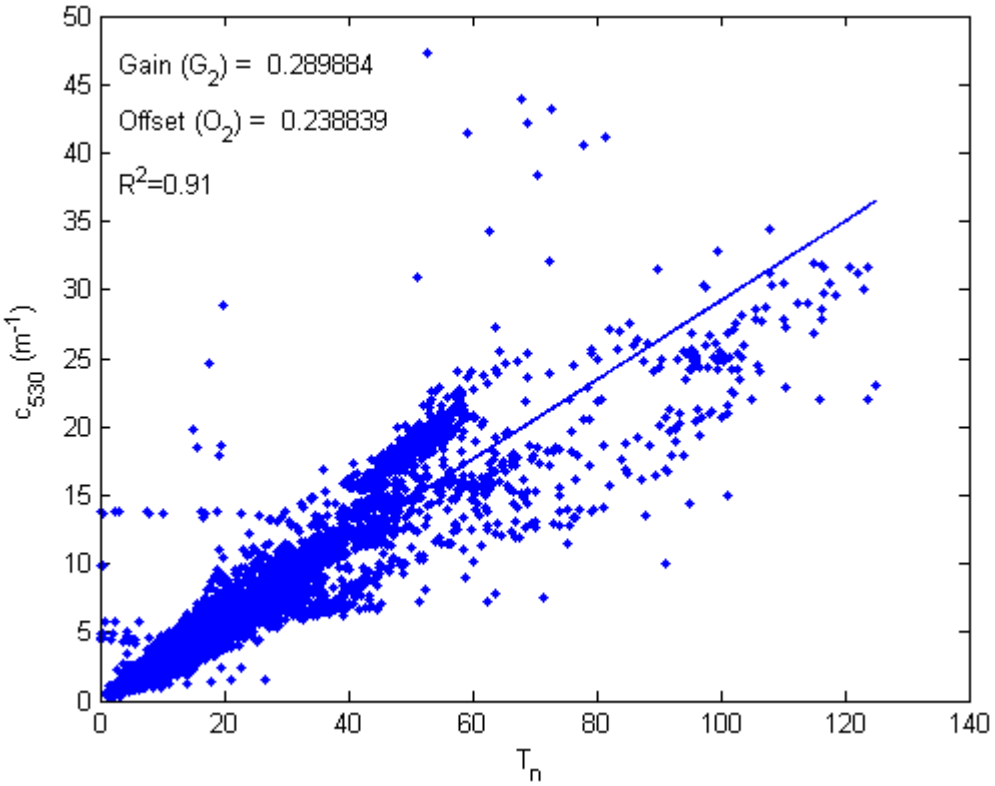

Figure 2-4: In-situ calibration of T_n versus c_{530}

Conversion of T_n into k_d.

T_n was related to k_d by using a linear relationship:

$$k_d = G_3 T_n + O_3 \quad (5)$$

where G_3 is the sensor gain (units of m^{-1} per NTU) and O_3 is the sensor offset (units of m^{-1}).

A regression was used to fit the linear relationship (Equation 5) to the calibration dataset (T_n versus k_d) to the determine G_3 and O_3(Figure 2-5). The estimates of k_d and T_n used in the calibration were both measured by the Bio-Fish.

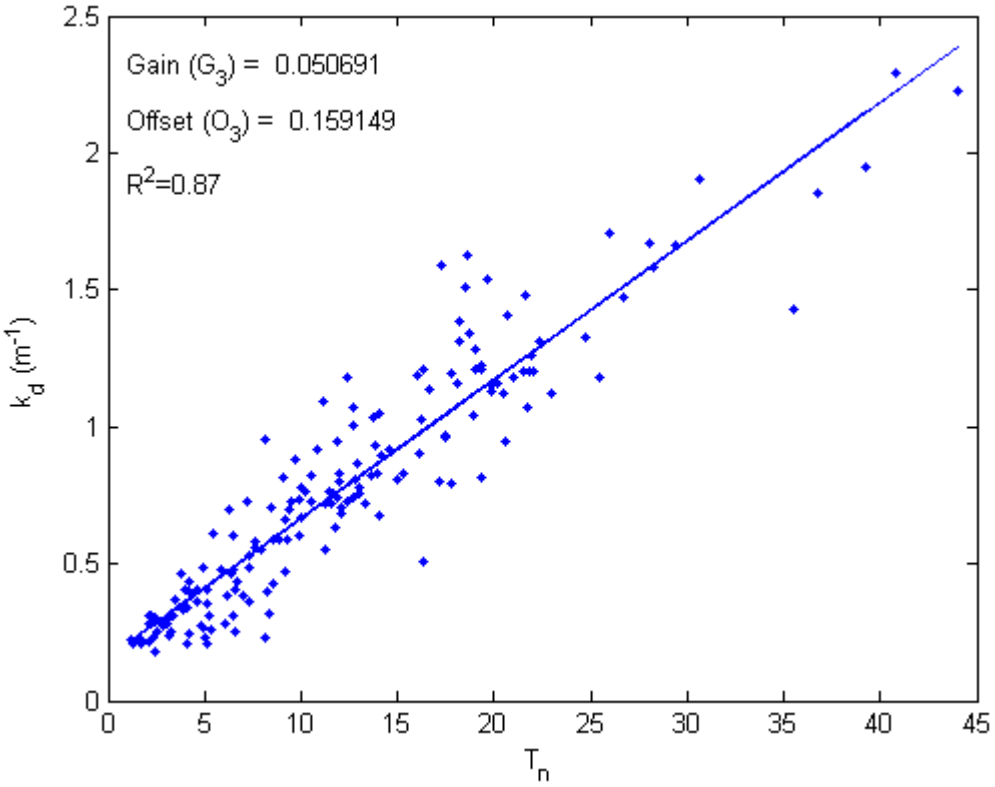

Figure 2-5: In-situ calibration of T_n versus k_d.

To summarise, the OBS data were processed firstly by applying Equation (2) to estimate T_n and then by applying Equations (3), (4) and (5) to estimate SSC, c_{530} and k_d, respectively.

2.2.4 Seabed sediments analysis

Seabed surface sediments were collected at each of the 6 instrument mooring sites on a single occasion. The surface sediments were collected by divers pushing a 15-cm-long plastic core into the seabed.

After returning to the laboratory, the sediment was washed several times with fresh water to remove any salt.

The washed sediment was then wet-sieved into 1 ϕ size fractions, where $\phi = -\log_2(d)$, with d the particle diameter in millimetres. The apertures of sieve sizes used in the analysis are shown in Table 2-2.

Table 2-2: Sieve sizes used in the analysis of the beach sediments.

	Sieve aperture							
d (mm)	8.000	4.000	2.000	1.000	0.500	0.250	0.125	0.063
φ	-3	-2	-1	0	1	2	3	4

The particle size distribution (PSD) was then derived from weighing the sediment (once it had been dried) that was retained on each sieve.

2.3 Surf-zone water samples

Due to the combination of shallow water depths and breaking waves in the surf-zone it was not possible during the boat surveys to make measurements (or collect water samples) in the shallows very close to the shore. Therefore, additional water samples were collected by wading out into the surf-zone. At each site a 4 L water sample and a 20 L bucket water sample were collected.

To minimise degradation, the water samples were sent within 24 hours to NIWA's Hamilton laboratory for analysis. The water samples collected in the 4 L bottle were analysed to yield estimates of: SSC, coloured dissolved organic matter (CDOM), chlorophyll a (Chl-a) and particle size distribution. Before analysis, the water samples were filtered through a 0.063 mm sieve to remove any sand-sized particles, since it is the fine sediments that have the greatest effect on the optics. Once sieved, the water samples were analysed according to the procedures described in Section 2.1.2.

The 20 L (bucket) samples were used to estimate y_{BD}, which was done using the equipment shown in Figure 2-6. Once sieved, the 20 L sample was emptied into a galvanised trough. Located at one end of the trough is an underwater viewer equipped with a 45˚ mirror, which allows an observer to view horizontally down the length of the trough. With the observer watching, a second person moves a black disc away from the observer down the trough until the black disc can no longer be seen. The distance at which the observer first losses sight of the disc is defined as y_{BD}. When the horizontal visibility was less than 0.5 m, a 2 cm diameter black disc was used. For visibility between 0.5 m and 1.5 m, a 6 cm diameter black disc was used.

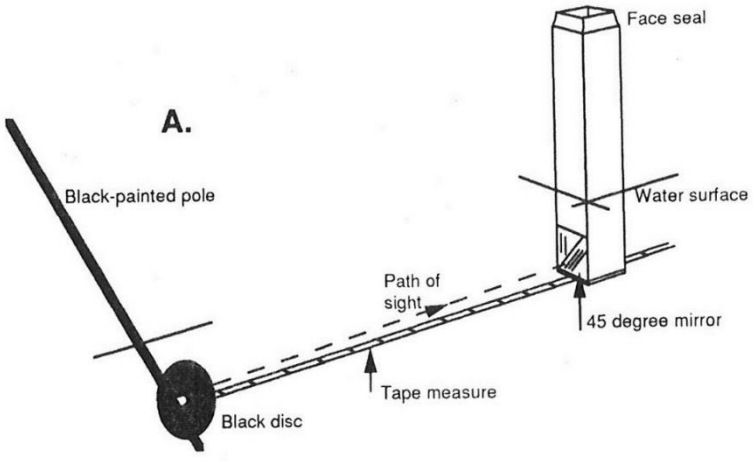

Figure 2-6: Black disc equipment used for measuring visual water clarity (y_{BD}) from the surf-zone water samples.(After, Davies-Colley et al. 2003).

2.4 Deployment considerations

2.4.1 Boat surveys

Figure 2-7: Aerial photography of the nearshore region in the STB. Picture shows a cross-shore gradient in SSC, with SSC decreasing with distance from the shore (photography courtesy of Boffa Miskell).

Figure 2-7 shows a cross-shore (normal to the shoreline) gradient in SSC, with SSC decreasing with distance from the shore. This is a consistent feature along the entire coastline of the STB.

Due to the influence of rivers, it is anticipated the SSC will also vary significantly in the long-shore (parallel to the shoreline) direction. Accordingly, the boat surveys were planned to capture both the cross-shore and long-shore variability in SSC, spanning the area of interest from Wanganui to Hawera.

2.4.2 Moored deployments

The 6-week moorings were positioned to measure the effects of the Patea, Waitotara and Wanganui Rivers, where it is anticipated that SSC levels would be elevated relative to other parts of the STB. The remaining sites were positioned away from the major rivers, thus providing a contrasting set of conditions to those experienced at the river sites. Ideally, the sites would be roughly equispaced along the area of interest from approximately Wanganui to Hawera.

2.4.3 Surf-zone water sampling sites

The surf-zone water sampling sites were selected using the following criteria:

1. sites must have public beach access, so that repeat trips do not present difficulties with access through private land, and
2. sites must be spaced to span the area of interest from approximately Wanganui to Hawera.

2.4.4 Winds and Rainfall

Wind and rainfall data during the deployment period were obtained from the Electronic Weather Station (EWS) at Spriggens Park in Wanganui (NIWA Climate Database Agent number 3715). The EWS at Spriggens Park is located 15 m above sea level. The location of the Spriggens Park EWS is shown in Figure 2-8.

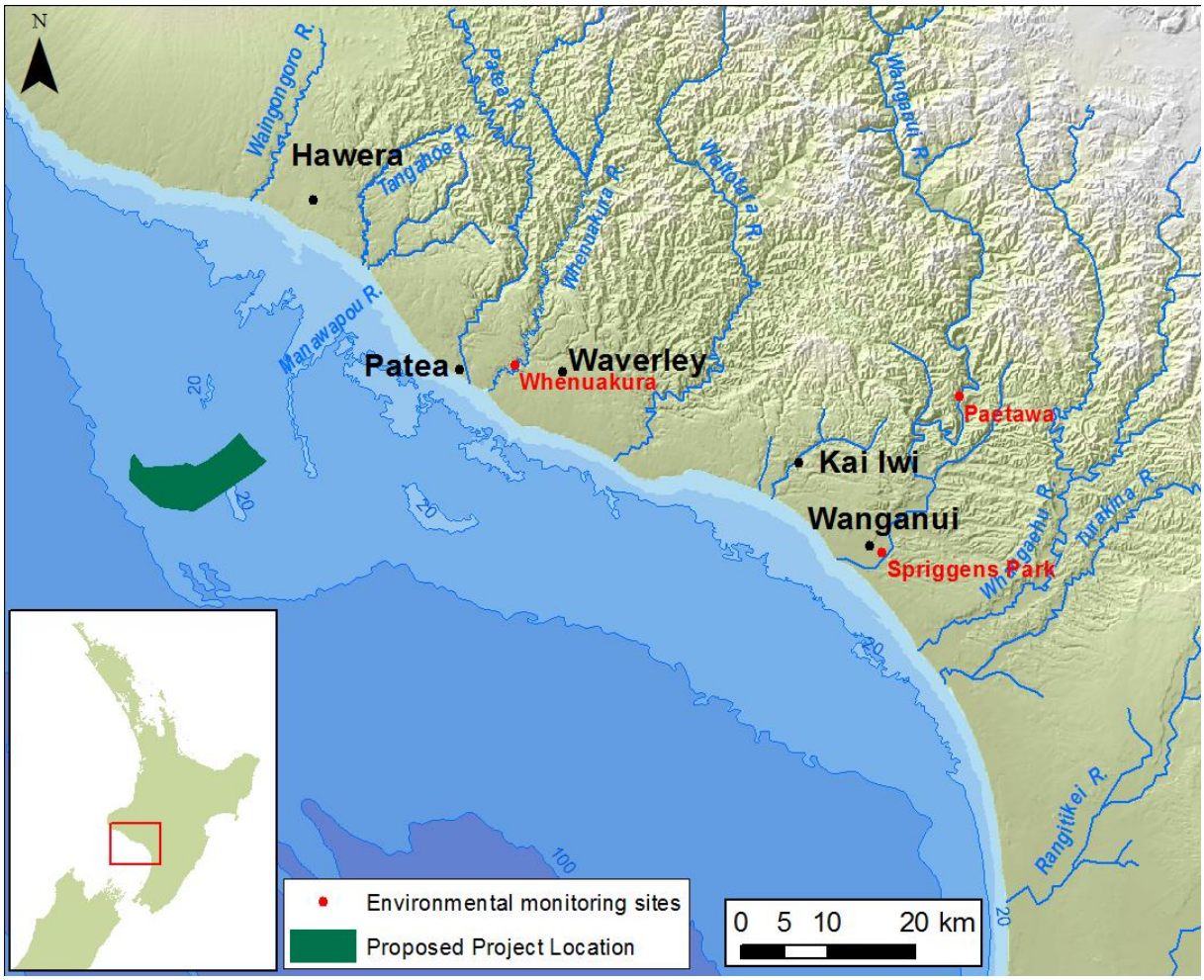

Figure 2-8: Site map showing the locations of environmental monitoring stations.

2.4.5 River flows

River discharges during the deployments were obtained from gauging stations on the Wanganui River at Paetawa and on the Whenuakura River (near Patea) (Figure 2-8).

3 Results

3.1 Site selection and deployment information

Following a consideration of the logistics and the issues discussed in section 2.4, a field programme was designed.

3.1.1 Boat surveys

The locations of the profiles for the first and second boat surveys are shown in Figure 3-1 and Figure 3-2, respectively. The profiles span the area of interest from Wanganui to Hawera and were positioned to assess the cross-shore and long-shore variability. During both surveys, profiles were also measured at the 6 moored instrument sites.

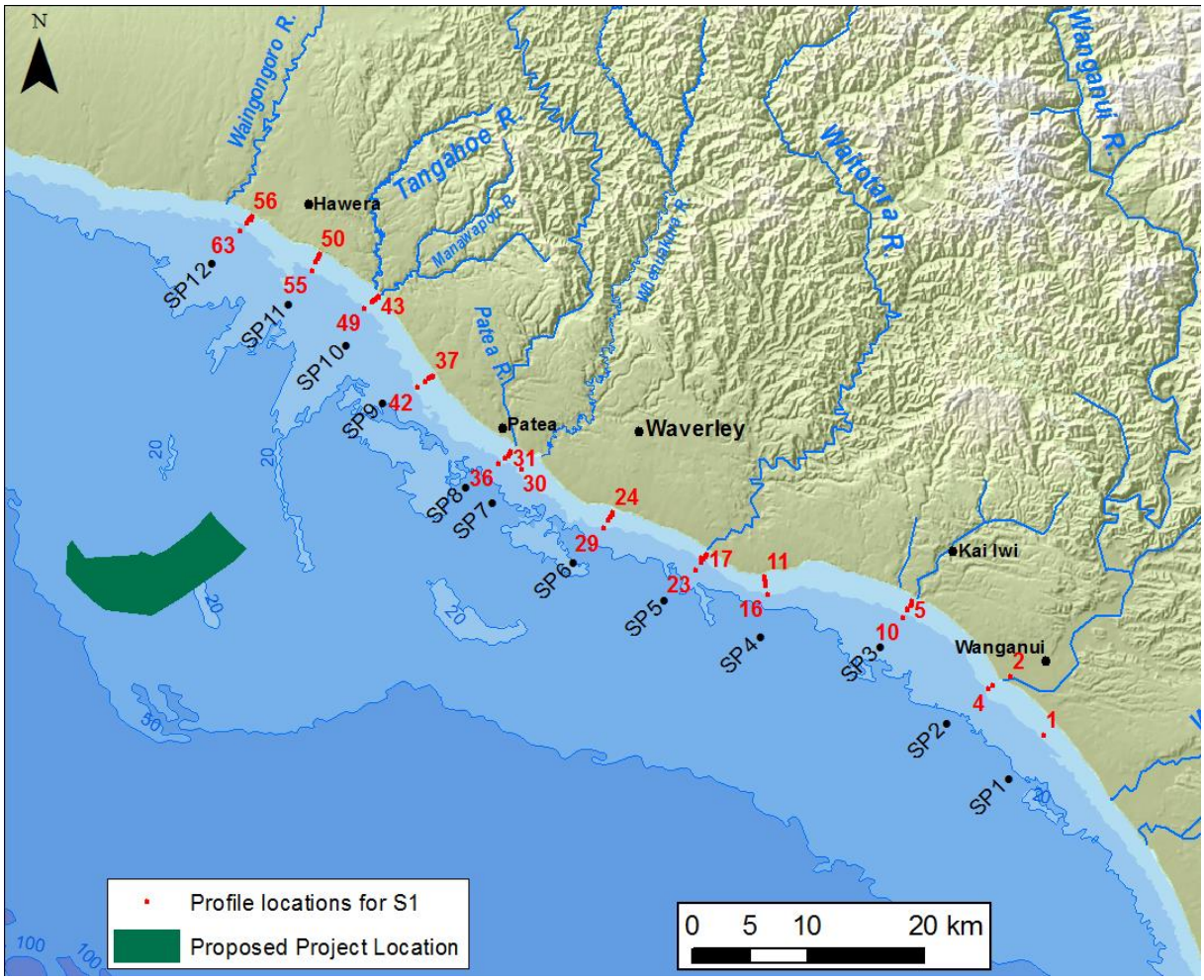

Figure 3-1: Site map showing profile locations from the first boat survey (S1).

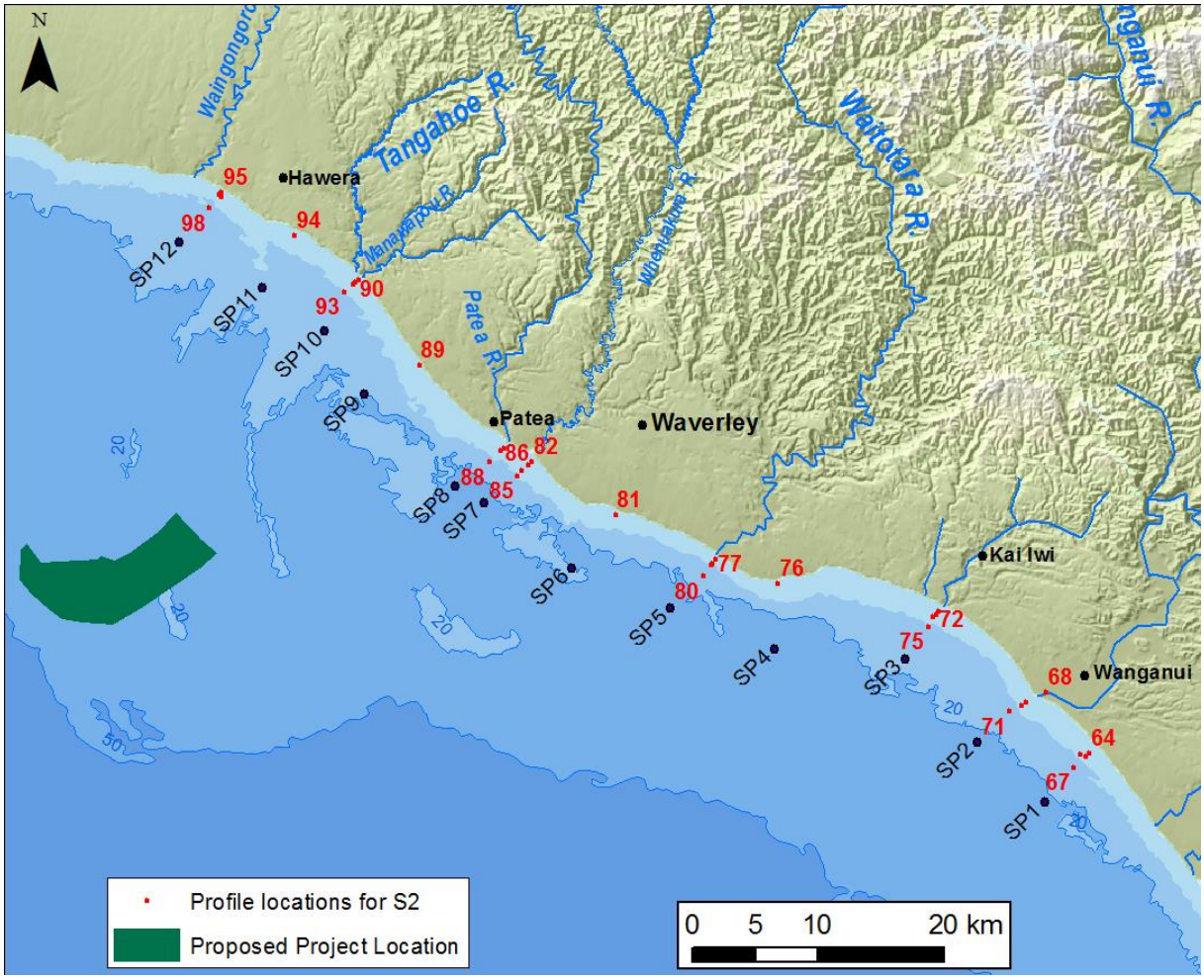

Figure 3-2: Site map showing profile locations from the second boat survey (S2).

Summary information relating to the boat surveys is shown in Table 3-1. Additional information relating to the locations of the profiles is shown in Table A-1 in Appendix A.

Table 3-1: Summary information about the boat surveys.

Boat Survey	Survey ID	Period	Number of profiles collected
1	S1	11/03/13 to 12/03/13	63
2	S2	01/05/13 to 02/05/13	35

Locations of the profiles in this report will be referenced by either the profile number as shown in Figure 3-1 and Figure 3-2, or by profile position along the coast. For example, the profile numbers 5 to 10 (see Figure 3-1) may be referenced as SP3.

The profile locations at which water samples were collected during the boat surveys are shown in Table 3-2. When a series of profiles formed a shore-normal transect (e.g., profiles 5 to 10 at SP3 in Figure 3-1) water samples were collected at the inner and outer ends of the transect (e.g., at profiles 5 and 10 on SP3). During both surveys, water samples were also collected at the 6 moored instrument sites.

Table 3-2: Locations of the water samples collected during the boat surveys. (Profile numbers in bold correspond to profiles collected at the moored instrument sites).

Survey	Number of water samples collected	Profile number
S1	26	**1**, 2, 4, 5, **8**, 10, 11, 16, 17, **21**, 23, 24, 29, **30**, 31, 36, 37, 42, 43, **47**, 49, 50, 55, 56, **60**, 63.
S2	27	64, **66**, 67, 68, 69, 71, 72, **74**, 75, 76, 77, **79**, 80, 81 82, **84**, 85, 86, 88, 89, 90, **92**, 93, 94, 95, **97**, 98.

3.1.2 Moored deployments

Figure 3-3 shows the locations of the 6 nearshore moored deployment sites. Sites 11, 13, 14 and 15 were chosen to measure the effects of the Wanganui, Waitotara, Patea/Whenuakura and Manawapou/Tangahoe Rivers, respectively. Sites 12 and 16 were positioned away from the major rivers, to provide a contrasting set of conditions to the river sites.

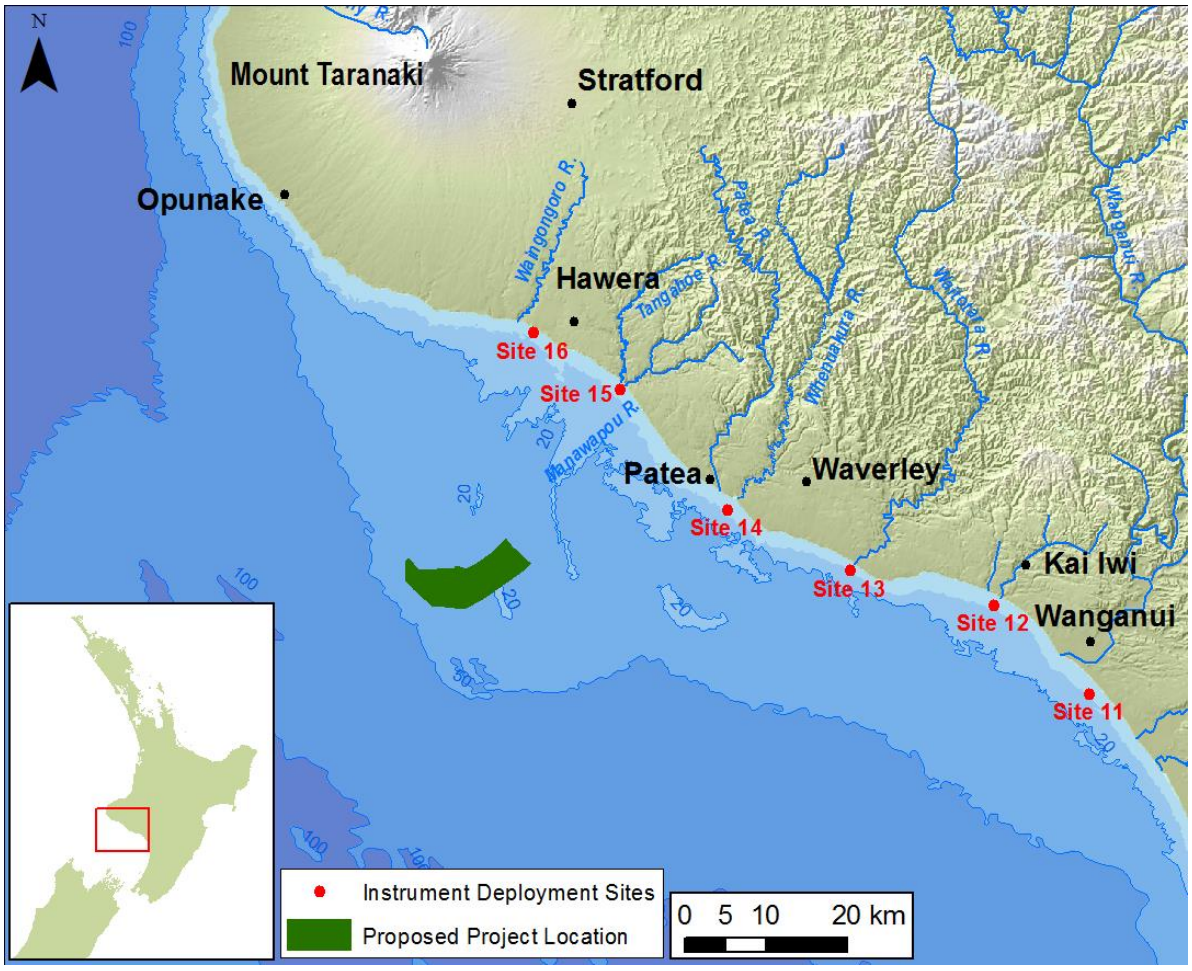

Figure 3-3: Site map, showing the locations of the moored instruments.

Summary information about the moored deployments is shown in Table 3-3.

Table 3-3: Summary information about the moored deployments. The records at sites 13 and 15 ended earlier than anticipated as a resut of an unexpected memory issue.

Site No.	Latitude (S)	Longitude (E)	Approximate distance from shoreline (m)	Time period (NZST)	Duration (days)	Depth below water surface (m)	Mean water depth (m)
11	39˚ 59.415	175˚ 01.689	1450	26/02/13 13:00 to 01/05/13 11:45	63	3.0	11.5
12	39˚ 53.631	174˚ 53.268	1250	26/02/13 14:00 to 01/05/13 13:45	63	3.0	11.5
13	39˚ 51.524	174˚ 40.782	960	26/02/13 15:00 to 20/04/13 16:00	53	3.0	11.5
14	39˚ 47.622	174˚ 30.056	1590	27/02/13 07:30 to 02/05/13 14:45	64	3.0	11.5
15	39˚ 39.728	174˚ 20.523	880	27/02/13 09:00 to 08/04/13 21:00	40	3.0	11.5
16	39˚ 35.994	174˚ 13.054	508	27/02/13 10:00 to 02/05/13 09:15	64	3.0	11.5

Additional information relating to the measurements at the mooring sites is shown in Table A-2 in Appendix A.

3.1.3 Surf-zone water sampling

Figure 3-4 shows the location of 11 sites that were selected for the surf-zone water sampling network. These are the few locations on the coast that can be accessed by public road.

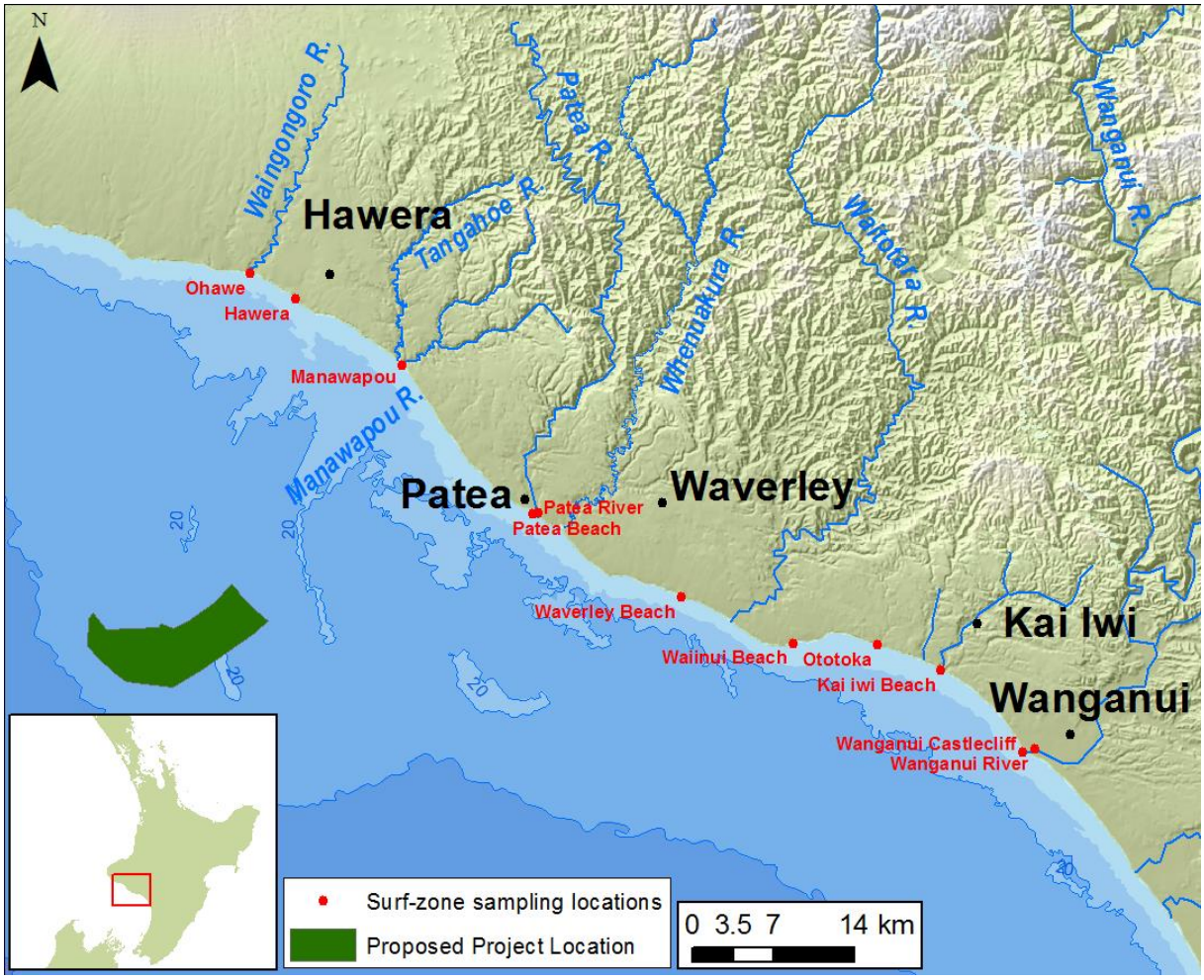

Figure 3-4: Site map showing the 11 sites selected for the surf-zone sampling.

Summary information relating to the surf-zone water sampling is shown in Table 3-4.

Table 3-4: Summary information for the surf-zone water sampling.

Surf-zone water sampling survey	Survey ID	Date	Number of samples collected
1	SZ1	23/04/2013	11
2	SZ2	18/07/2013	11
3	SZ3	05/08/2013	11

3.2 Conditions experienced during the study period

The sampling period spanned the late-summer to early-autumn period.

3.2.1 Winds

The long-term wind climate for the STB was derived from hourly observations at Spriggens Park (Wanganui) EWS over a 17-year period from March 1996 to June 2013. The wind rose is shown in Figure 3-5.

The mean wind speed over the 17-year period was 3.5 m/s, with a maximum of 19.0 m/s on 22 October 2003 from the S (160˚). The wind directions exhibit a bi-modal distribution, dominated by winds from the N and W.

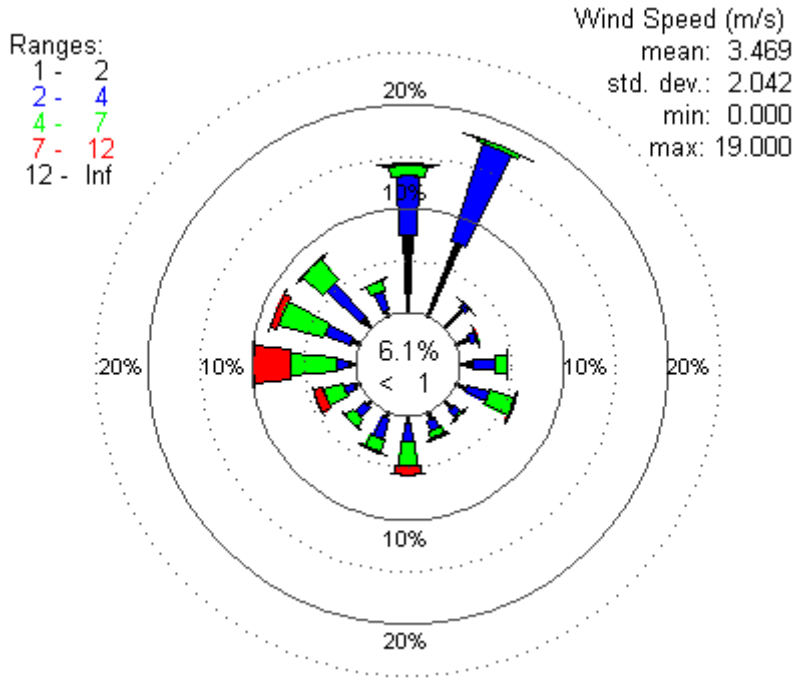

Figure 3-5: Wind rose for winds measured at Wanganui over a period of 17-years (March 1996 to June 2013). Meteorological convention is used in expressing the direction that the wind "blows from".

The wind rose for the deployment period (26 February 2013 to 02 May 2013) is shown in Figure 3-6. The mean wind speed over the deployment period was 2.8 m/s, which is less than the long term mean value of 3.5 m/s. The maximum wind speed during the deployment period was 9.8 m/s, which was reached on 4 March 2013 when the wind blew from the W (274˚). Overall, it was less windy during the deployment period (Feb-May) compared to the long term climate (cf. Figure 3-5 and Figure 3-6). However, the distribution of wind directions during the field deployment was similar to the long-term wind climate.

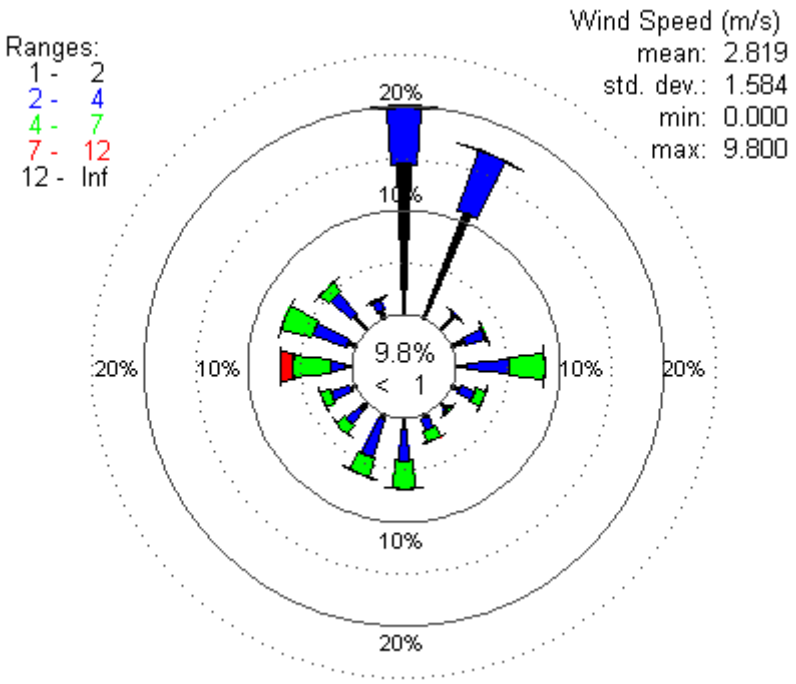

Figure 3-6: Wind rose for winds measured at Wanganui over the deployment period February 2013 to April 2013.

3.2.2 Rainfall and River flows

Table 3-5 provides a summary of the amount of rainfall that fell at Wanganui and Hawera during the 4-month period from January 2013 to April 2013. It compares the monthly rainfall to the long-term monthly averages, with the difference between the two expressed as the "Difference from normal (mm)". The table shows that for most of the deployment period the amount of rainfall that fell in the STB was less than normal. This is consistent with the drought being experienced by most of New Zealand at this time.

Table 3-5: Rainfall in the South Taranaki Bight for the 4-month period from January to April 2013 (source https://www.niwa.co.nz/climate/summaries).

Month	Wanganui			Hawera		
	Total fall (mm)	No. of Rain days	Difference from normal (mm)	Total fall (mm)	No. of Rain days	Difference from normal (mm)
January 2013	47	7	-12	70	9	-6
February 2013	64	3	-13	43	3	-30
March 2013	66	5	+3	20	7	-63
April 2013	57	15	-12	111	21	+28

Time series plots of river discharges at Paetawa (Wanganui River) and at Whenuakura (Whenuakura River) are shown in Figure 3-7A. The region bounded by the vertical red lines indicate the period in which the instruments were in the water. During the deployment period the flows at the two sites displayed very similar temporal patterns and, as one would expect, the times of increased river flows coincide with times of rain (cf. Figure 3-7A and Figure

3-7B). The blue and black horizontal dashed lines in Figure 3-7A show the long-term average flow at Paetawa and at Whenuakura, respectively. From the long-term averages it is apparent that the majority of the river flows during the deployment period were well below average.

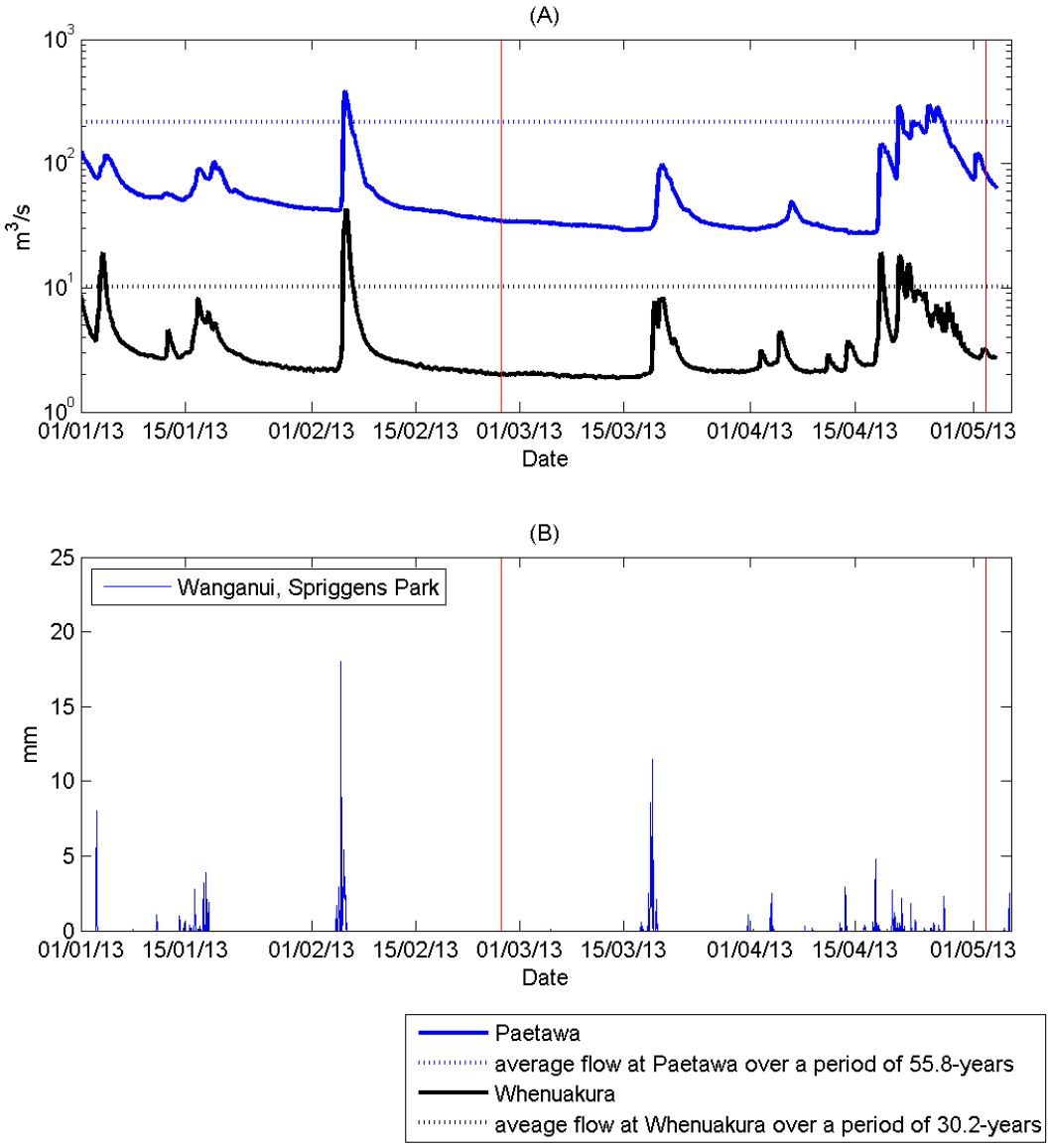

Figure 3-7: River flow and rainfall time series over the period 1/1/2013 to 2/5/2013. Regions bounded by the vertical red lines indicate the period over which the instruments were in the water. Panels show: (A) river flow at Paetawa (Wanganui River) and Whenuakura (Whenuakura River) and (B) hourly rainfall at Wanganui.

Additional summary information about the river flows at these two sites is shown in Table 3-6.

Table 3-6: Summary of river flows at Paetawa and Whenuakura.

Site	Deployment period			Long-term record		
	Mean flow (m^3/s)	Maximum flow (m^3/s)	Minimum flow (m^3/s)	Mean flow (m^3/s)	Maximum flow (m^3/s)	Minimum flow (m^3/s)
Paetawa	62.0	294.5 (24-Apr-2013)	27.6 (14-Apr-2013)	214.2	4100 (10-Mar-1990)	22.2 (15-Mar-1974)
Whenuakura	3.3	19.1 (18-Apr-2013)	1.9 (14-Mar-2013)	10.2	352.7 (16-Feb-2004)	0.9 (22-Nov-1995)

3.2.3 Summary of the conditions experienced during the study period

From Table 3-5 and Table 3-6 it is clear that deployment took place during a period of lower than expected rainfall for that time of the year, and consequently during a period of low river flows. Given that the rivers are likely to be the major source of fine sediments into the coastal environment it is likely that deployment took place during conditions that are representative of comparatively clear water conditions found in the STB.

3.3 Boat surveys

Time series of wind speed, wind direction and river flows in the period leading up to and including the boat surveys are shown in Figure 3-8. S1 was during a period of low river flows and wind speeds during this time were typically around 5 m/s (gentle breeze on the Beaufort scale), with a direction starting out as a southerly then swinging around to the east. During S2 the wind speed was typically less than 5 m/s (light breeze), starting out as an easterly then swinging around to the north. River flows during S2 were higher than those experienced during S1.

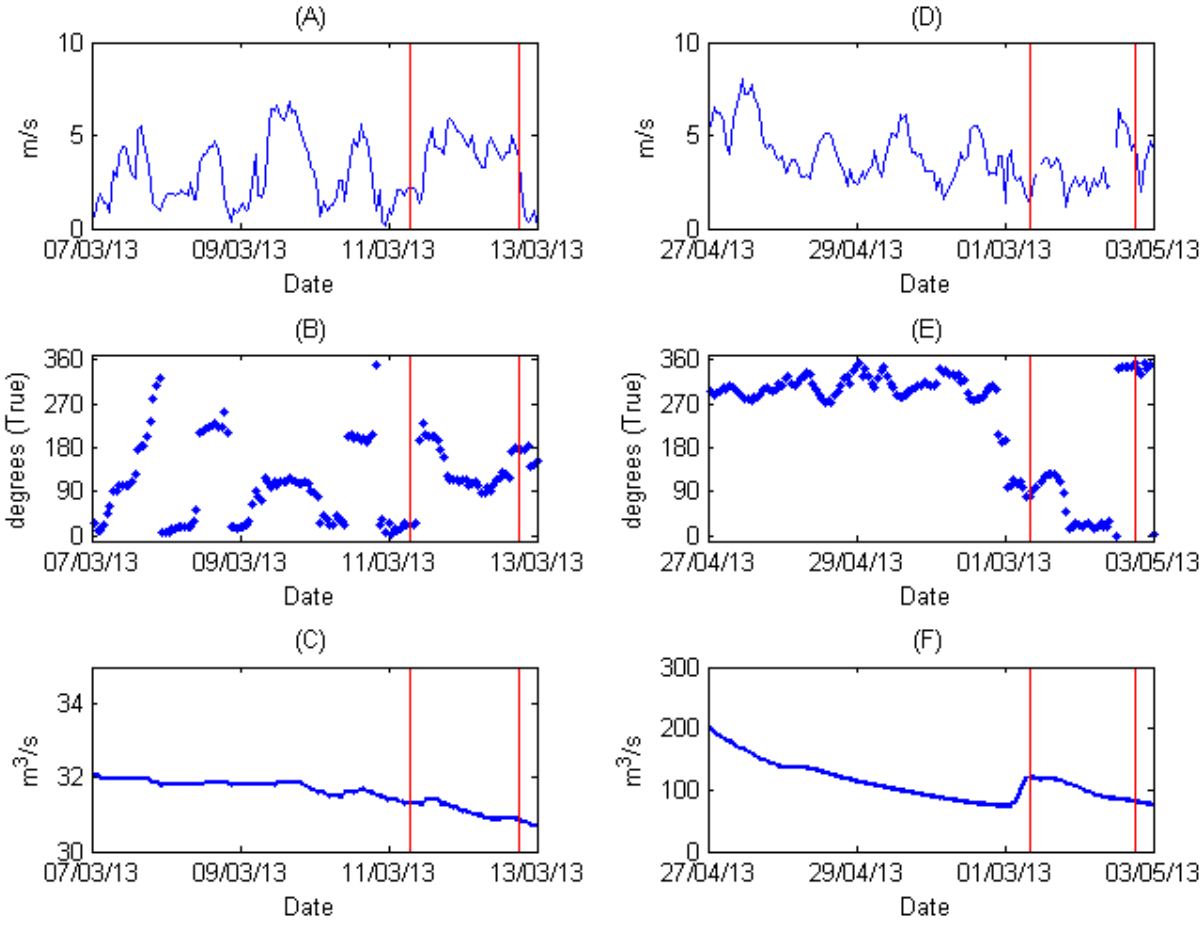

Figure 3-8: Wind and flow conditions around the times of the boat surveys. Panels (A to C) relate to S1, while panels (D to F) relate to S2. (A and D) wind speed, (B and E) wind direction, and (C and F) river flows at Paetawa. Regions bound by the vertical red lines indicate the periods during which the boat surveys took place.

3.3.1 Bio-Fish data

The measurements from the Bio-Fish are shown in this section in the form of:

- profiles plots which display the measured variables as a function of depth below the water surface, and
- bar plots of the profile data.

To aid with interpretation, the measured profiles of salinity (S), T_n, c_{530} and E_d (from which k_d was derived) for the 98 transects collected during S1 and S2 are shown in Appendix B (Figure B-1 to Figure B-17). The profile data shown in those figures are now used to explore the cross-shore and alongshore variability in SSC, y_{BD} and k_d.

Cross-shore variability

Figure 3-9 to Figure 3-11 displays bar plots of SSC, y_{BD} and k_d measured at locations SP3, SP8 and SP9 as a function of distance from the shoreline. In these figures the measured profile data are represented by the central mark (the solid dot) which corresponds to the

mean value, and by the "whiskers" which extend to the 25th and 75th percentiles. The interquartile[2] range gives an indication of the vertical variability in the measurements.

Figure 3-9 clearly shows a cross-shore gradient in SSC, y_{BD} and k_d. SSC and k_d are highest closest to the shoreline, and decrease appreciably with distance from the shore. Reflecting this, the visual clarity (y_{BD}) is greatest offshore, and decreases shoreward. This cross-shore gradient is also clearly evident in Figure 3-10 and Figure 3-11, and is in fact a consistent feature along the entire coastline of STB. For completeness, the cross-shore bar plots at SP1, SP2, SP4, SP5, SP6, SP7, SP9, SP10 and SP11 are shown in Figure B-18 to Figure B-26 in Appendix B.

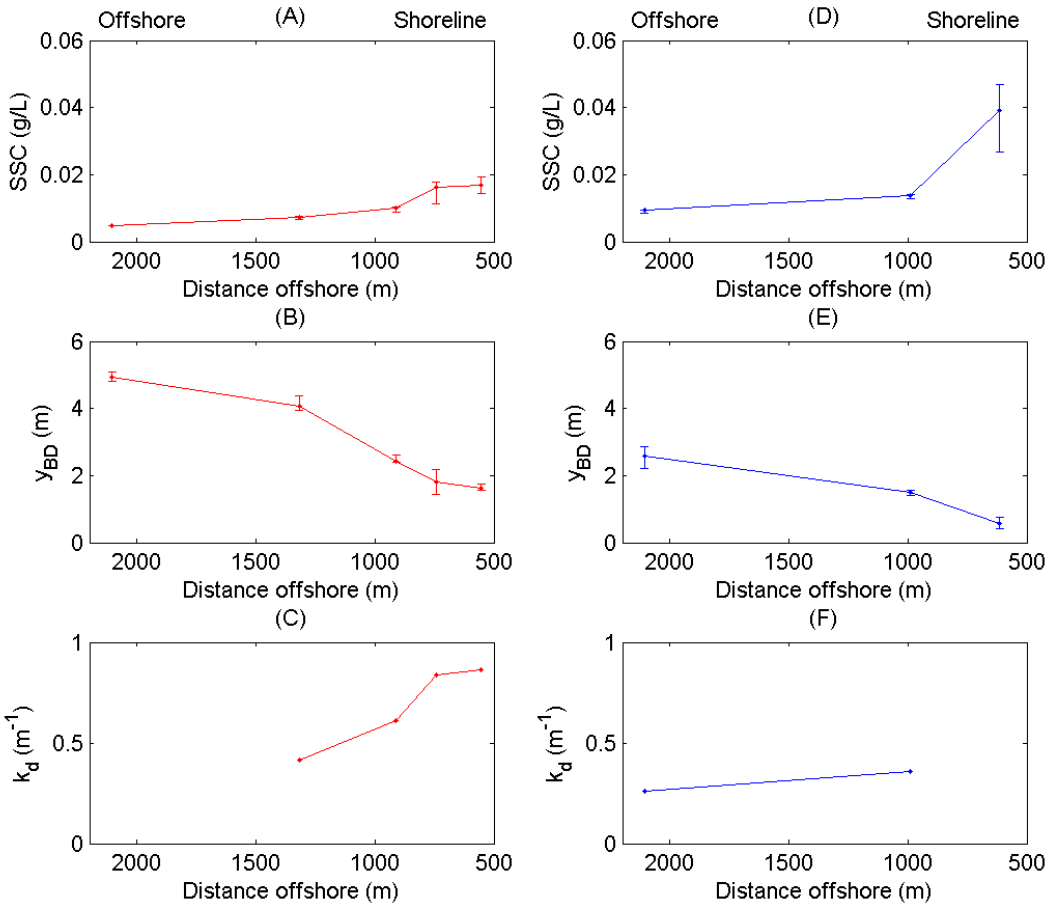

Figure 3-9: Cross-shore variability in SSC, y_{BD} and k_d at SP3. Panels: A to C relate to S1 and D to F relate to S2. (A and D) SSC, (B and E) y_{BD} and (C and F) k_d.

[2] The interquartile range is the difference between the 25th and 75th percentiles

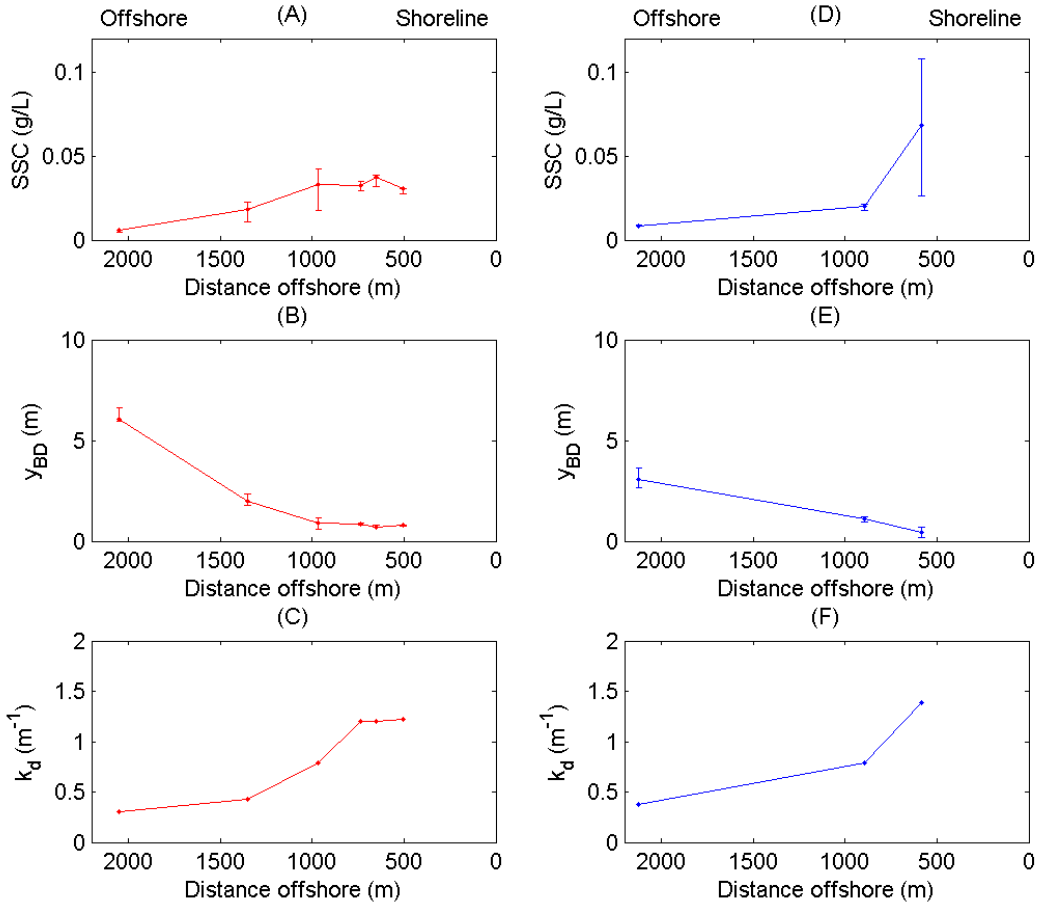

Figure 3-10: Cross-shore variability in SSC, y_{BD} and k_d at SP8. Panels: A to C relate to S1 and D to F relate to S2. (A and D) SSC, (B and E) y_{BD} and (C and F) k_d.

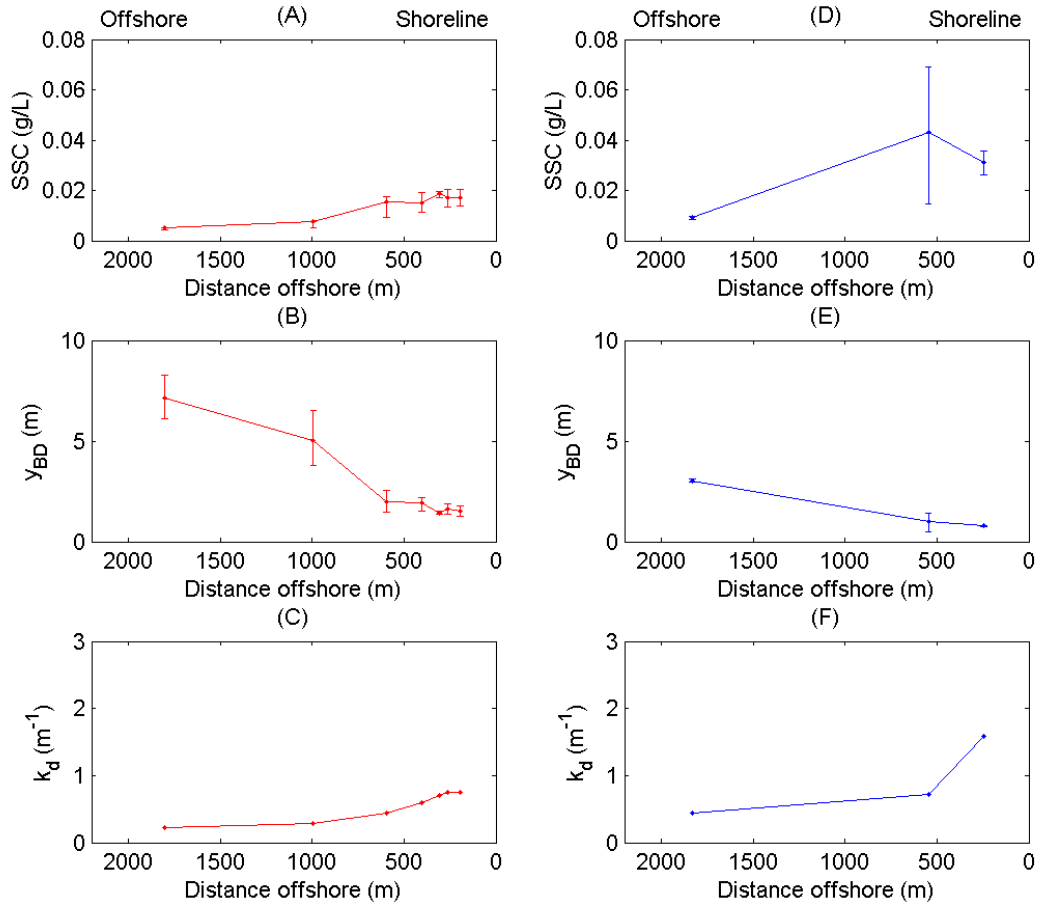

Figure 3-11: Cross-shore variability in SSC, y_{BD} and k_d at SP12. Panels: A to C relate to S1 and D to F relate to S2. (A and D) SSC, (B and E) y_{BD} and (C and F) k_d.

Alongshore variability

Figure 3-12 displays bar plots of SSC, y_{BD} and k_d from the measurements collected at the shoreward-most profile from each transect (e.g., profile # 11 for SP4). The measurements from both S1 and S2 are shown in this figure.

Figure 3-12 shows appreciably spatial variability in SSC, y_{BD} and k_d along the coast. With the data suggesting a reduction in SSC (and hence an increase in y_{BD} and a decrease in k_d) moving down the coast in a S SE direction (i.e., from SP12 to SP1). This feature is evident from the measurements taken during S1 and S2. The figure also shows that SSC and k_d were greater (y_{BD} lower) during S2 than during S1, probably as a result of higher river flows (and sediment loads). The maximum (averaged over the water column) SSC measured during S2 was 0.068 g/L at SP11 near Hawera.

Figure 3-12B shows that during S2 that the horizontal visibility along the study area was always less than 1 m.

In making this assessment of the alongshore variability we are assuming that the conditions remained approximately constant over the 36 hours that it took to complete each survey.

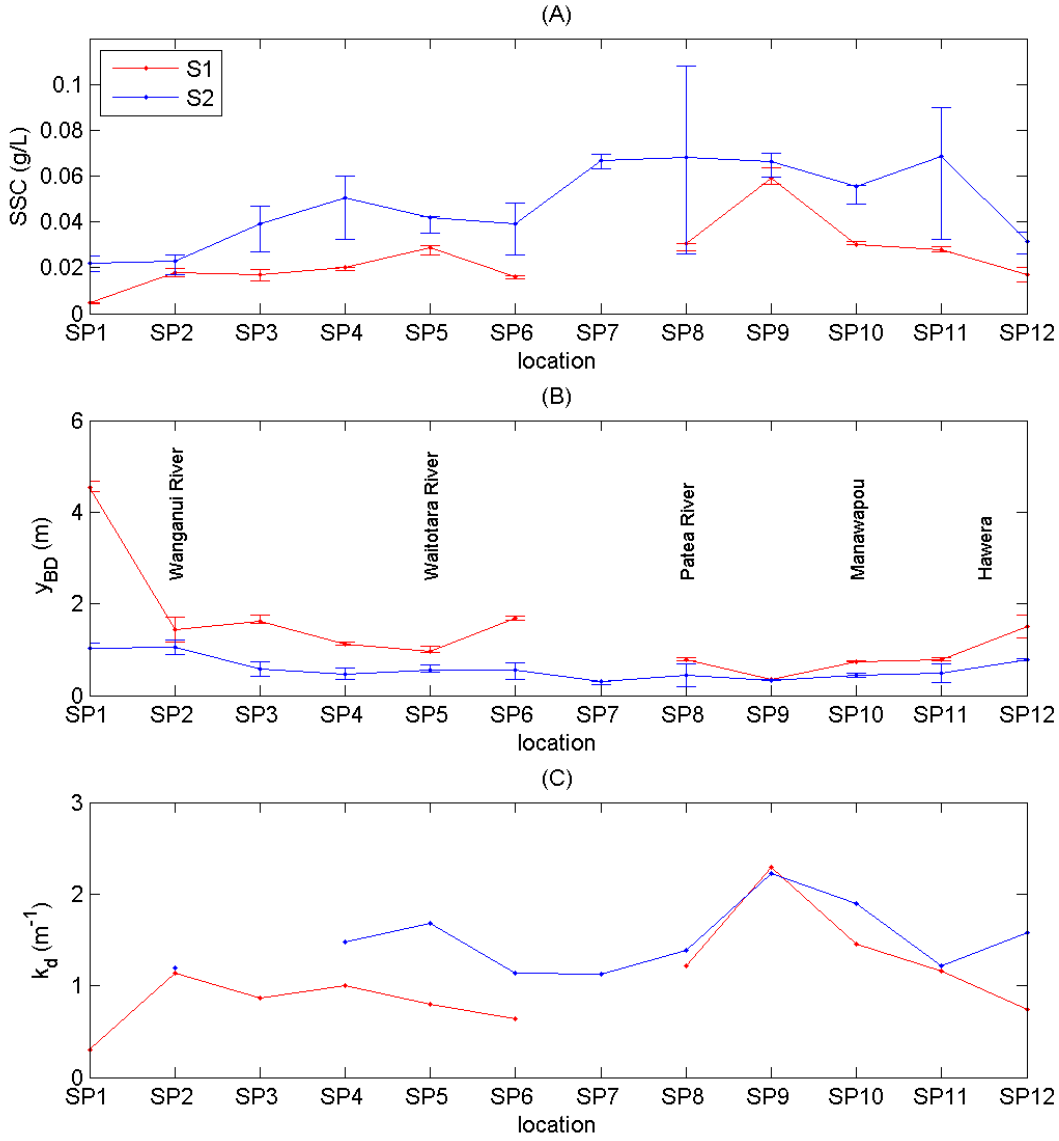

Figure 3-12: Alongshore variability in SSC, y_{BD} and k_d. Panels (A) SSC, (B) y_{BD} and (C) k_d. Note, no profile was collected at SP7 during S1 and the missing k_d values occur when a poor linear relationship between z and ln(E_d) was obtained (section 2.1.1).

3.3.2 Boat survey water sample results

The estimates for suspended sediment concentration (SSC), chlorophyll a concentration (Chl-a) and coloured dissolved organic matter (CDOM, indexed by g_{340}) derived from the analysis of the water samples collected during S1 and S2 are shown in Table 3-7 and Table 3-8, respectively.

Table 3-7 shows that for S1:

- SSC varied by more than an order of magnitude, from 0.0027 g/L to 0.0618 g/L, with a mean value of 0.0156 g/L. SSC was highest near the shore and decreased with distance offshore.

- g_{340} varied more than four-fold from 0.35 m^{-1} to 1.73 m^{-1}, with a mean value of 0.50 m^{-1}. The highest values came from the measurements taken in and at the mouth of the Wanganui River (Profiles 2 and 4). Typically, g_{340} was highest near the shore and decreased with distance offshore.
- Chl-a varied between 0.3 mg/m^3 and 2.4 mg/m^3, with a mean value of 1.0 mg/m^3. Typically, Chl-a was highest near the shore and decreased with distance offshore.

Table 3-7: Water sample results from boat survey 1 (S1). Note, profile number 2 has a negative offshore distance as this profile was collected in the Wanganui River at the wharf, which is inland from the assumed shoreline position.

Survey	Shoreline position	Profile number	Distance Offshore (m)	SSC (g/L)	Chl-a (mg/m^3)	g_{340} (m^{-1})
S1	SP1	1	1429	0.0036	0.4	0.35
S1	SP2	2	-1059	0.0179	1.3	1.73
S1	SP2	4	1160	0.0114	1.0	1.21
S1	SP3	5	553	0.0153	1.2	0.40
S1	SP3	8	1273	0.0062	0.8	0.40
S1	SP3	10	2106	0.0033	0.9	0.40
S1	SP4	11	351	0.0235	1.4	0.40
S1	SP4	16	1872	0.0040	0.6	0.35
S1	SP5	17	452	0.0479	1.9	0.46
S1	SP5	21	944	0.0132	1.4	0.40
S1	SP5	23	2055	0.0073	0.6	0.35
S1	SP6	24	371	0.0272	1.2	0.52
S1	SP6	29	1941	0.0069	0.6	0.35
S1	SP7	30	1730	0.0150	0.7	0.29
S1	SP8	31	506	0.0231	1.5	0.46
S1	SP8	36	2049	0.0083	0.7	0.52
S1	SP9	37	276	0.0618	2.4	0.58
S1	SP9	42	1953	0.0093	1.0	0.40
S1	SP10	43	236	0.0343	0.8	0.58
S1	SP10	47	840	0.0141	1.1	0.52
S1	SP10	49	1812	0.0042	0.8	0.40
S1	SP11	50	234	0.0251	1.3	0.46
S1	SP11	55	1812	0.0037	0.6	0.46
S1	SP12	56	193	0.0076	0.5	0.40
S1	SP12	60	492	0.0081	0.7	0.35
S1	SP12	63	1801	0.0027	0.3	0.35

Table 3-8 shows that for S2:

- SSC varied more than an order of magnitude from 0.0028 g/L to 0.0626 g/L, with a mean value of 0.0182 g/L. SSC was highest near the shore and decreased with distance offshore.
- g_{340} varied seventeen-fold from 0.20 m^{-1} to 3.50 m^{-1}, with a mean value of 0.74 m^{-1}. As with S1, the g_{340} values measured in and at the mouth of the Wanganui River (profiles 68 and 69) were elevated compared to the rest of the STB. Typically, g_{340} was highest near the shore and decreased with distance offshore.
- Chl-a varied between 0.9 mg/m^3 and 3.5 mg/m^3, with a mean value of 1.9 mg/m^3. Typically, Chl-a was highest near the shore and decreased with distance offshore.

Table 3-8: Water sample results from boat survey 2 (S2). Note, profile number 68 has a negative offshore distance as this profile was collected in the Wanganui River at the wharf, which is inland from the assumed shoreline position.

Survey	Shoreline position	Profile number	Distance Offshore (m)	SSC (g/L)	Chl-a (mg/m^3)	g_{340} (m^{-1})
S2	SP1	64	879	0.0145	2.5	0.40
S2	SP1	66	1511	0.0081	1.9	0.35
S2	SP1	67	2558	0.0048	1.6	0.35
S2	SP2	68	-1059	0.0416	1.5	3.50
S2	SP2	69	690	0.0128	1.7	1.32
S2	SP2	71	2202	0.0066	1.3	0.29
S2	SP3	72	615	0.0202	2.7	0.34
S2	SP3	74	1267	0.0116	1.7	0.22
S2	SP3	75	2107	0.0052	1.9	0.35
S2	SP4	76	308	0.0245	1.6	0.28
S2	SP5	77	410	0.0367	3.5	0.35
S2	SP5	79	952	0.0176	2.4	0.35
S2	SP5	80	2092	0.0028	0.9	0.40
S2	SP6	81	360	0.0199	1.4	0.52
S2	SP7	82	712	0.0157	2.4	0.40
S2	SP7	84	1570	0.0119	1.4	0.46
S2	SP7	85	2109	0.0041	1.2	0.29
S2	SP8	86	584	0.0187	2.5	0.46
S2	SP8	88	2122	0.0064	1.2	0.41
S2	SP9	89	248	0.0626	2.9	0.59
S2	SP10	90	379	0.0374	2.1	0.41
S2	SP10	92	892	0.0300	1.7	0.30
S2	SP10	93	1812	0.0110	1.3	0.41

Survey	Shoreline position	Profile number	Distance Offshore (m)	SSC (g/L)	Chl-a (mg/m^3)	g_{340} (m^{-1})
S2	SP11	94	445	0.0228	2.4	0.37
S2	SP12	95	244	0.0276	1.8	0.46
S2	SP12	97	554	0.0100	1.8	0.39
S2	SP12	98	1832	0.0073	1.5	0.20

Particle Size Distribution

The PSDs of the suspended sediments that were collected in the water samples during the boat surveys are shown in Figure 3-13. It is worth noting that the majority of the water samples collected had insufficient sediment mass to accurately measure the PSD. The ones that did have sufficient mass are shown in Figure 3-13.

The PSDs shown in Figure 3-13 all display a unimodal distribution, with peaks around 0.02 mm (fine to medium silt).

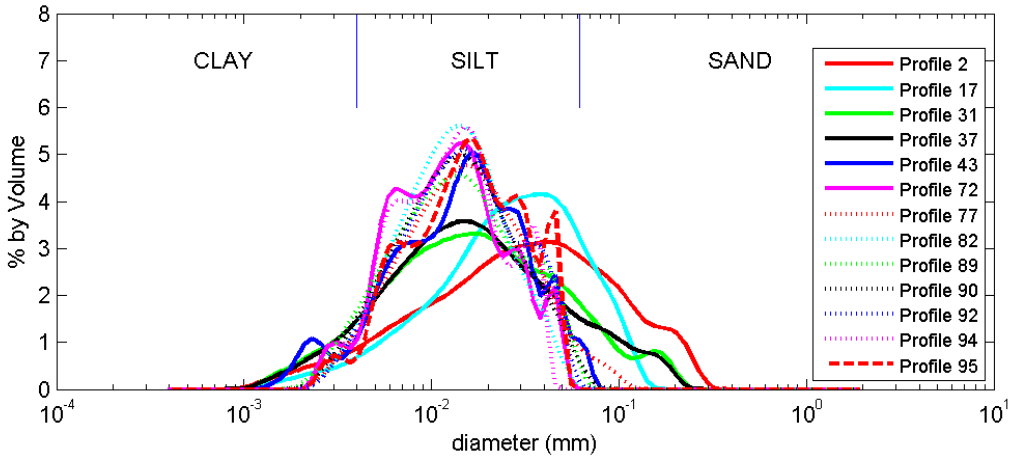

Figure 3-13: Particle size distibution of the suspended sediments.

Particle absorption spectra

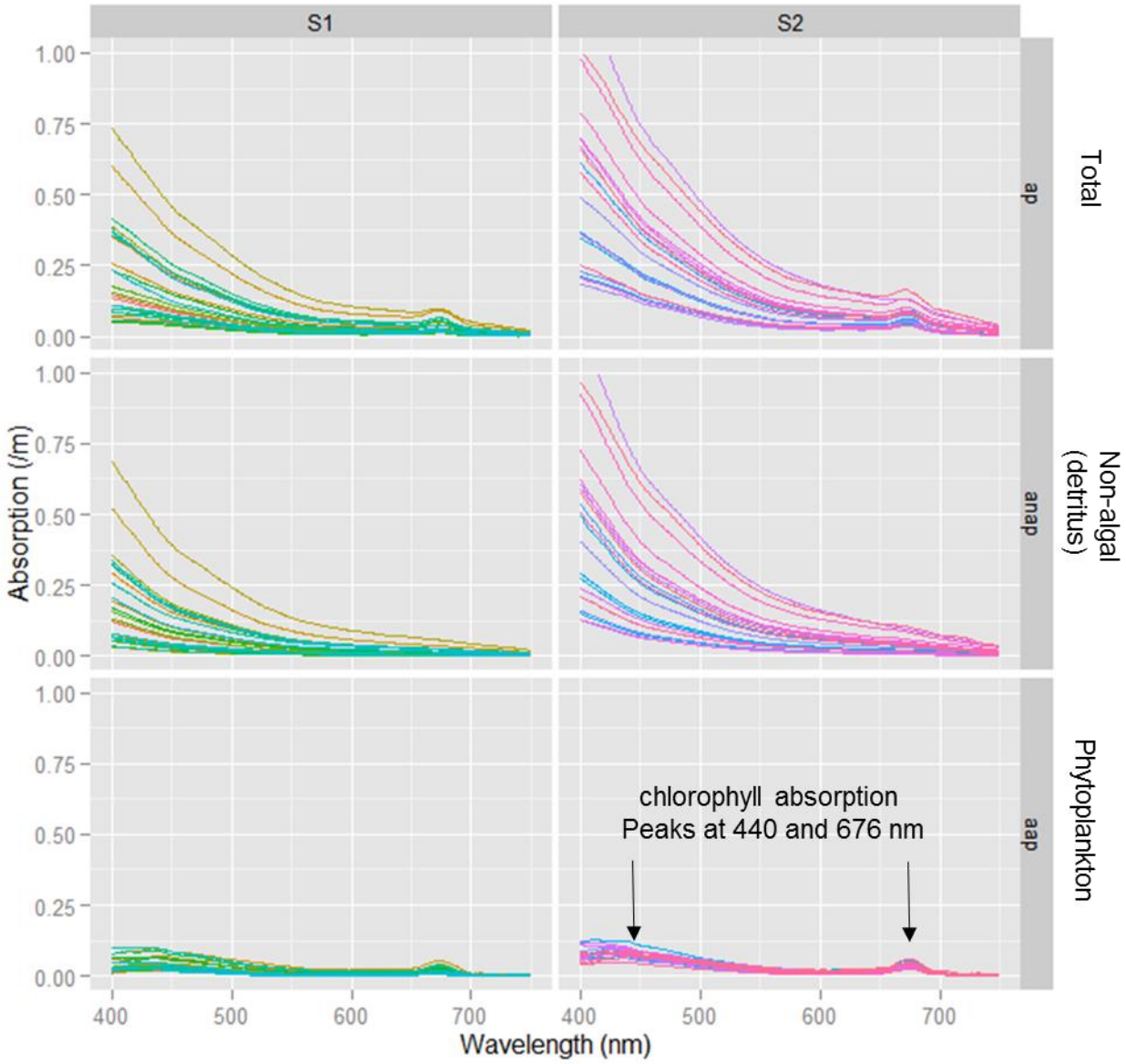

Figure 3-14: Absorption spectra. List of symbols: S1 = survey 1, S2 = survey 2, a_p = particle absorption, a_{nap} = absorption by non-algal particles and a_{ap} = absorption by algal particles.

Figure 3-14 shows the absorption spectra obtained from the PABS analysis (section 2.1.2). The top row of panels in Figure 3-14 displays estimates of the total particle absorption (a_p). The variability shown in the a_p spectra is expected, and result from spatial variability in the concentrations of the absorbing constituents (e.g., CDOM). The middle and bottom rows present the results from partitioning the total particulate matter absorption into the absorption due to non-algal particles (a_{nap}) and the absorption due to algal particles (a_{ap}). From these plots it evident that the non-algal matter is responsible for the majority of the total absorption. There are also some differences between surveys, illustrating temporal variability.

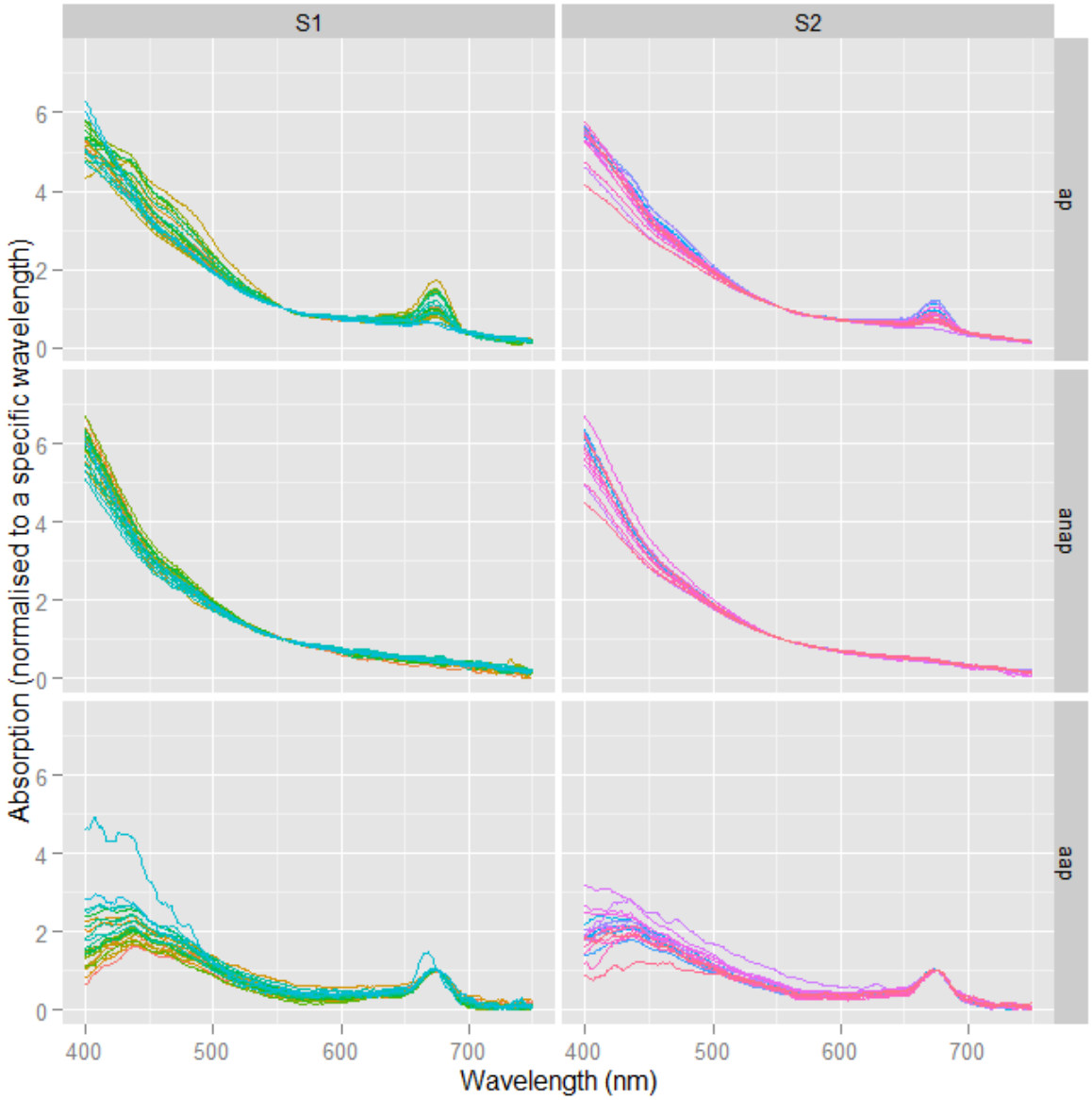

Figure 3-15: Normalised absorption spectra. List of symbols: S1 = survey 1, S2 = survey 2, a_p = particle absorption, a_{nap} = absorption by non-algal particles and a_{ap}=absorption by algal particles.

Figure 3-15 shows absorption spectra normalised to a specific wavelength (550 nm). This provides perspective on how the changes in the shape of spectra may influence beam attenuation and light penetration. There is little variation (especially below 500 nm) in the normalised spectra for both a_p and a_{nap}, indicating that the absorption characteristics of constituents does not vary significantly throughout the STB (at least relative to concentration changes).The a_p shape varies slightly more and could be due to spatial variability in species and algal size differences, but these differences are relatively minor compared to concentration changes.

3.4 Moored deployment

In this section estimates of turbidity (T_n), SSC (suspended sediment concentration), k_d (diffuse light attenuation coefficient) and y_{BD} (from c_{530}) from the 6 moored deployment sites are presented. Details about the locations, periods and sampling schemes relating to these measurements can be found in Table 3-3 and in Table A-2 in Appendix A.

In this section all data are presented as burst (time) averages rather than instantaneous values.

3.4.1 Site 11 (Wanganui)

Time series plots for site 11 are shown in Figure 3-16 and Figure 3-17.

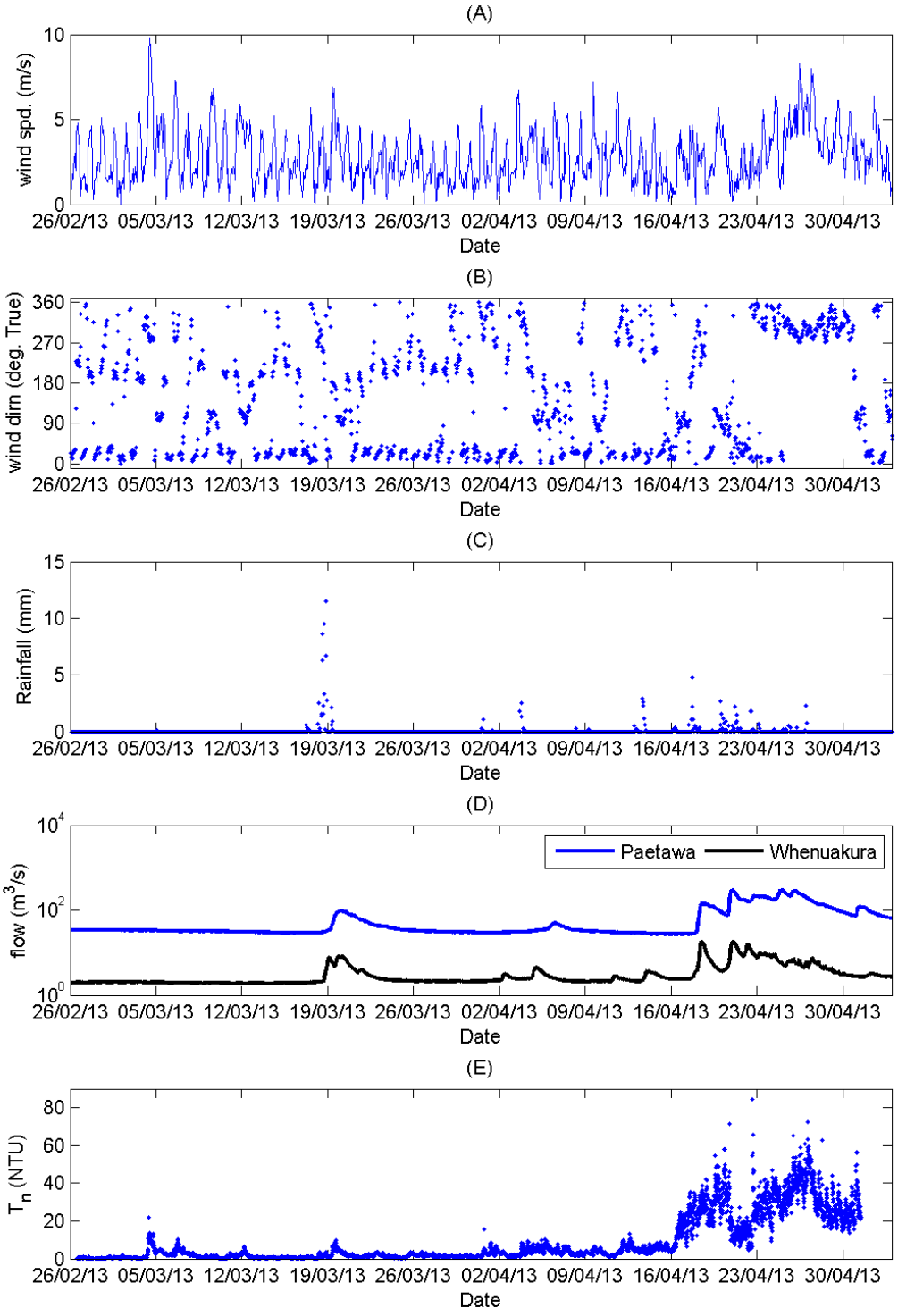

Figure 3-16: Time series of wind speed, direction, rainfall, river flows and turbidity at Site 11. Panels show: (A) wind speed, (B) wind direction (in meteorological convention "blowing from"), (C) rainfall, (D) river flows and (E) turbidity.

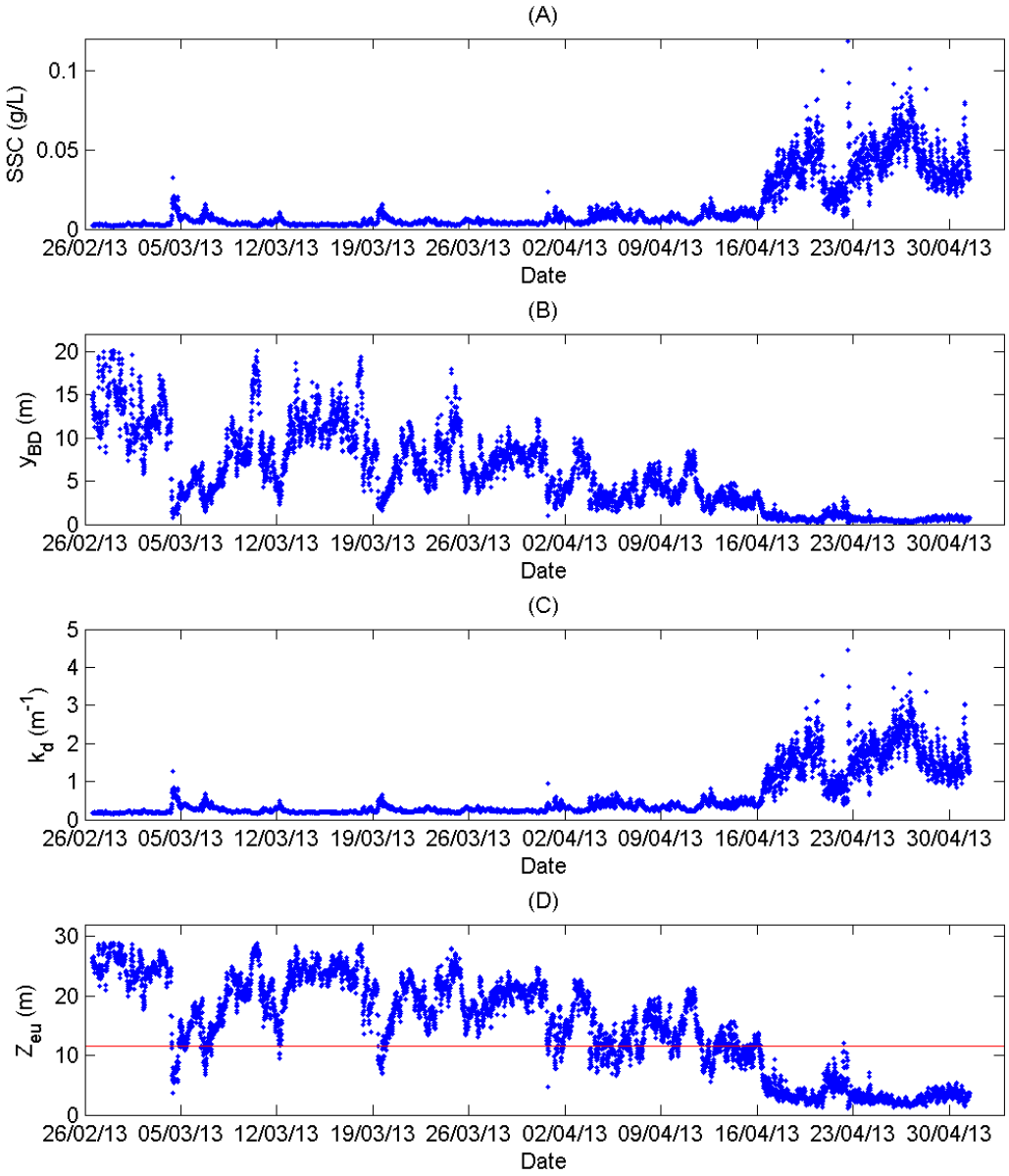

Figure 3-17: Time series of SSC and optical variables at Site 11. Panels show: (A) SSC, (B) y_{BD} (C) k_d and (D) euphotic depth (Z_{eu}) (red line mean water depth).

At site 11, the estimates of T_n, SSC, k_d, and y_{BD} all showed considerable temporal variability. During the last two weeks of the deployment period there was a significant increase in turbidity. A comparison of Figure 3-16D and Figure 3-16E shows that the increased turbidity coincided with times of increased river flow. It is likely at these times that the rivers were discharging fine sediments into the STB, which were then being transported in suspension through the measurement site.

Some of the peaks in turbidity also coincided with times of high wind speed, e.g., see the period of high winds that occurred around 05/03/13. This peak in turbidity is most likely to be wave-driven; note that this peak occurred during a long dry period, so it cannot be explained by the input of fines into the STB from rivers. At these times, wave stirring is entraining fine sediments from the sea floor, which are subsequently being mixed into the water column.

The red line in Figure 3-17D plots the mean water level at site 11. During the wave and river events, the euphotic depth (Z_{eu}) is less than the water depth, meaning that less than 1% of the ambient light is reaching the benthos.

3.4.2 Site 12 (Kai iwi)

Time series plots for site 12 are shown in Figure 3-18 and Figure 3-19.

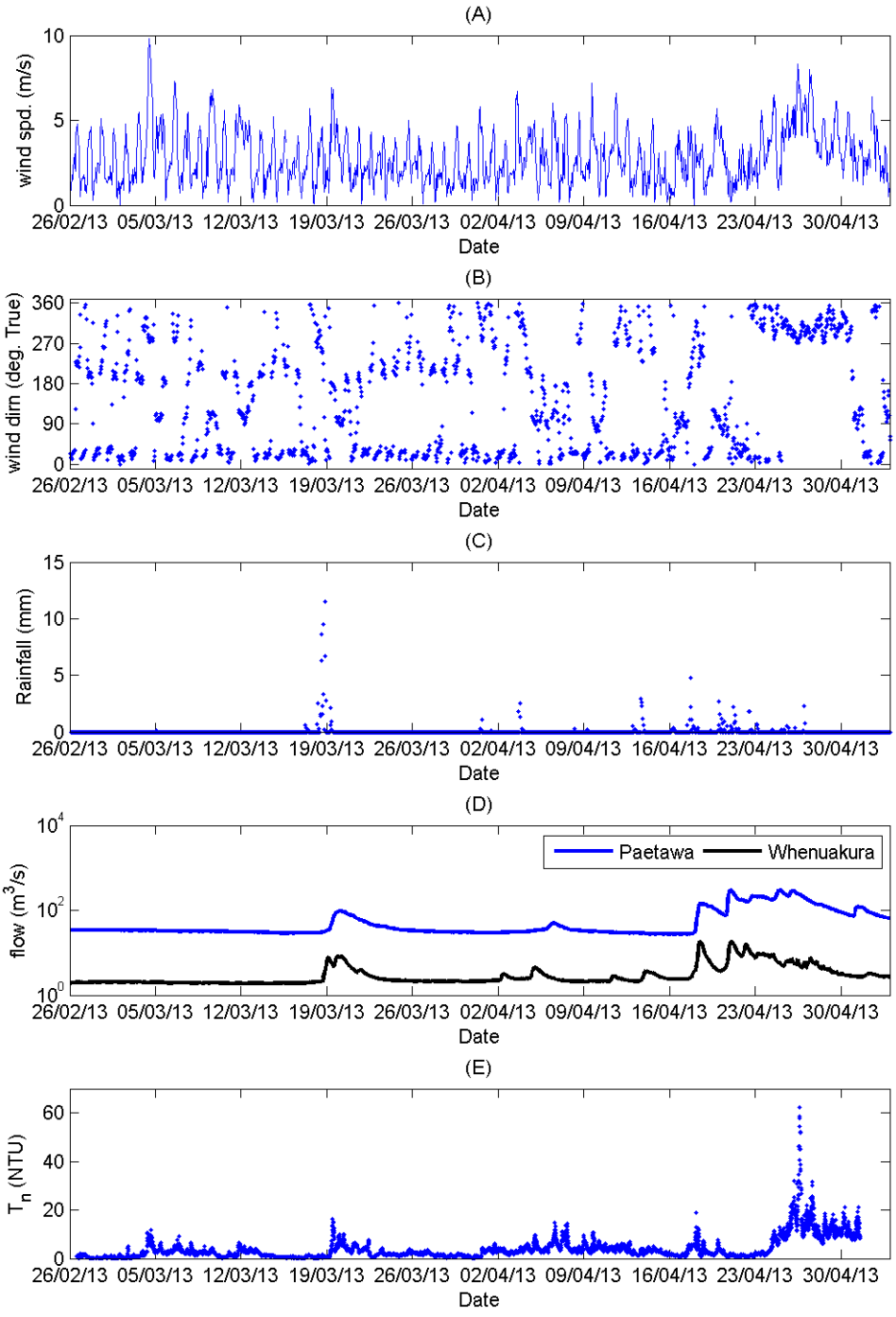

Figure 3-18: Time series of wind speed, direction, rainfall, river flows and turbidity at Site 12. Panels show show: (A) wind speed, (B) wind direction (in meteorological convention "blowing from"), (C) rainfall, (D) river flows and (E) turbidity.

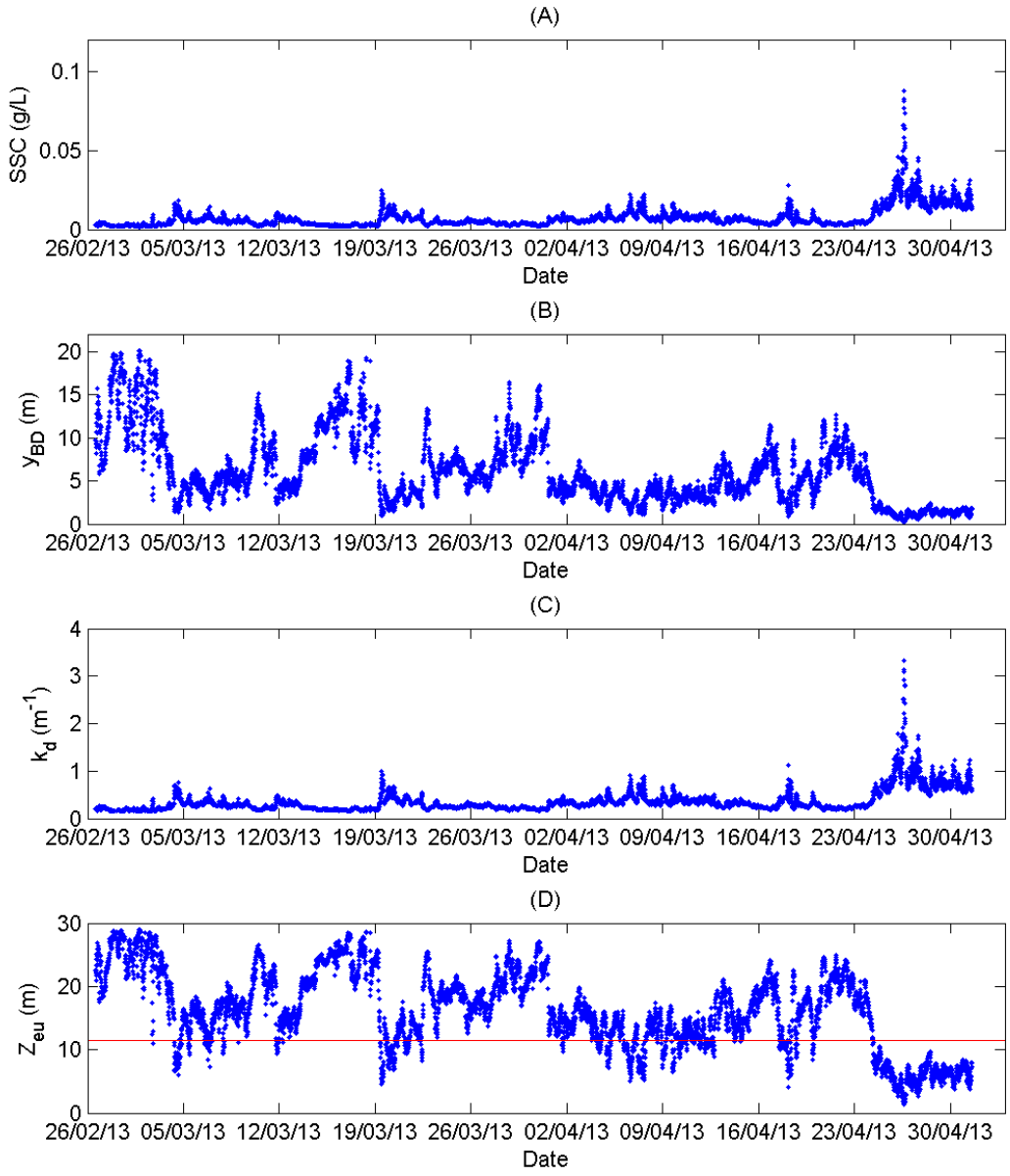

Figure 3-19: Time series of SSC and optical variables at Site 12. Panels show: (A) SSC, (B) y_{BD} (C) k_d and (D) euphotic depth (Z_{eu}) (red line mean water depth).

At site 12, the estimates of T_n, SSC, k_d, and y_{BD} all showed considerable temporal variability. As with site 11 the periods of increased turbidity are driven by the discharge of fine sediments from nearby rivers and by the resuspension of fines by wave action.

The red line in Figure 3-19D plots the mean water level at site 12. During the wave and river events, the euphotic depth (Z_{eu}) is less than the water depth, meaning that less than 1% of the ambient light is reaching the benthos.

3.4.3 Site 13 (Waitotara River)

Time series plots for site 13 are shown in Figure 3-20 and Figure 3-21.

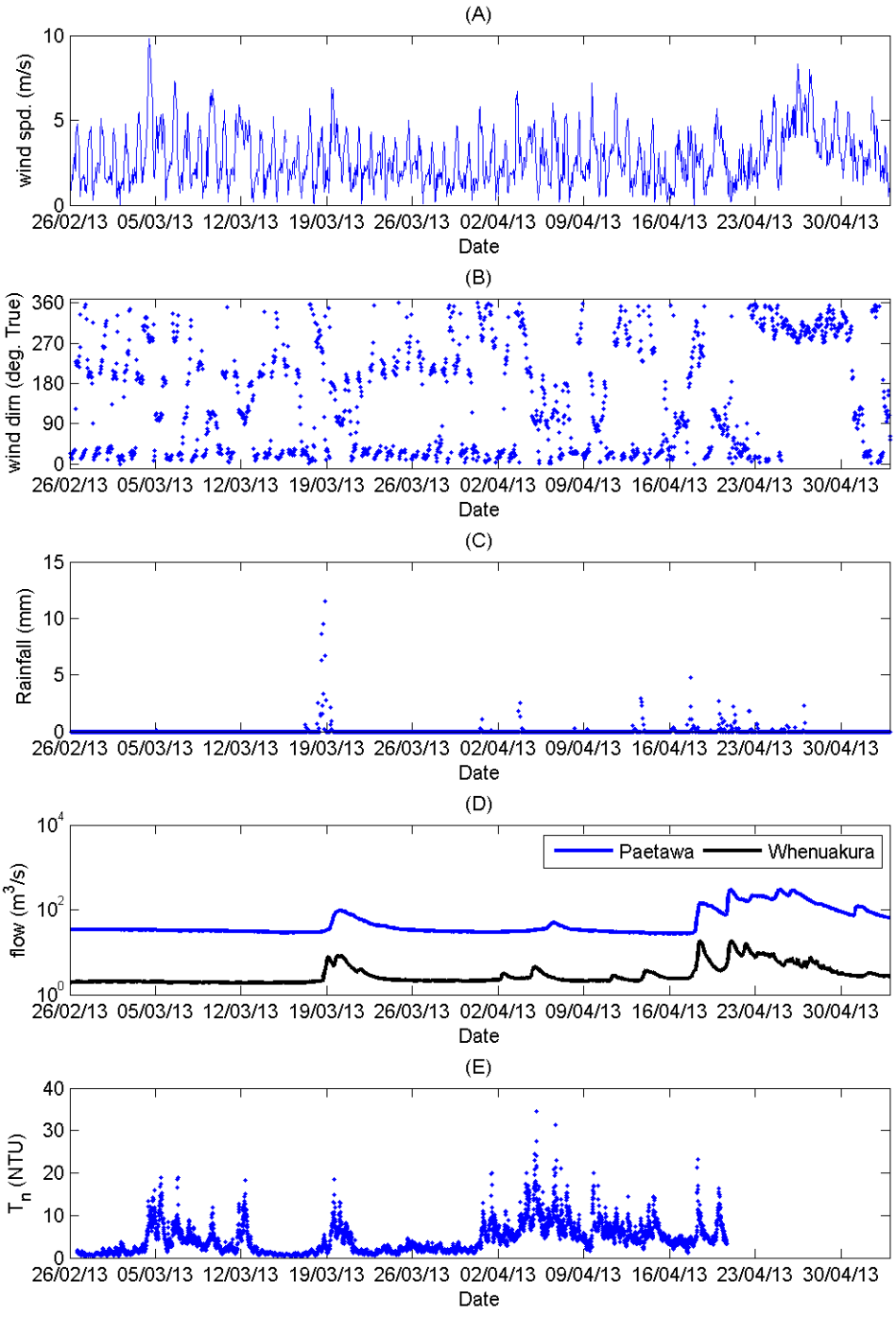

Figure 3-20: Time series of wind speed, direction, rainfall, river flows and turbidity at Site 13. Panels show: (A) wind speed, (B) wind direction (in meteorological convention "blowing from"), (C) rainfall, (D) river flows and (E) turbidity. The record at site 13 ended earlier than anticipated as a resut of an unexpected memory issue.

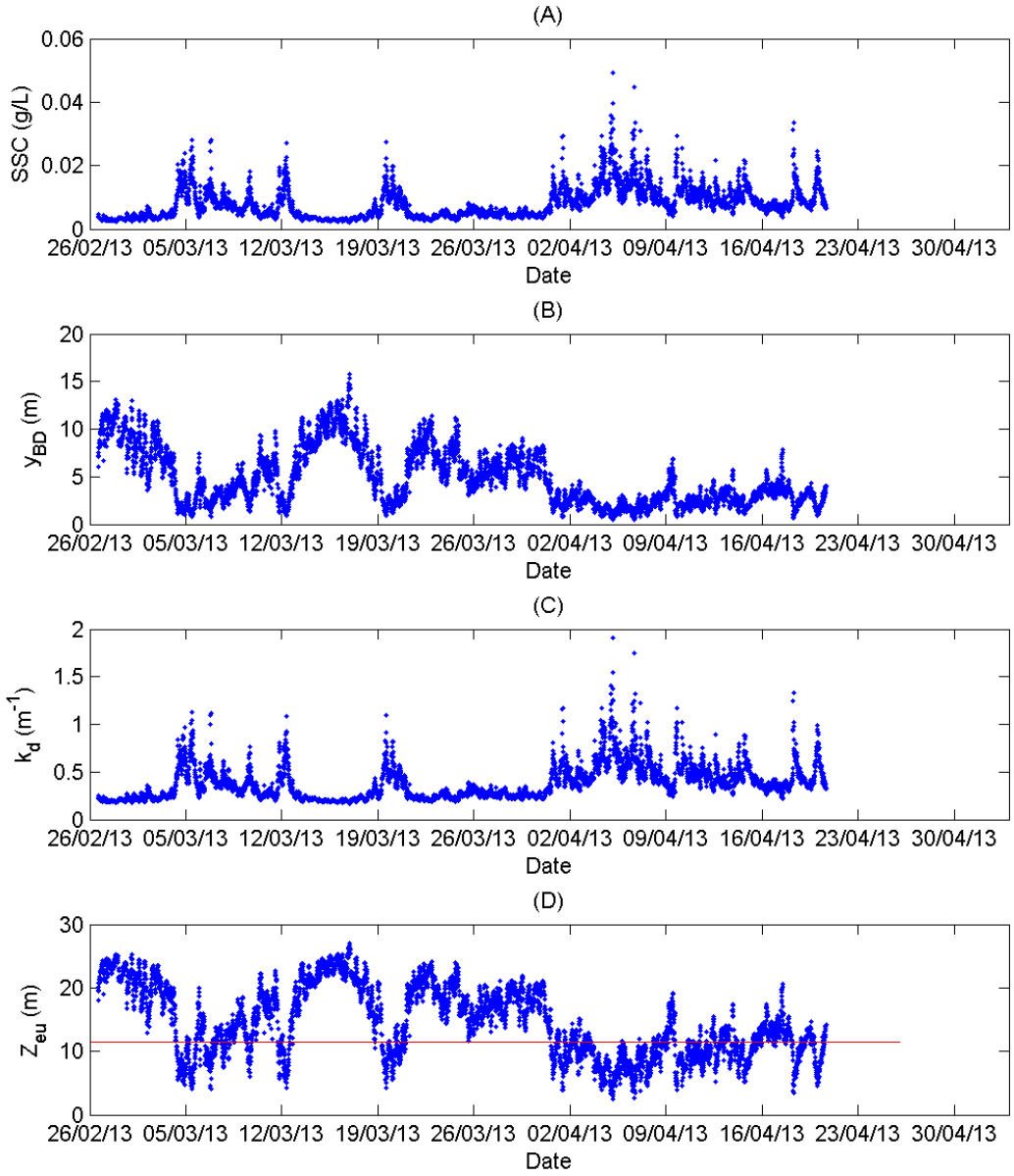

Figure 3-21: Time series of SSC and optical variables at Site 13. Panels show: (A) SSC, (B) y_{BD} (C) k_d and (D) euphotic depth (Z_{eu}) (red line mean water depth). The record at site 13 ended earlier than anticipated as a resut of an unexpected memory issue.

At site 13, the estimates of T_n, SSC, k_d, and y_{BD} all showed considerable temporal variability. As with the previous sites, the periods of increased SSC are driven by the discharge of fine sediments from nearby rivers and by the resuspension of fines by wave action.

The red line in Figure 3-21D plots the mean water level at site 13. During the wave and river events, the euphotic depth (Z_{eu}) is less than the water depth, meaning that less than 1% of the ambient light is reaching the benthos.

3.4.4 Site 14 (Patea)

Time series plots for site 14 are shown Figure 3-22 in and Figure 3-23.

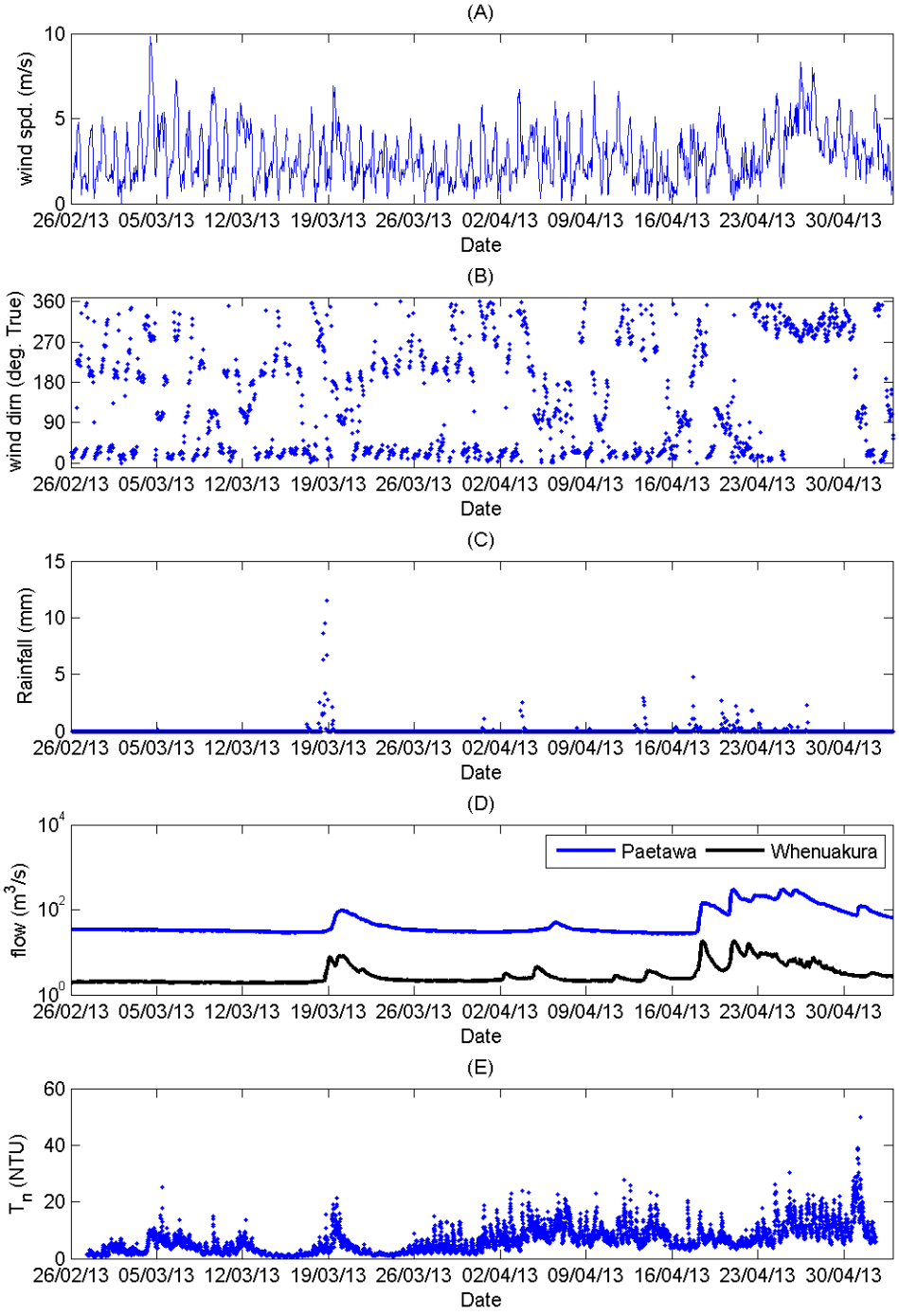

Figure 3-22: Time series of wind speed, direction, rainfall, river flows and turbidity at Site 14. Panels show: (A) wind speed, (B) wind direction (in meteorological convention "blowing from"), (C) rainfall, (D) river flows and (E) turbidity.

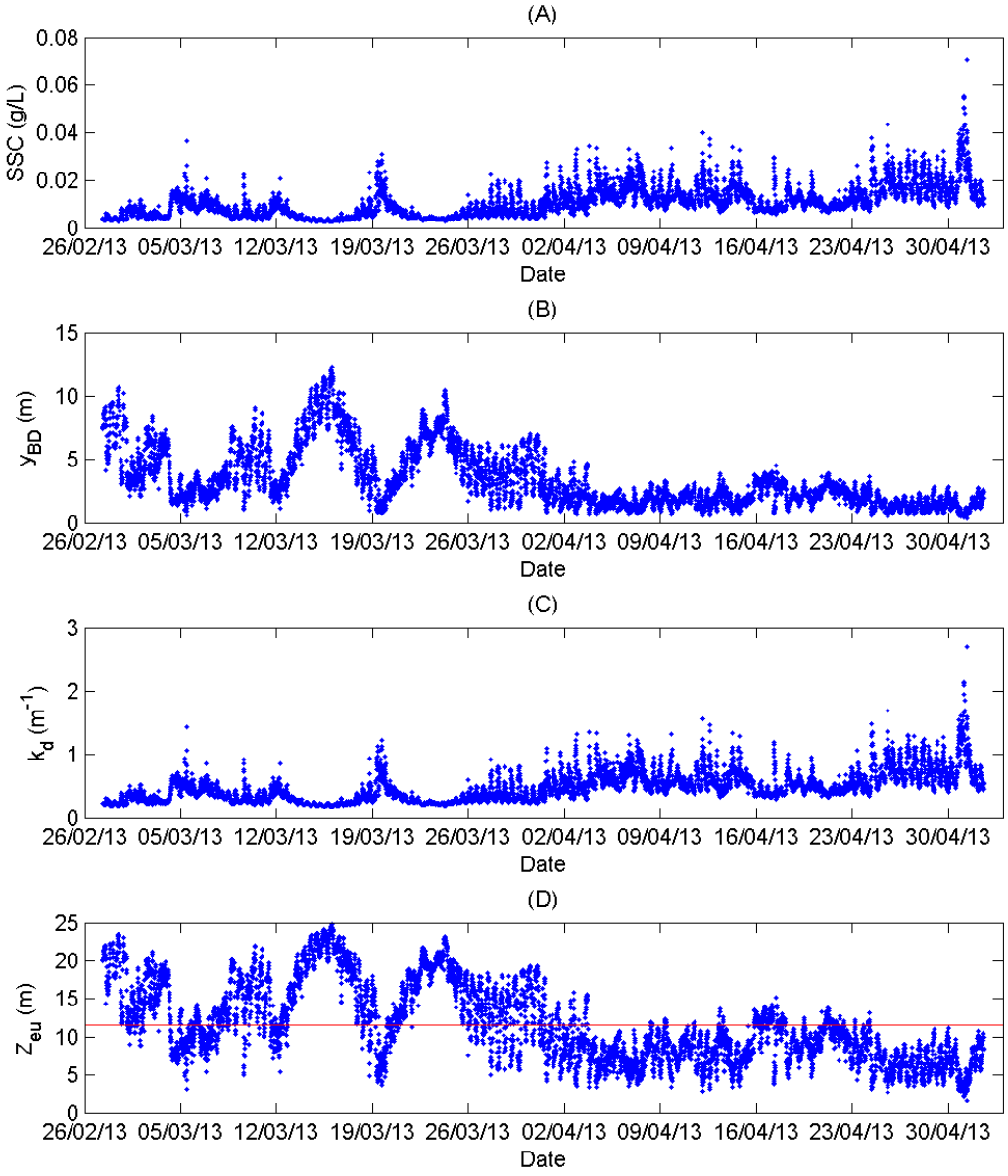

Figure 3-23: Time series of SSC and optical variables at Site 14. Panels show: (A) SSC, (B) y_{BD} (C) k_d and (D) euphotic depth (Z_{eu}) (red line mean water depth).

At site 14, the estimates of T_n, SSC, k_d, and y_{BD} all showed considerable temporal variability. As with the previous sites, the periods of increased SSC are driven by the discharge of fine sediments from nearby rivers and by the resuspension of fines by wave action.

The red line in Figure 3-23D plots the mean water level at site 14. During the wave and river events, the euphotic depth (Z_{eu}) is less than the water depth, meaning that less than 1% of the ambient light is reaching the benthos.

3.4.5 Site 15 (Manawapou)

Time series plots for site 15 are shown in Figure 3-24 and Figure 3-25.

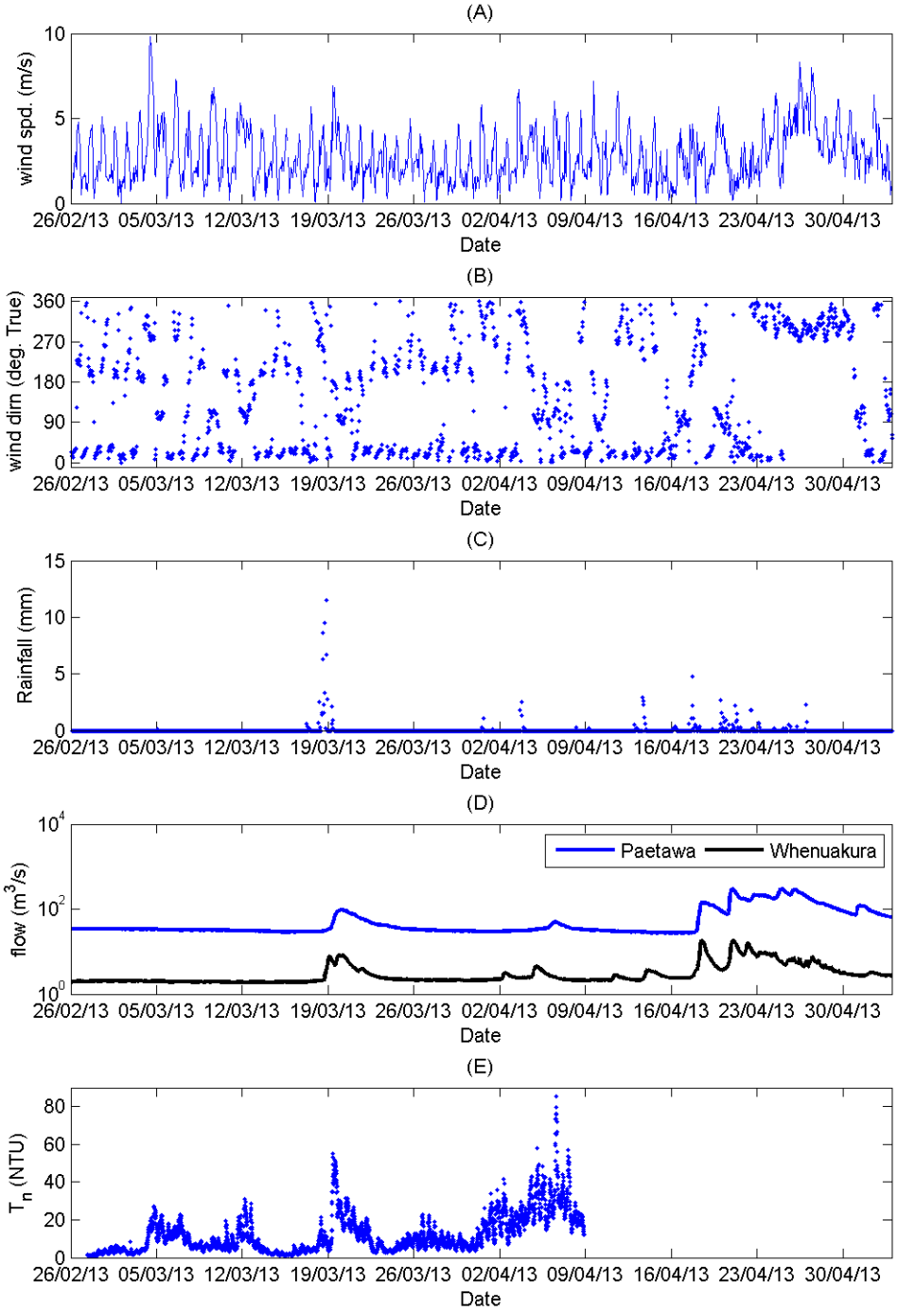

Figure 3-24: Time series of wind speed, direction, rainfall, river flows and turbidity at Site 15. Panels show: (A) wind speed, (B) wind direction (in meteorological convention "blowing from"), (C) rainfall, (D) river flows and (E) turbidity. The record at site 15 ended earlier than anticipated as a resut of an unexpected memory issue.

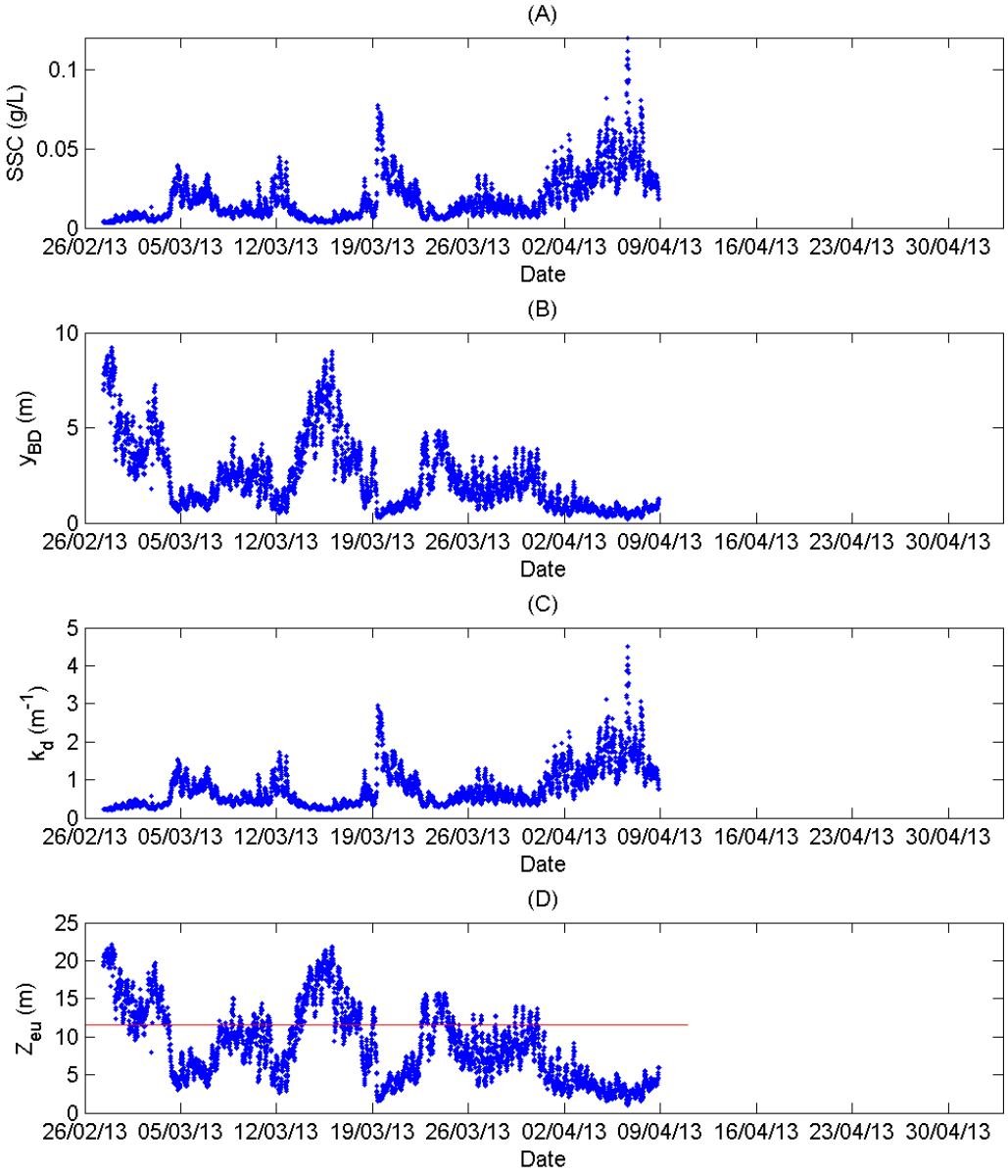

Figure 3-25: Time series of SSC and optical variables at Site 15. Panels show: (A) SSC, (B) y_{BD} (C) k_d and (D) euphotic depth (Z_{eu}) (red line mean water depth). The record at site 15 ended earlier than anticipated as a resut of an unexpected memory issue.

Despite the shorter record at site 15, the estimates of T_n, SSC, k_d, and y_{BD} all showed considerable temporal variability. As with the previous sites, the periods of increased turbidity are driven by the discharge of fine sediments from nearby rivers (see event around 19/03/13) and by the resuspension of fines by wave action (see event around 05/03/13).

The red line in Figure 3-25D plots the mean water level at site 15. During the wave and river events, the euphotic depth (Z_{eu}) is less than the water depth, meaning that less than 1% of the ambient light is reaching the benthos.

3.4.6 Site 16 (Ohawe)

Time series plots for site 16 are shown in Figure 3-26 and Figure 3-27.

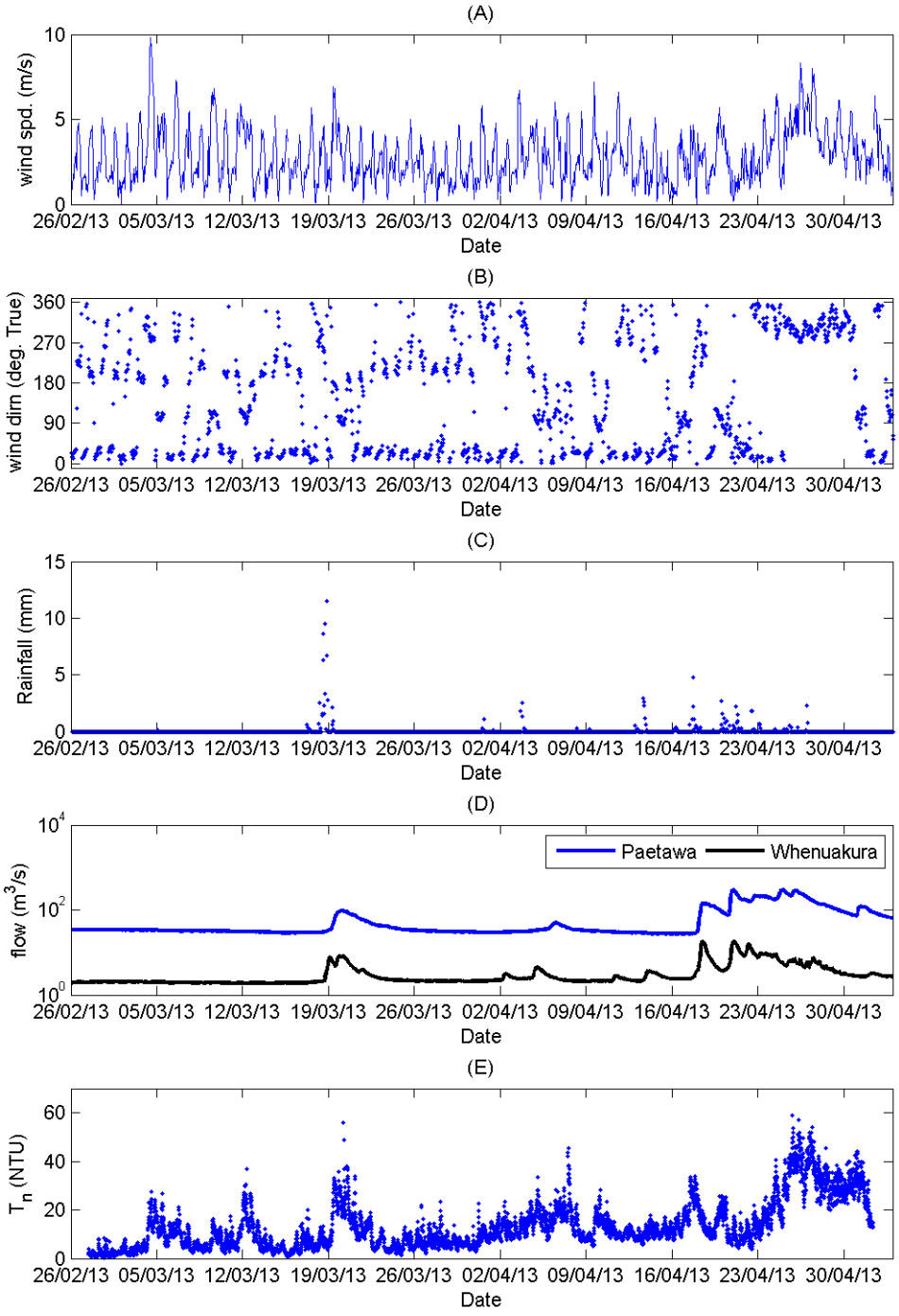

Figure 3-26: Time series of wind speed, direction, rainfall, river flows and turbidity at Site 16. Panels show: (A) wind speed, (B) wind direction (in meteorological convention "blowing from"), (C) rainfall, (D) river flows and (E) turbidity.

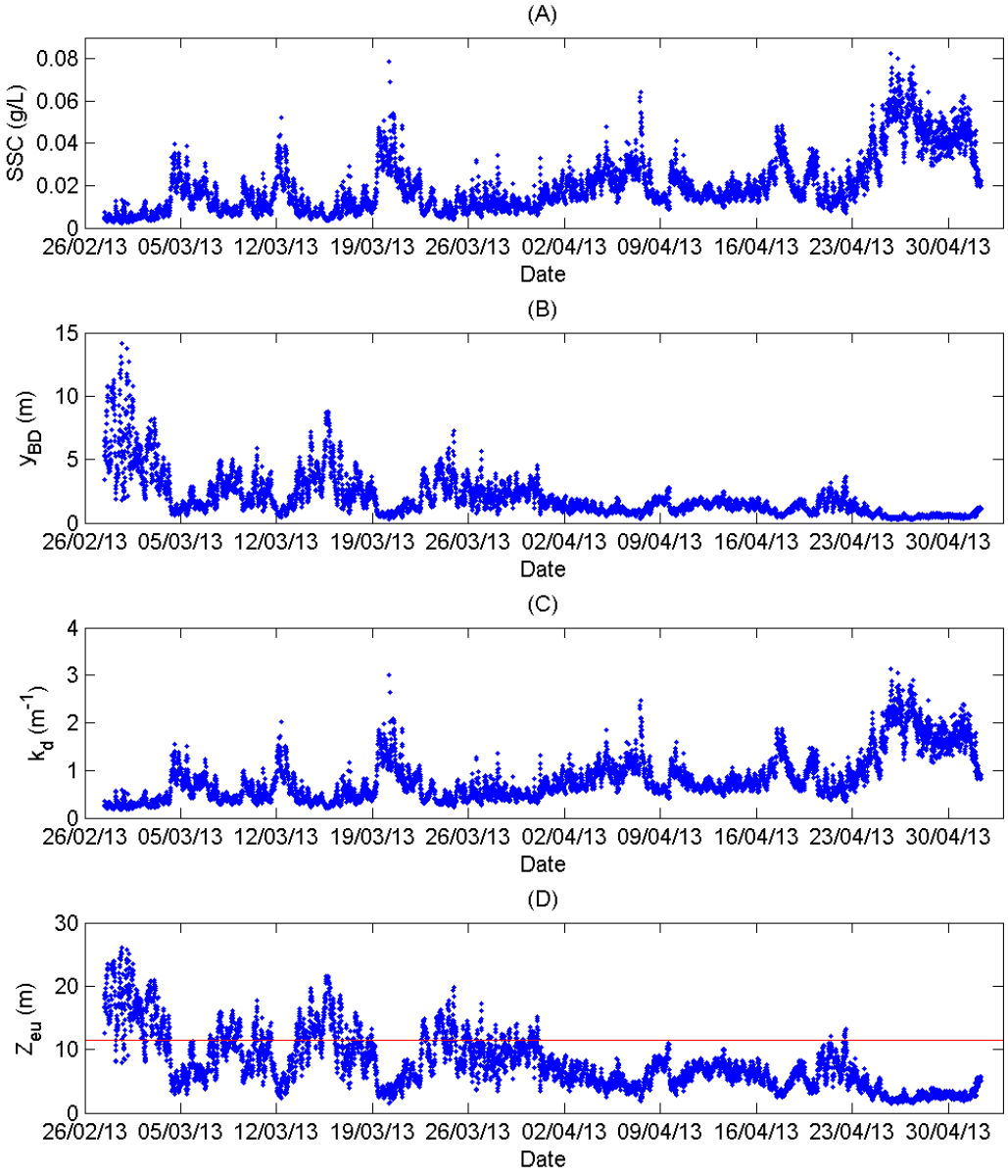

Figure 3-27: Time series of SSC and optical variables at Site 16. Panels show: (A) SSC, (B) y_{BD} (C) k_d and (D) euphotic depth (Z_{eu}) (red line mean water depth).

At site 16, the estimates of T_n, SSC, k_d, and y_{BD} all showed considerable temporal variability. As with the previous sites, the periods of increased SSC are driven by the discharge of fine sediments from nearby rivers and by the resuspension of fines by wave action.

The red line in Figure 3-27D plots the mean water level at site 16. During the wave and river events, the euphotic depth (Z_{eu}) is less than the water depth, meaning that less than 1% of the ambient light is reaching the benthos.

3.4.7 Comparison

Given that the boat surveys showed an obvious decrease in turbidity with distance from the shoreline, and that the measurements at the 6 sites were all made at varying distances from the shoreline (Table 3-3), a comparison of the time series at the 6 sites to assess the

alongshore variation would likely be more confusing than helpful and therefore was not attempted.

3.4.8 Bed sediments

The particle size distributions (PSD) of the bed sediments collected at the 6 moored instrument sites are presented in this section. The results are given in Table 3-9, which shows the percentage of bed sediment by mass that was retained on each sieve after sieving.

At sites 11 to 15 the bed sediment composition was dominated by fine to very fine sands. In comparison to these sites, at site 16 the bed sediment composition was broader, containing a much larger percentage of coarser sediments.

The proportion of fines (< 0.063 mm "muds") was significantly greater at Sites 14 and 15 than at the other four sites.

Table 3-9: Bed sediment grain size (from sieving). List of symbols: MP = medium pebbles; FP = fine pebbles; VFP = very fine pebbles; VCS = very coarse sand; CS = coarse sand; MS = medium sand; FS = fine sand and VFS = very fine sand.

d (mm)	8.000	4.000	2.000	1.000	0.500	0.250	0.125	0.063	<0.063
φ	-3	-2	-1	0	1	2	3	4	
Size term[3]	MP	FP	VFP	VCS	CS	MS	FS	VFS	Muds
Site 11	0.0%	0.0%	0.5%	0.1%	0.1%	0.5%	9.4	84.8	4.7
Site 12	0.0%	0.0%	0.3%	0.5%	1.0%	1.8%	41.5	50.5	4.5
Site 13	0.0%	0.0%	0.4%	0.1%	0.2%	1.4%	51.7	42.6	3.7
Site 14	0.0%	0.0%	0.0%	0.0%	0.1%	0.3%	4.9	75.7	19.0
Site 15	0.0%	0.0%	0.1%	0.1%	0.3%	1.3%	8.7	74.6	14.8
Site 16	4.2%	5.8%	7.4%	14.0%	34.6%	24.1%	6.8	2.8	0.3

3.5 Surf-zone water sampling

In this section estimates of SSC, Chl-a, g_{340} and y_{BD} from the surf-zone water sampling are presented. Details about the locations and periods relating to these measurements can be found in Table 3-4.

SSC, Chl-a, g_{340} and y_{BD}

The surf-zone estimates of SSC, Chl-a, g_{340} and y_{BD} derived from the analysis of the water samples collected during SZ1, SZ2 and SZ3 are shown in Table 3-10, Table 3-11 and Table 3-12, respectively. These results are also displayed in Figure 3-28.

Table 3-10 and Figure 3-28 shows that for SZ1:

- SSC varied four-fold between 0.0243 g/L and 0.0976 g/L, with a mean value of 0.0582 g/L.

[3] After Wentworth.

- Chl-a varied between 0.7mg/m^3 and 4.0 mg/m^3, with a mean value of 2.4 mg/m^3.
- g_{340} varied between 0.4 m^{-1} and 18.25 m^{-1}, with a mean value of 3.69 m^{-1}. The highest values came from the samples collected in the Whanganui and Patea Rivers and at Ohawe.
- y_{BD} varied between 0.21 m and 0.82 m, with a mean value of 0.39 m.

Table 3-11 and Figure 3-28 shows that for SZ2:

- SSC varied five-fold between 0.0252 g/L and 0.1310 g/L, with a mean value of 0.0876g/L.
- Chl-a varied between 0.4 mg/m^3 and 4.1 mg/m^3, with a mean value of 1.9 mg/m^3.
- g_{340} varied between 0.75 m^{-1} and 7.77 m^{-1}, with a mean value of 1.96 m^{-1}. The highest values came from the samples collected in the Whanganui and Patea Rivers and at Ohawe.
- y_{BD} varied between 0.11 m and 0.39 m, with a mean value of 0.19 m.

Table 3-12 and Figure 3-28 shows that for SZ3:

- SSC varied ten-fold between 0.0088 g/L and 0.0923 g/L, with a mean value of 0.0260 g/L.
- Chl-a varied between 0.4 mg/m^3 and 2.1 mg/m^3, with a mean value of 1.5 mg/m^3.
- g_{340} varied between 0.46 m^{-1} and 5.88m^{-1}, with a mean value of 1.22 m^{-1}. The highest values came from the samples collected in the Whanganui and Patea Rivers and at Ohawe.
- y_{BD} varied between 0.17 m and 0.82 m, with a mean value of 0.56 m.

Table 3-10: Water sample results from SZ1.

Site	SSC (g/L)	Chl-a (mg/m^3)	g_{340} (m^{-1})	y_{BD} (m)
Wanganui River	0.0337	0.7	18.25	0.21
Wanganui Castlecliff	0.0656	4.0	2.76	0.50
Kai iwi	0.0798	2.8	0.75	0.36
Ototoka	0.0296	2.6	0.40	0.83
Waiinui	0.0976	3.8	0.58	0.28
Waverley	0.0812	3.4	0.69	0.30
Patea River	0.0469	3.1	6.39	0.33
Patea Beach	0.0636	1.8	1.09	0.31
Manawapou	0.0707	1.7	1.50	0.26
Hawera	0.0477	1.1	0.58	0.43
Ohawe	0.0243	1.3	7.60	0.45

Table 3-11: Water sample results from SZ2.

Site	SSC (g/L)	Chl-a (mg/m^3)	g_{340} (m^{-1})	y_{BD} (m)
Wanganui River	0.0252	0.4	7.77	0.39
Wanganui Castlecliff	0.1180	1.6	0.86	0.12
Kai iwi	0.1290	4.1	0.81	0.11
Ototoka	0.0463	3.1	0.75	0.13
Waiinui	0.1310	2.1	1.15	0.11
Waverley	0.0957	1.8	1.04	0.13
Patea River	0.0319	1.2	4.61	0.34
Patea Beach	0.1160	1.5	1.05	0.13
Manawapou	0.1070	0.7	0.92	0.19
Hawera	0.0707	1.1	0.86	0.24
Ohawe	0.0930	2.9	1.78	0.20

Table 3-12: Water sample results from SZ3.

Site	SSC (g/L)	Chl-a (mg/m^3)	g_{340} (m^{-1})	y_{BD} (m)
Wanganui River	0.0124	1.3	0.921	0.67
Wanganui Castlecliff	0.0103	1.8	0.471	0.71
Kai iwi	0.0226	2.1	0.654	0.48
Ototoka	0.0125	1.3	0.711	0.82
Waiinui	0.0192	1.1	0.586	0.57
Waverley	0.0189	1.6	0.586	0.58
Patea River	0.0088	1.4	5.882	0.79
Patea Beach	0.0923	1.8	0.816	0.18
Manawapou	0.0463	1.2	0.461	0.26
Hawera	0.0266	1.0	0.518	0.45
Ohawe	0.0165	2.1	1.795	0.71

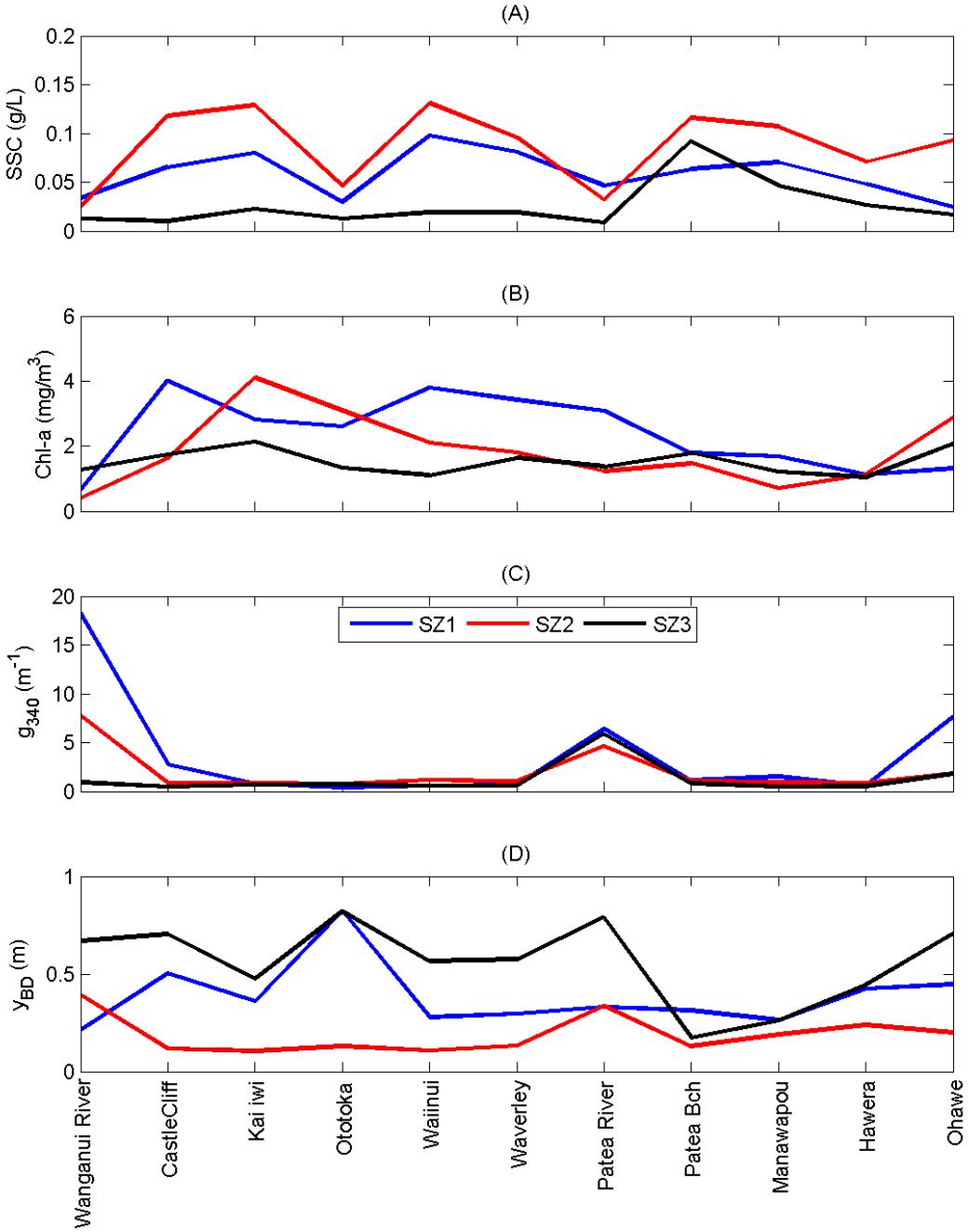

Figure 3-28: Surf-zone estimates of SSC, Chl-a, g_{340} and y_{BD}. Panels show: (A) SSC, (B) Chl-a, (C) g_{340} and (D) y_{BD}.

Particle size distribution

The PSDs of the sediments in suspension in the surf-zone are shown Figure 3-29. The surf-zone samples from SZ1 were not sieved, but this does not affect in the interpretation as sand-sized particles are optically irrelevant. Thus, it is the peaks in the silt-sized classes that are of most interest here. In the silt-sized classes, the majority of the PSDs shown in Figure 3-29 have peaks around 0.02 mm (fine to medium silt). The one major exception to the above is the PSD from the Wanganui River for SZ1, which has a peak around 0.007 mm (fine to very fine silt).

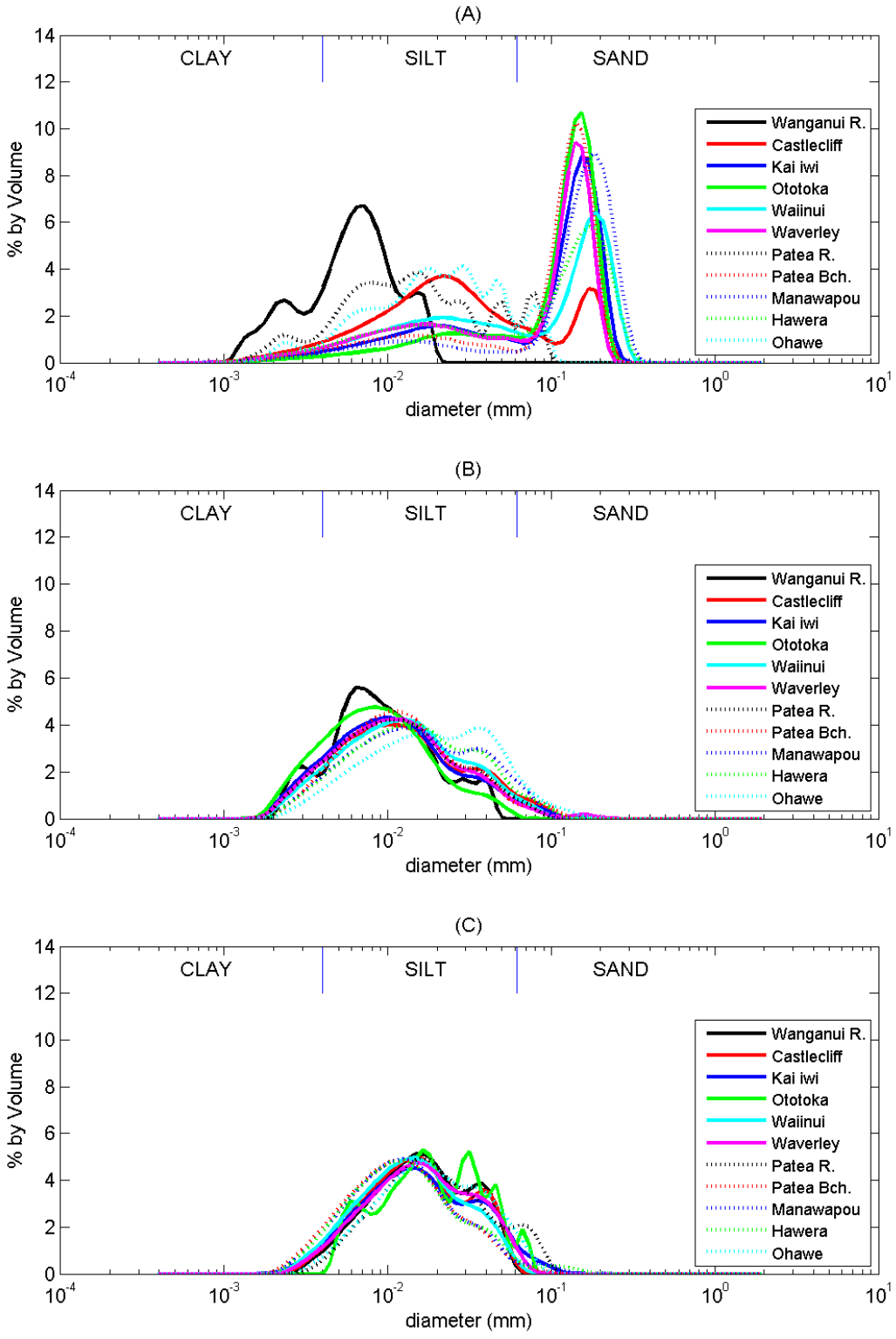

Figure 3-29: Particle size distribution of sediments suspended in the surf-zone. Panels: (A) SZ1, (B) SZ2 and (C) SZ3.

4 Summary

A comprehensive set of measurements have been made to characterise the background optical water quality and suspended sediment concentration (SSC) in the nearshore region of the STB.

A summary of the key findings is as follows.

Measurements from both boat surveys (S1 and S2) showed that SSC and optical variables vary significantly with distance offshore, with SSC and diffuse light attenuation (k_d) being greatest closest to the shore, and visual clarity (as indexed by the horizontal black disc visibility) increasing rapidly with distance offshore. Both coloured dissolved organic matter (CDOM) and chlorophyll-a concentration also decrease with distance offshore.

Both boat surveys suggest a reduction in SSC (and hence an increase in visual clarity and a decrease in k_d) moving down the coast in a S SE direction. Measured SSC was greater during S2 than during S1, which was probably the result of higher river flows (and sediment loads). The maximum (averaged over the water column) SSC measured during S2 was 0.068 g/L near Hawera. During S2, in the waters ~500m offshore, the horizontal black disc visibility (y_{BD}) was less than 1 m along the entire length of the STB, which is a rather low visual clarity.

Using the boat survey data, statistically robust in-situ relationships were determined relating the nephelometric turbidity (T_n) as measured by an optical backscatter sensor to SSC, the beam attenuation coefficient (c) at 530 nm (from which y_{BD} is derived), and k_d. These relationships were applied to the optical backscatter data collected at the 6 moored instrument sites. The estimates of T_n, SSC, k_d, and y_{BD} from the 6 moored instrument sites all showed considerable temporal variability. During the last two weeks of the deployment period there was a significant increase in SSC, coinciding with increased river flows. At these times it is likely that the rivers were discharging fine sediments into the STB, which were then being transported in suspension through the measurement site. Some of the peaks in SSC also coincided with times of high wind speed but low river flows. These peaks in SSC are most likely wave-driven. At these times, wave stirring is entraining fine sediments from the sea floor, which are subsequently mixed into the water column.

During river and wave events, the euphotic depth is less than the mean water depth at the instrument sites. This is significant, as it means that less than 1% of the ambient light is reaching the benthos at these times.

Rainfall data have shown that the deployment took place during a period of lower than expected rainfall for that time of year, and consequently during a period of low river flows. Since rivers are a major source of fine sediments into the STB, it is likely that the data are representative of conditions with clearer water.

Overall, the field dataset provides a comprehensive picture of the background optical water quality and SSC in the STB. These results can be used with confidence to help assess the potential effects of offshore sand extraction on the surrounding environment, and in particular the effect of sediment plume dispersal in the nearshore environment.

Information relating to TTR's additional scientific work undertaken since 2014 has been provided and the conclusions is this report remain valid.

5 Acknowledgements

We thank the many people who assisted in the field, especially Rod Budd, Scott Edhouse and the crew of the Ikatere. We would also like to thank Dr Mal Green and Dr Rob Davies-Colley for reviewing this report.

6 References

Davies-Colley, R.J., Nagels, J.W. (2008) Predicting light penetration into river waters. *Journal of Geophysical Research: Biogeosciences*, 113(G3): G03028. 10.1029/2008JG000722.

Davies-Colley, R.J., Vant, W.N., Smith, D.G. (2003) *Colour and Clarity of Natural Waters: Science and Management of Optical Water Quality*. The Blackburn Press: 310.

Hadfield, M. (2011) *Sediment Plume Modelling for South Tarnaki Bight Sand Mining*, WLG2011-37: 39.

Kirk, J.T.O. (2011) *Light and Photosynthesis in Aquatic Ecosystems*. Cambridge University Press.

MacDonald, I.T., Budd, R., Bremner, D., Edhouse, S. (2012) *South Taranaki Bight Iron Sand Mining: Oceanographic measurments data report*: 109.

Tassan, S., Ferrari, G.M. (1995) An alternative approach to absorption measurements of aquatic particles retained on filters. *Limnol. Oceanogr*. 40(8): 1358–1368.

Zaneveld, J.R., Pegau, W. (2003) Robust underwater visibility parameter. *Opt. Express*, 11(23): 2997–3009.

Appendix A Additional information

Table A-1: Additional information for the boat surveys. Note: Profile numbers 2 and 68 have negative offshore distances as these profiles were taken in the Wanganui River at the wharf, which is upstream from the assumed shoreline position.

Survey number	Profile Number	Distance offshore (m)	Latitude (S)	Longitude (E)	Time
S1	1	1429	-39.9895	175.0278	12/03/2013 16:08
S1	2	-1059	-39.9449	174.9928	12/03/2013 16:56
S1	3	645	-39.9519	174.9751	12/03/2013 16:36
S1	4	1160	-39.9545	174.9701	12/03/2013 16:26
S1	5	553	-39.888	174.8911	12/03/2013 14:39
S1	6	744	-39.8899	174.8908	12/03/2013 15:05
S1	7	910	-39.8913	174.8901	12/03/2013 15:13
S1	8	1273	-39.8937	174.887	12/03/2013 14:23
S1	9	1318	-39.89435	174.8874	12/03/2013 15:18
S1	10	2106	-39.9005	174.8828	12/03/2013 15:27
S1	11	351	-39.8713	174.7421	12/03/2013 12:48
S1	12	373	-39.87175	174.7414	12/03/2013 13:16
S1	13	468	-39.8725	174.742	12/03/2013 13:23
S1	14	692	-39.8745	174.7425	12/03/2013 13:31
S1	15	1063	-39.8778	174.7433	12/03/2013 13:40
S1	16	1872	-39.8849	174.7454	12/03/2013 13:51
S1	17	452	-39.8549	174.683	12/03/2013 11:24
S1	18	559	-39.8558	174.6825	12/03/2013 11:32
S1	19	628	-39.8563	174.682	12/03/2013 11:47
S1	20	898	-39.8579	174.6795	12/03/2013 11:56
S1	21	944	-39.8574	174.678	12/03/2013 11:09
S1	22	1258	-39.8608	174.6775	12/03/2013 12:05
S1	23	2055	-39.8667	174.6722	12/03/2013 12:16
S1	24	371	-39.8233	174.5872	12/03/2013 09:38
S1	25	461	-39.8246	174.5875	12/03/2013 09:52
S1	26	526	-39.8251	174.5871	12/03/2013 09:58
S1	27	782	-39.827	174.5854	12/03/2013 10:08
S1	28	1159	-39.8298	174.5829	12/03/2013 10:18
S1	29	1941	-39.8359	174.5783	12/03/2013 10:30
S1	30	1730	-39.7913	174.4941	12/03/2013 08:51
S1	31	506	-39.777	174.4835	11/03/2013 15:29
S1	32	652	-39.7785	174.4831	11/03/2013 15:42
S1	33	734	-39.7786	174.4818	11/03/2013 15:56
S1	34	965	-39.7805	174.4805	11/03/2013 16:06

Survey number	Profile Number	Distance offshore (m)	Latitude (S)	Longitude (E)	Time
S1	35	1350	-39.7828	174.4771	11/03/2013 16:22
S1	36	2049	-39.7867	174.4706	11/03/2013 16:38
S1	37	276	-39.7198	174.4041	11/03/2013 13:53
S1	38	405	-39.7205	174.4029	11/03/2013 14:13
S1	39	504	-39.7207	174.4017	11/03/2013 14:21
S1	40	726	-39.7217	174.3995	11/03/2013 14:31
S1	41	1110	-39.7243	174.3963	11/03/2013 14:41
S1	42	1953	-39.7286	174.3882	11/03/2013 14:54
S1	43	236	-39.6584	174.3478	11/03/2013 12:28
S1	44	304	-39.6588	174.3472	11/03/2013 12:38
S1	45	406	-39.6593	174.3462	11/03/2013 12:46
S1	46	589	-39.6603	174.3445	11/03/2013 12:53
S1	47	840	-39.6618	174.3423	11/03/2013 12:12
S1	48	997	-39.6626	174.3408	11/03/2013 13:03
S1	49	1812	-39.6674	174.3336	11/03/2013 13:14
S1	50	234	-39.6258	174.2872	11/03/2013 11:11
S1	51	336	-39.6268	174.2871	11/03/2013 11:22
S1	52	431	-39.6276	174.2867	11/03/2013 11:30
S1	53	625	-39.6292	174.2858	11/03/2013 11:37
S1	54	1023	-39.6324	174.2837	11/03/2013 11:46
S1	55	1812	-39.6388	174.2797	11/03/2013 11:55
S1	56	193	-39.5972	174.2189	11/03/2013 09:41
S1	57	262	-39.5978	174.2186	11/03/2013 09:50
S1	58	306	-39.598	174.2181	11/03/2013 09:56
S1	59	403	-39.5988	174.2176	11/03/2013 10:04
S1	60	492	-39.5999	174.218	11/03/2013 09:31
S1	61	595	-39.6001	174.2161	11/03/2013 10:13
S1	62	993	-39.6029	174.2132	11/03/2013 10:25
S1	63	1801	-39.6085	174.2072	11/03/2013 10:37
S2	64	879	-39.988	175.0345	01/05/2013 10:00
S2	65	1292	-39.9908	175.0313	01/05/2013 10:30
S2	66	1511	-39.9893	175.0265	01/05/2013 09:37
S2	67	2558	-39.9987	175.0206	01/05/2013 10:50
S2	68	-1059	-39.9449	174.9928	01/05/2013 16:56
S2	69	690	-39.9524	174.9749	01/05/2013 16:41
S2	70	1171	-39.9548	174.9702	01/05/2013 16:32
S2	71	2202	-39.9594	174.9597	01/05/2013 16:19
S2	72	615	-39.8886	174.891	01/05/2013 13:05
S2	73	990	-39.8916	174.8889	01/05/2013 13:20

Survey number	Profile Number	Distance offshore (m)	Latitude (S)	Longitude (E)	Time
S2	74	1267	-39.8931	174.886	01/05/2013 12:48
S2	75	2107	-39.9002	174.8821	01/05/2013 13:34
S2	76	308	-39.8711	174.7415	02/05/2013 16:32
S2	77	410	-39.8546	174.6833	02/05/2013 15:45
S2	78	862	-39.8579	174.6802	02/05/2013 15:58
S2	79	952	-39.8584	174.6793	01/05/2013 14:54
S2	80	2092	-39.867	174.672	02/05/2013 16:11
S2	81	360	-39.8242	174.589	02/05/2013 15:23
S2	82	712	-39.78715	174.5104	02/05/2013 13:56
S2	83	1009	-39.7898	174.5072	02/05/2013 14:08
S2	84	1570	-39.7936	174.5012	02/05/2013 13:39
S2	85	2109	-39.7976	174.4975	02/05/2013 14:21
S2	86	584	-39.7782	174.4839	02/05/2013 12:51
S2	87	895	-39.78	174.481	02/05/2013 13:03
S2	88	2122	-39.788	174.4711	02/05/2013 13:17
S2	89	248	-39.7198	174.4045	02/05/2013 12:18
S2	90	379	-39.6592	174.3465	02/05/2013 10:49
S2	91	648	-39.66095	174.3443	02/05/2013 11:02
S2	92	892	-39.6626	174.3424	02/05/2013 10:25
S2	93	1812	-39.6676	174.3338	02/05/2013 11:13
S2	94	445	-39.6277	174.2866	02/05/2013 09:59
S2	95	244	-39.5976	174.2186	02/05/2013 08:22
S2	96	547	-39.5996	174.2162	02/05/2013 08:44
S2	97	554	-39.6005	174.218	02/05/2013 08:10
S2	98	1832	-39.6091	174.2076	02/05/2013 08:56

Table A-2: Deployment information for the moored deployments. List of symbols: Ibb = interval between bursts and BD = burst duration.

Site No.	Instrument Serial No. (DOBIE/OBS)	Time period (NZST)	Duration (weeks)	Ibb (mins)	BD (mins)	Depth below surface (m)	Mean water depth
11	2604/11871	26/02/13 12:00 to 01/05/13 12:00	9.14	15	3.41	3.0	11.5
12	2312/10081	26/02/13 13:30 to 01/05/13 14:00	9.15	15	3.41	3.0	11.5
13	2608/10704	26/02/13 14:15 to 20/04/13 16:00	7.58	15	3.41	3.0	11.5
14	2603/10596	27/02/13 06:45 to 02/05/13 13:50	9.19	15	3.41	3.0	11.5
15	2609/10599	27/02/13 07:45 to 08/04/13 21:00	5.79	15	3.41	3.0	11.5
16	2607/11870	27/02/13 09:15 to 02/05/13 09:30	9.14	15	3.41	3.0	11.5

Appendix B Bio-Fish data plots

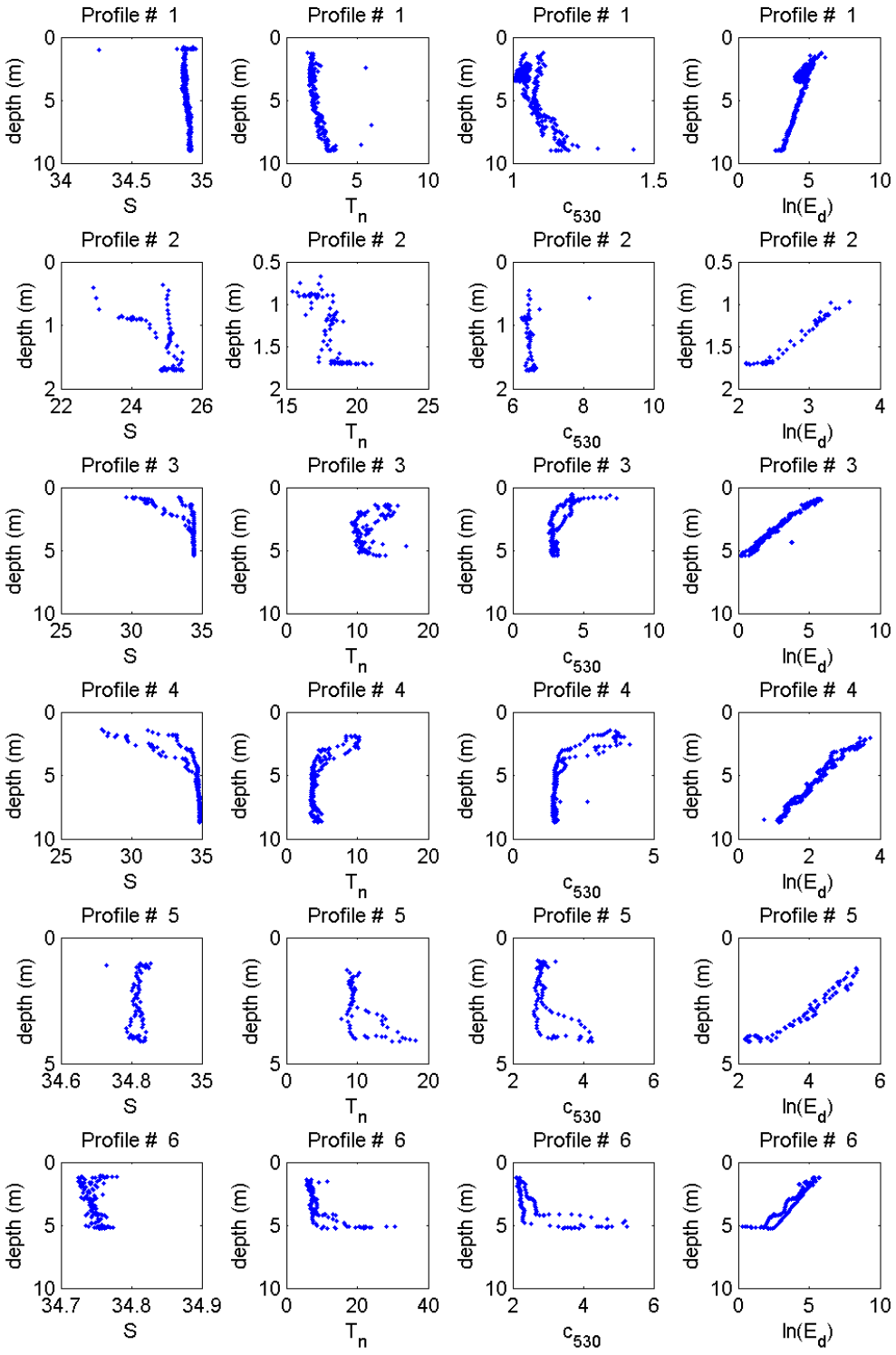

Figure B-1: Profiles of salinity, T_n, c_{530} and E_d (from which k_d is derived) for profiles 1 to 6.

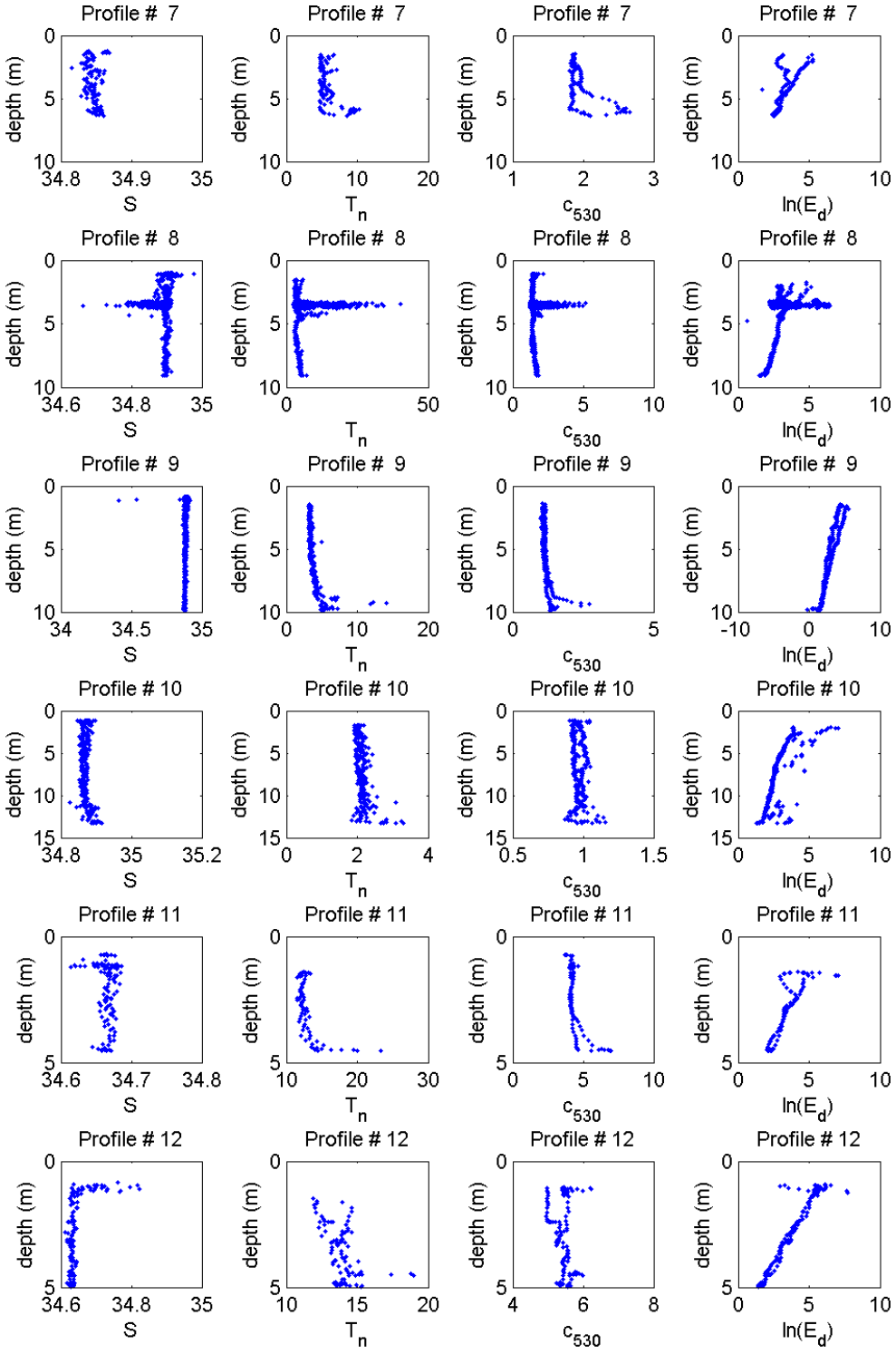

Figure B-2: Profiles of salinity, T_n, c_{530} and E_d (from which k_d is derived) for profiles 7 to 12.

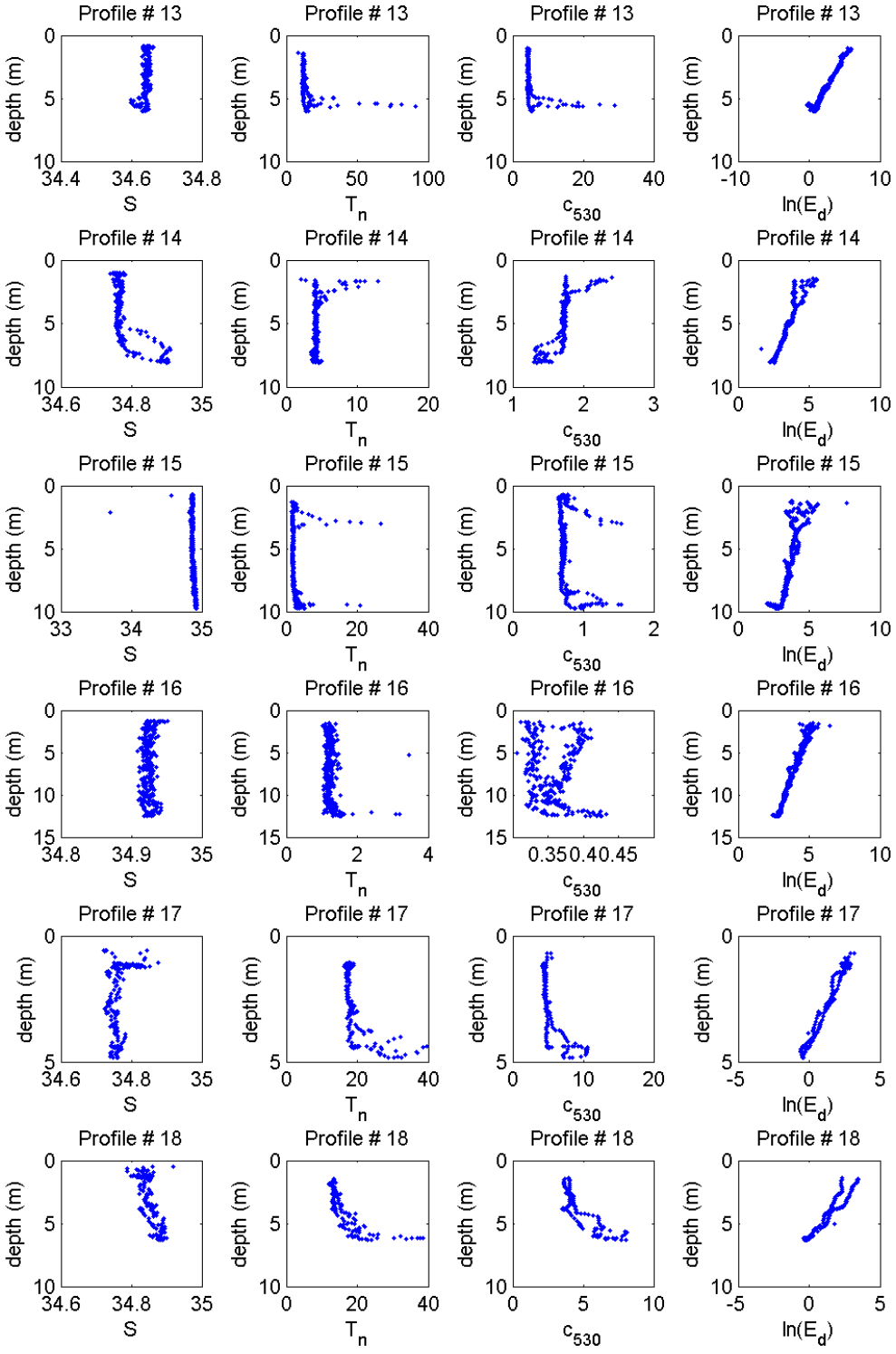

Figure B-3: Profiles of salinity, T_n, c_{530} and E_d (from which k_d is derived) for profiles 13 to 18.

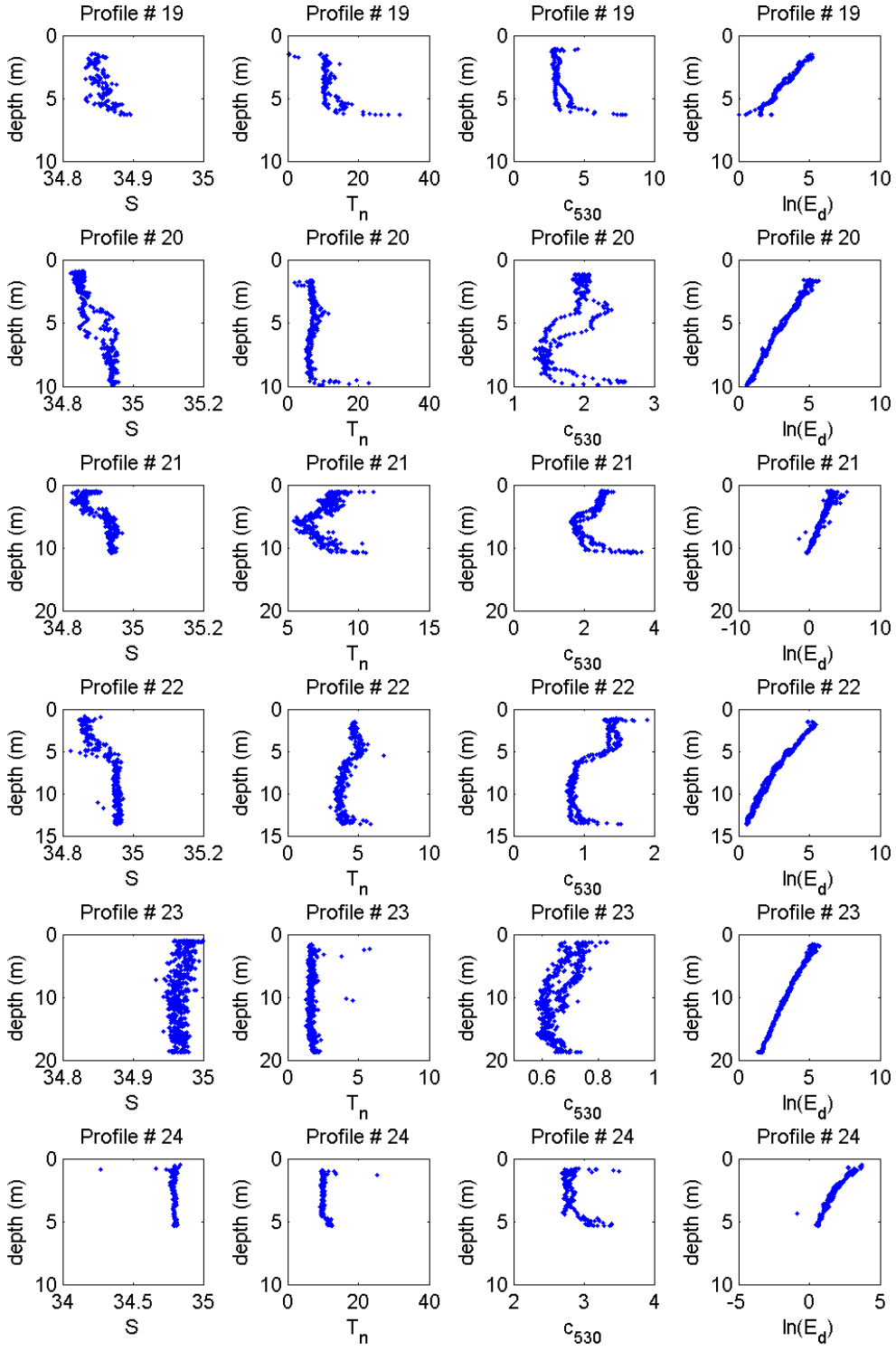

Figure B-4: Profiles of salinity, T_n, c_{530} and E_d (from which k_d is derived) for profiles 19 to 24.

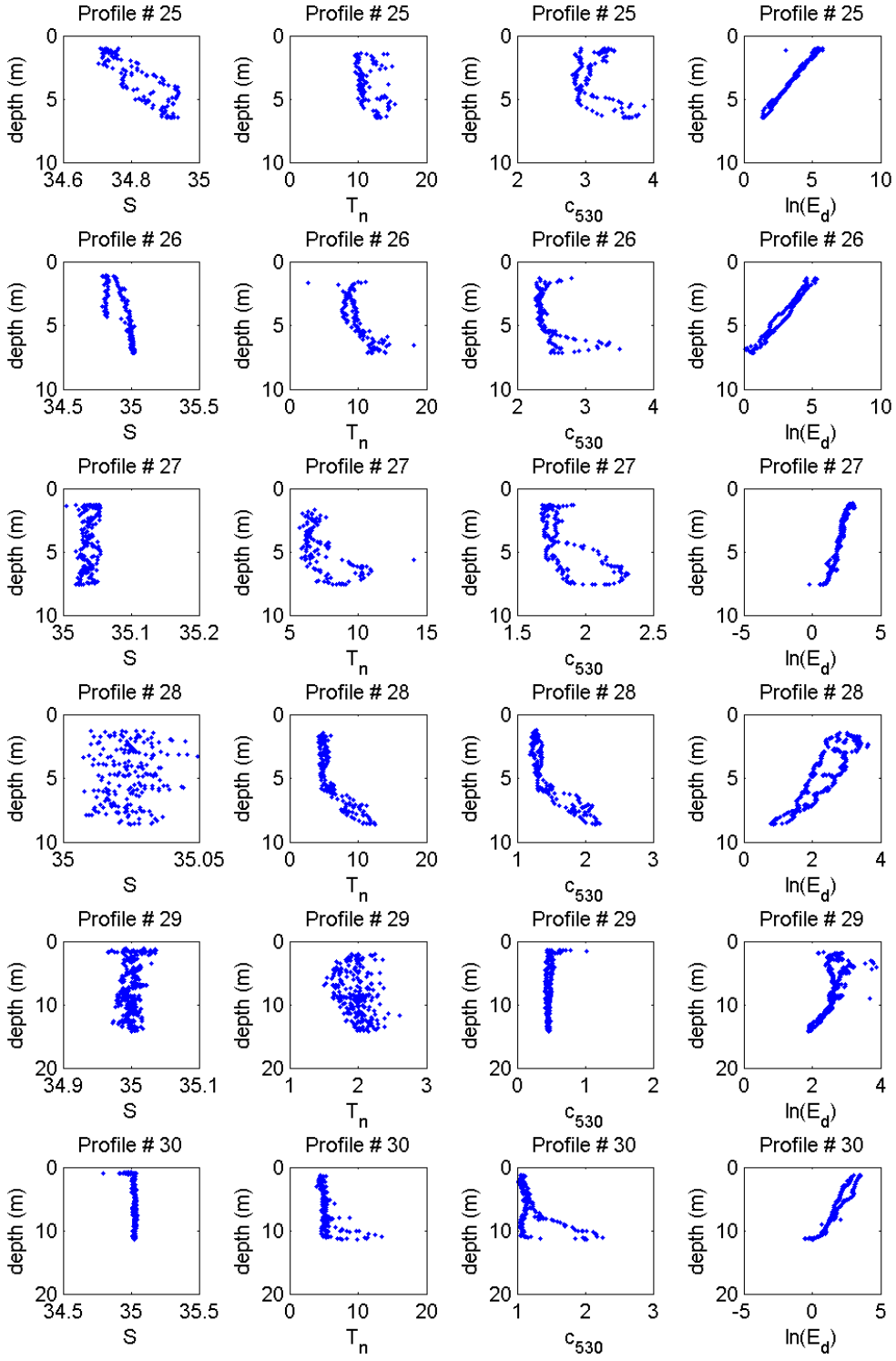

Figure B-5: Profiles of salinity, T_n, c_{530} and E_d (from which k_d is derived) for profiles 25 to 30.

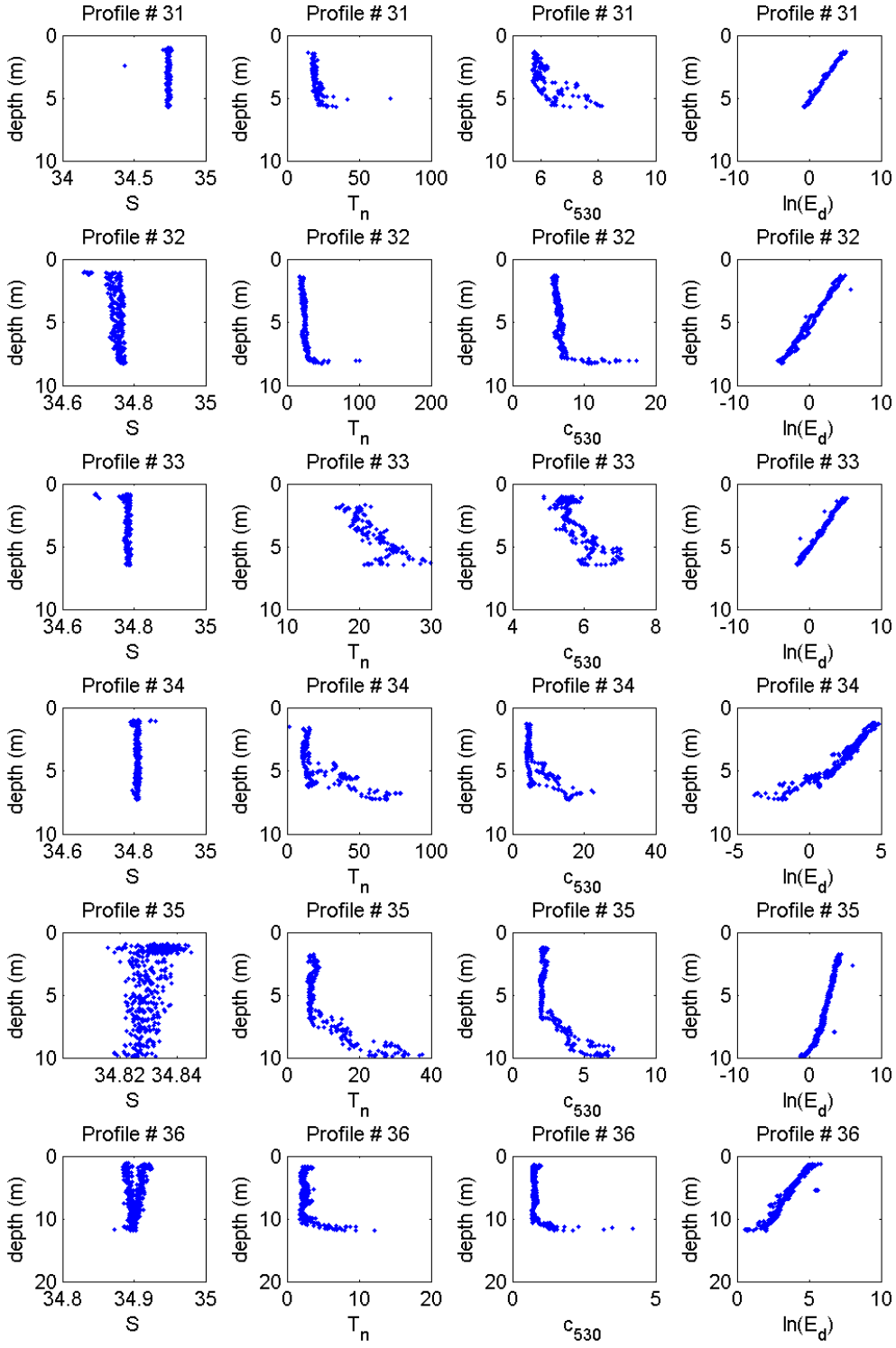

Figure B-6: Profiles of salinity, T_n, c_{530} and E_d (from which k_d is derived) for profiles 31 to 36.

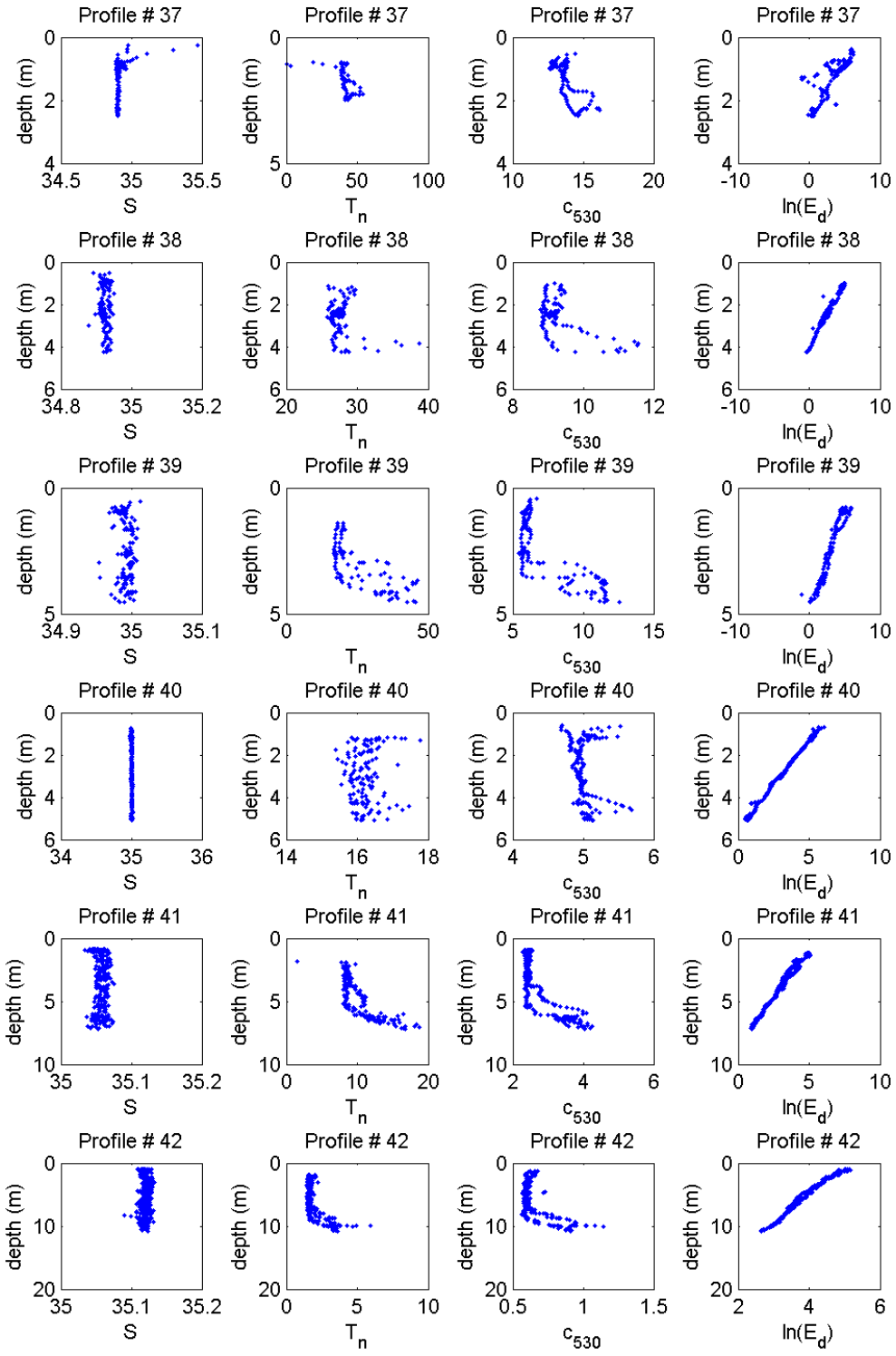

Figure B-7: Profiles of salinity, T_n, c_{530} and E_d (from which k_d is derived) for profiles 37 to 42.

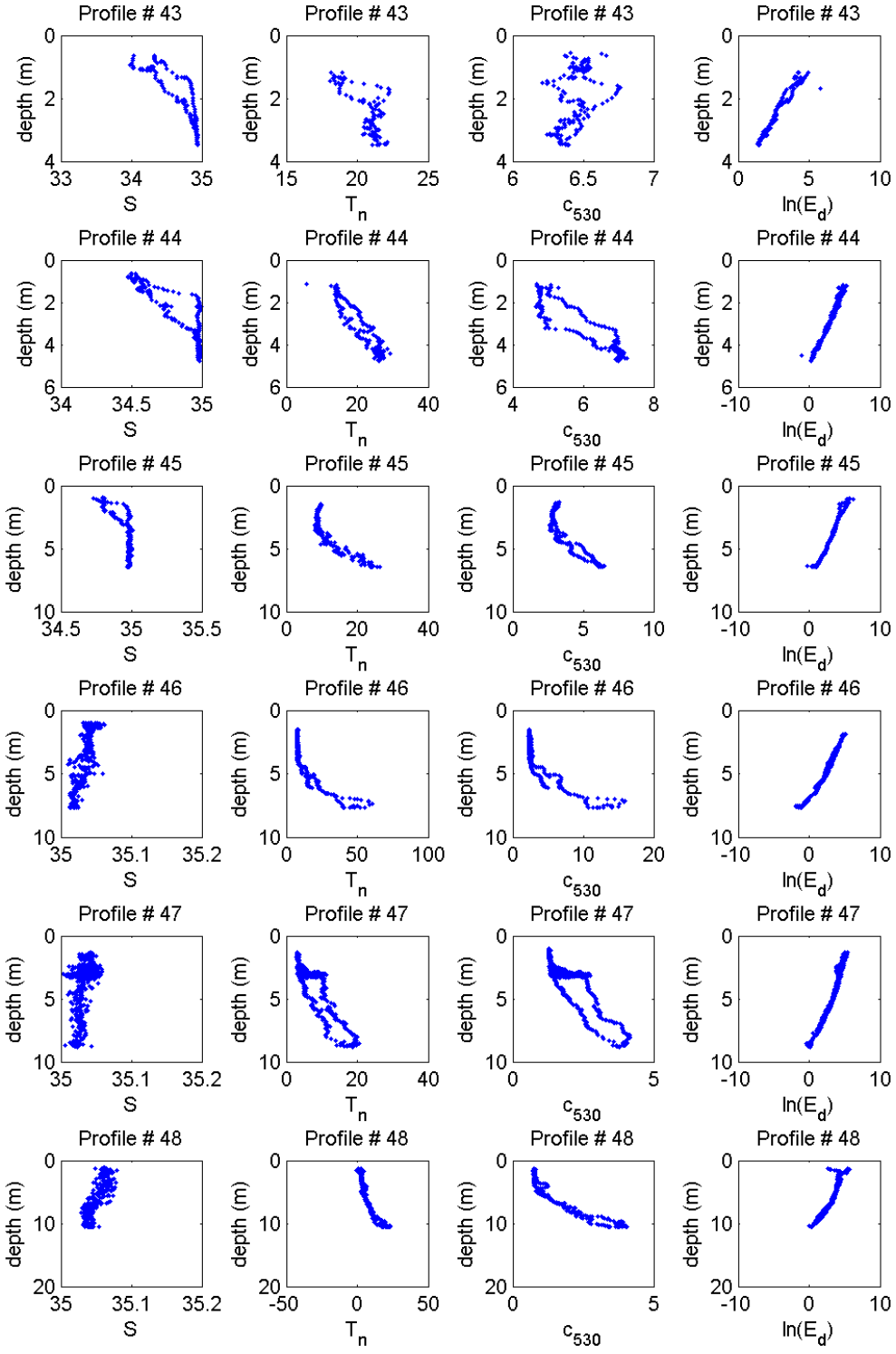

Figure B-8: Profiles of salinity, T_n, c_{530} and E_d (from which k_d is derived) for profiles 43 to 48.

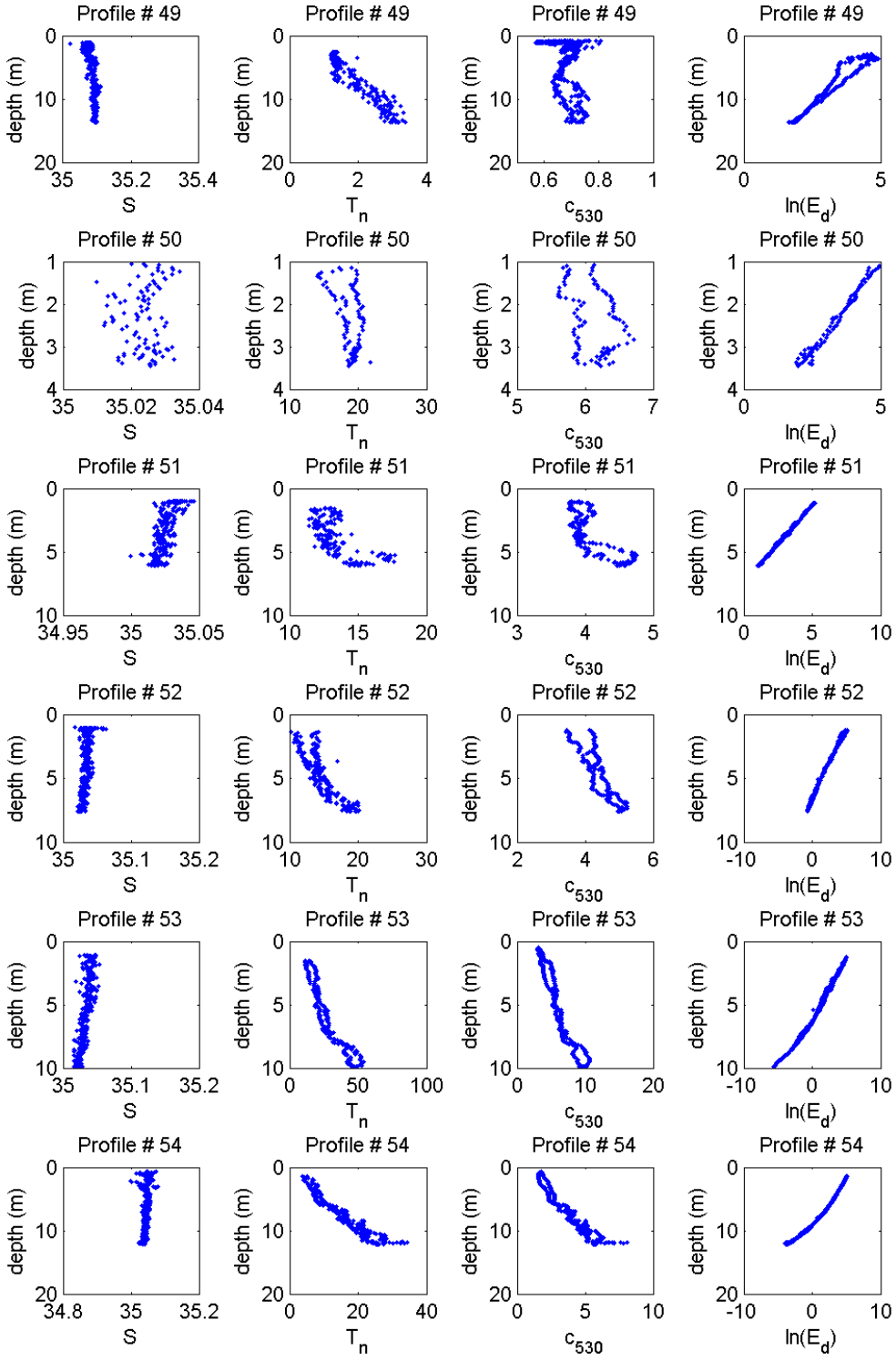

Figure B-9: Profiles of salinity, T_n, c_{530} and E_d (from which k_d is derived) for profiles 49 to 54.

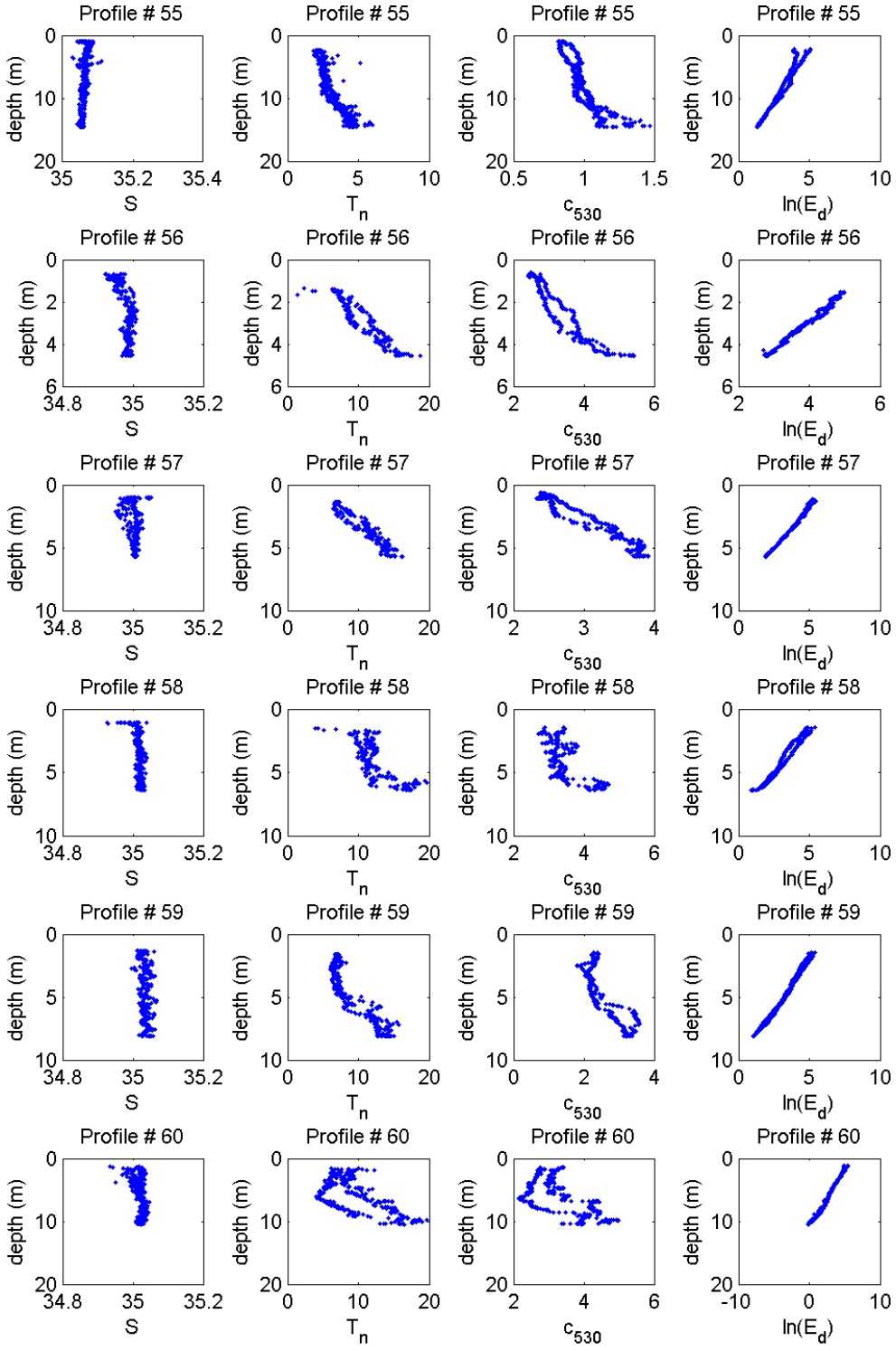

Figure B-10: Profiles of salinity, T_n, c_{530} and E_d (from which k_d is derived) for profiles 55 to 60.

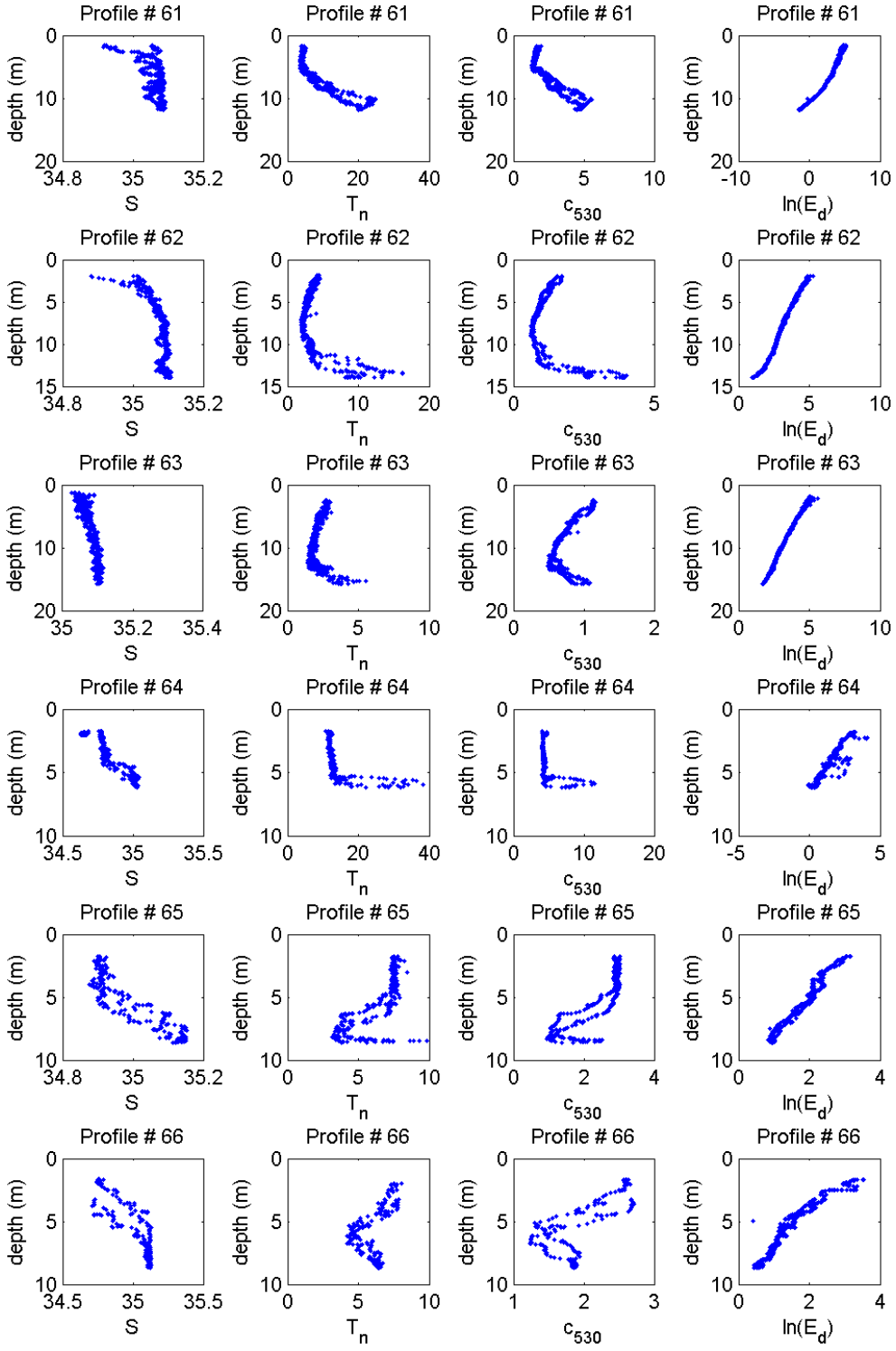

Figure B-11: Profiles of salinity, T_n, c_{530} and E_d (from which k_d is derived) for profiles 61 to 66.

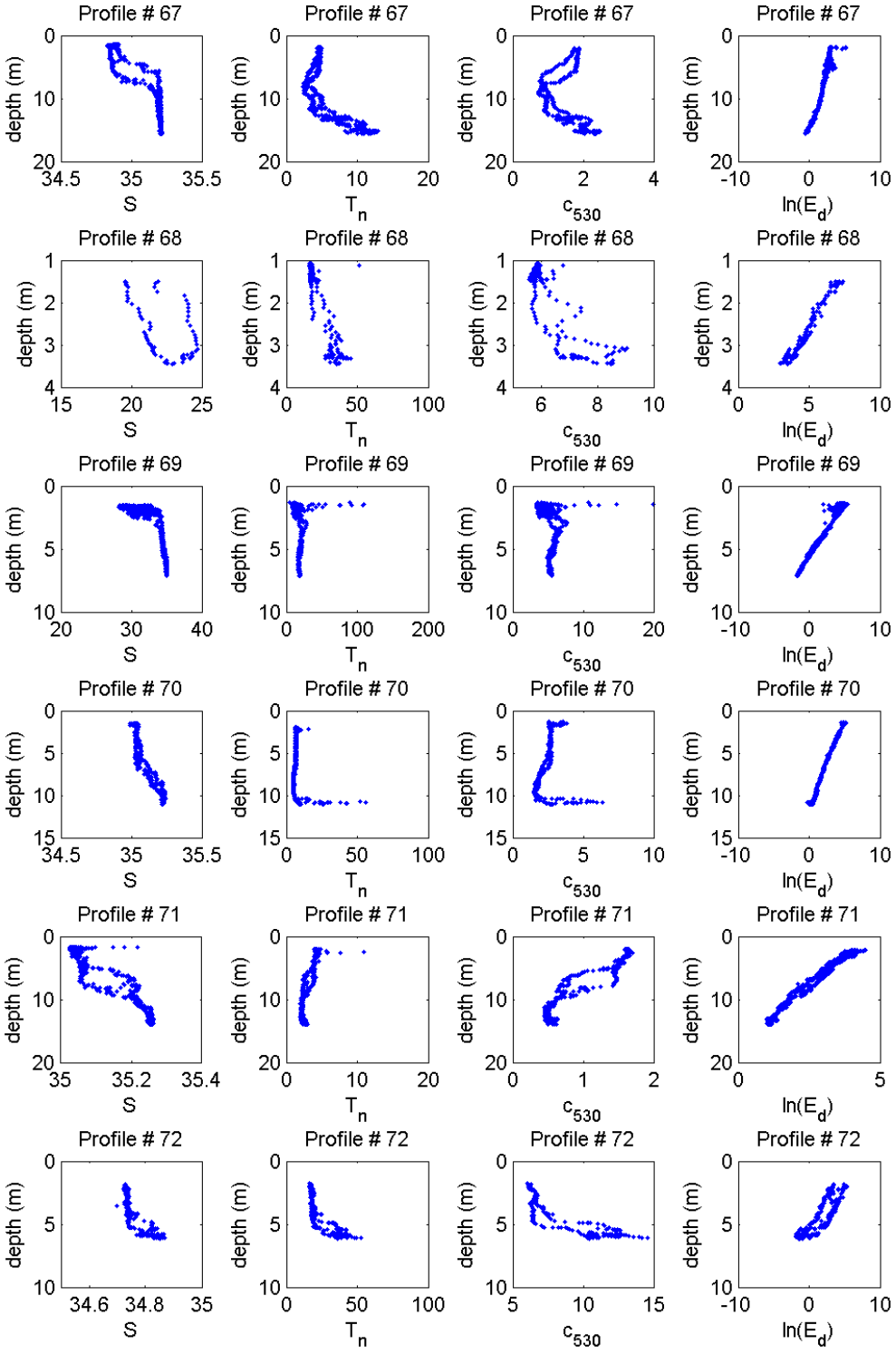

Figure B-12: Profiles of salinity, T_n, c_{530} and E_d (from which k_d is derived) for profiles 67 to 72.

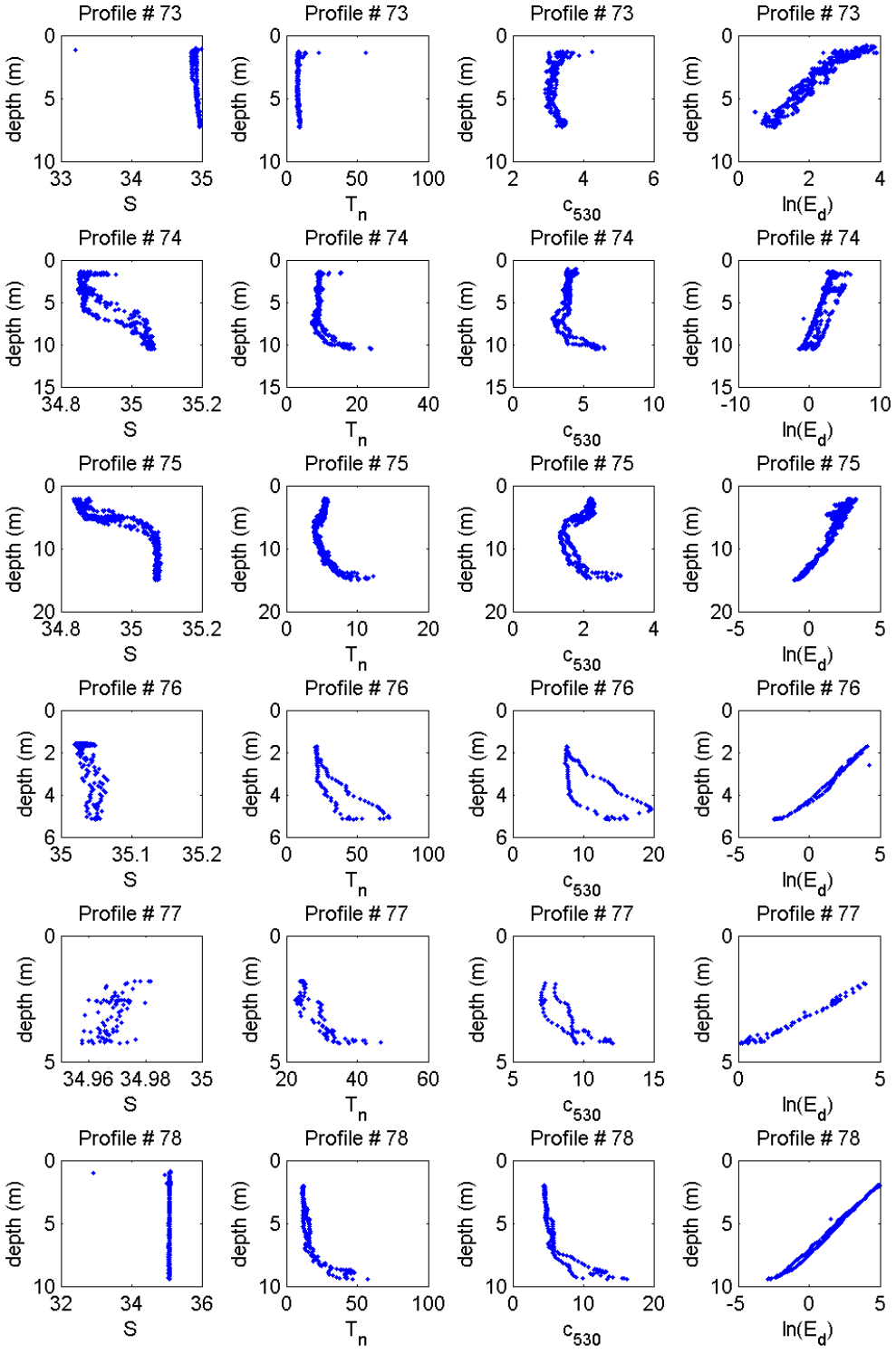

Figure B-13: Profiles of salinity, T_n, c_{530} and E_d (from which k_d is derived) for profiles 73 to 78.

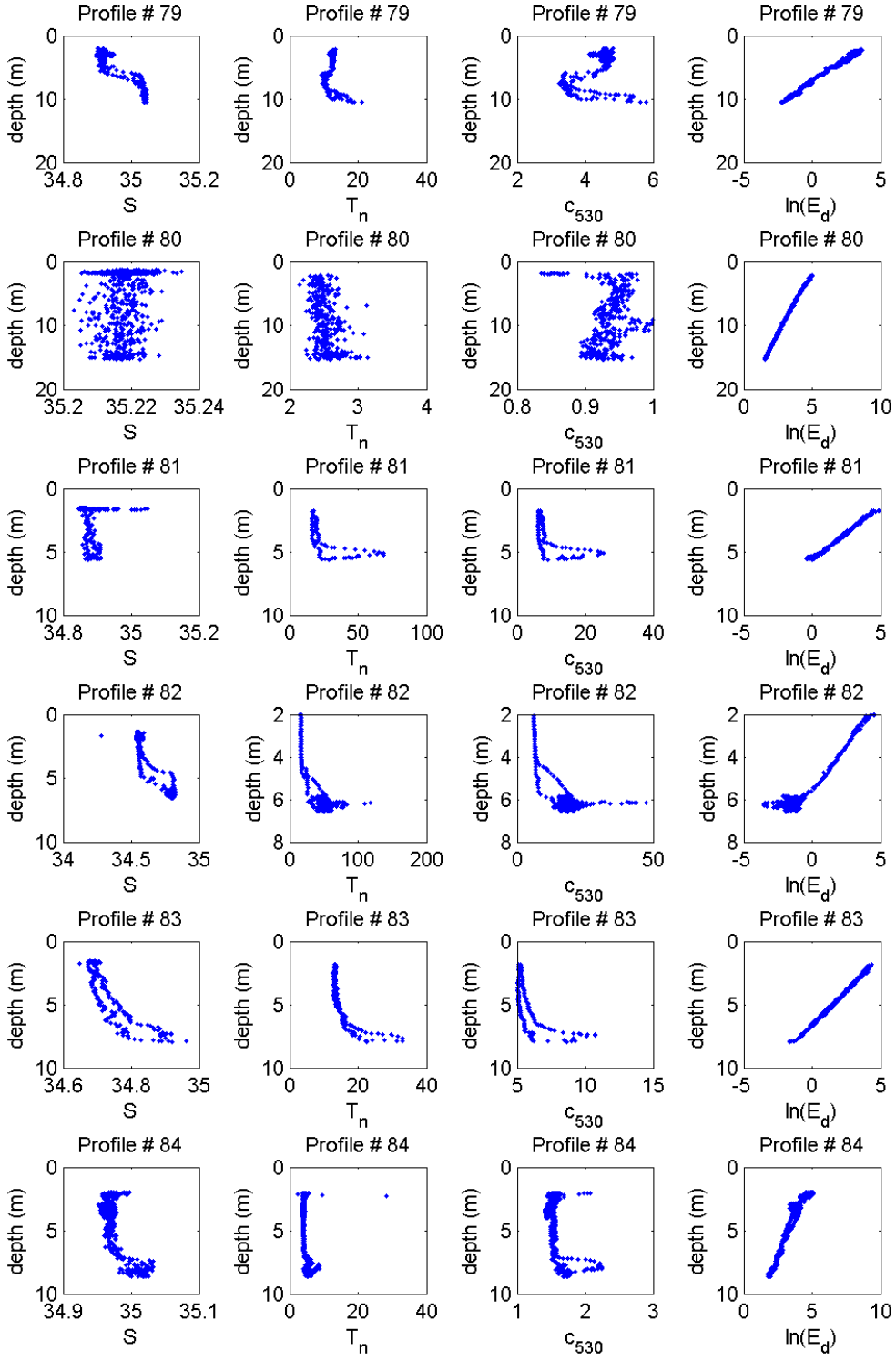

Figure B-14: Profiles of salinity, T_n, c_{530} and E_d (from which k_d is derived) for profiles 79 to 84.

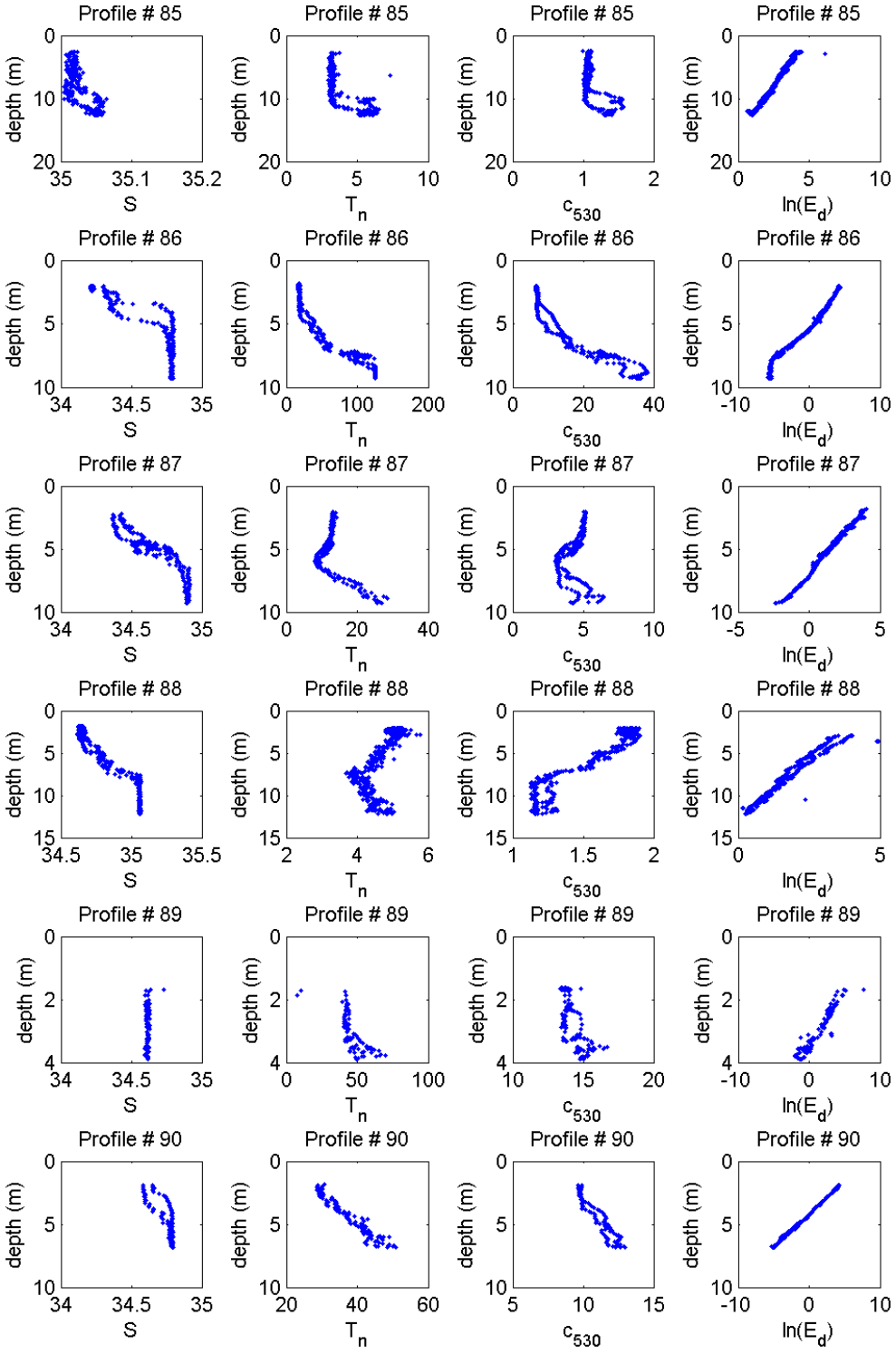

Figure B-15: Profiles of salinity, T_n, c_{530} and E_d (from which k_d is derived) for profiles 85 to 90.

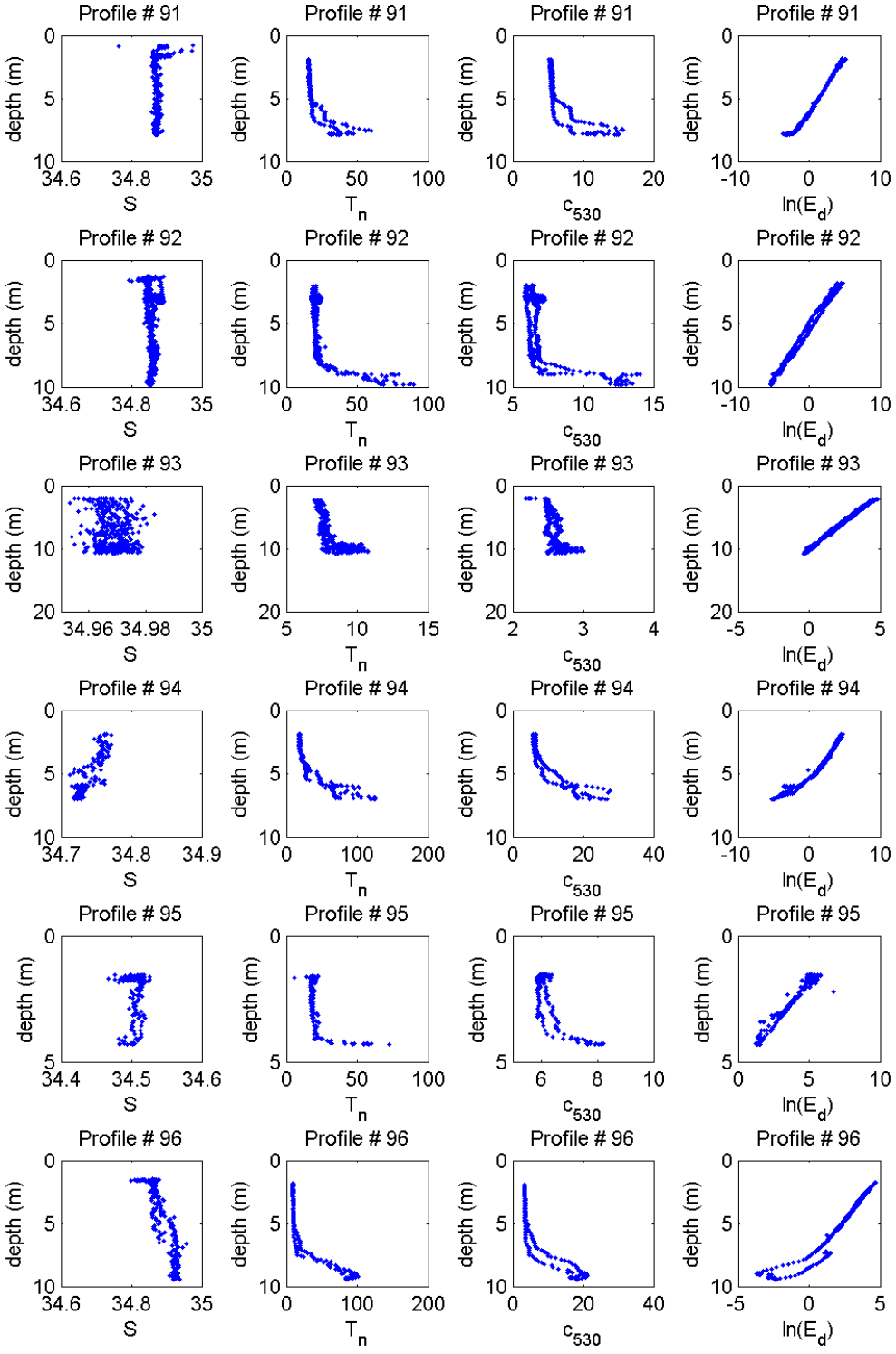

Figure B-16: Profiles of salinity, T_n, c_{530} and E_d (from which k_d is derived) for profiles 91 to 96.

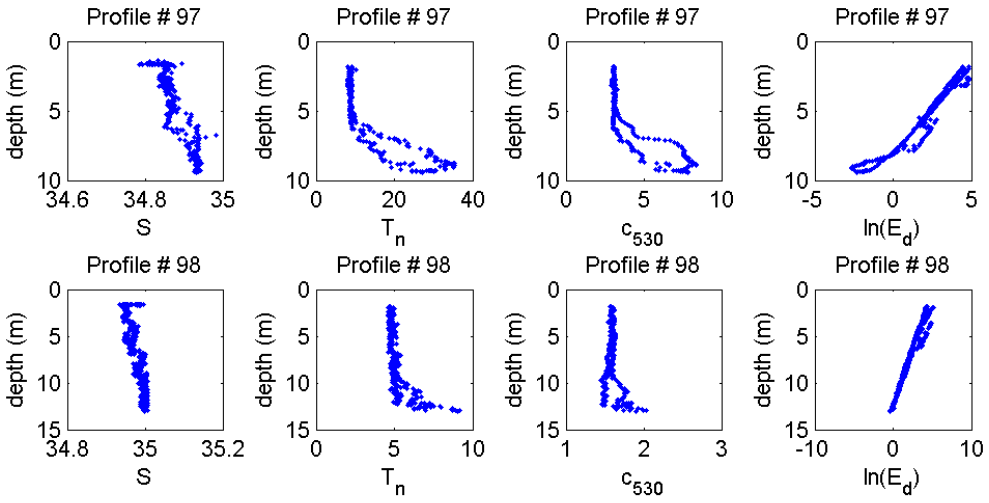

Figure B-17: Profiles of salinity, T_n, c_{530} and E_d (from which k_d is derived) for profiles 97 to 98.

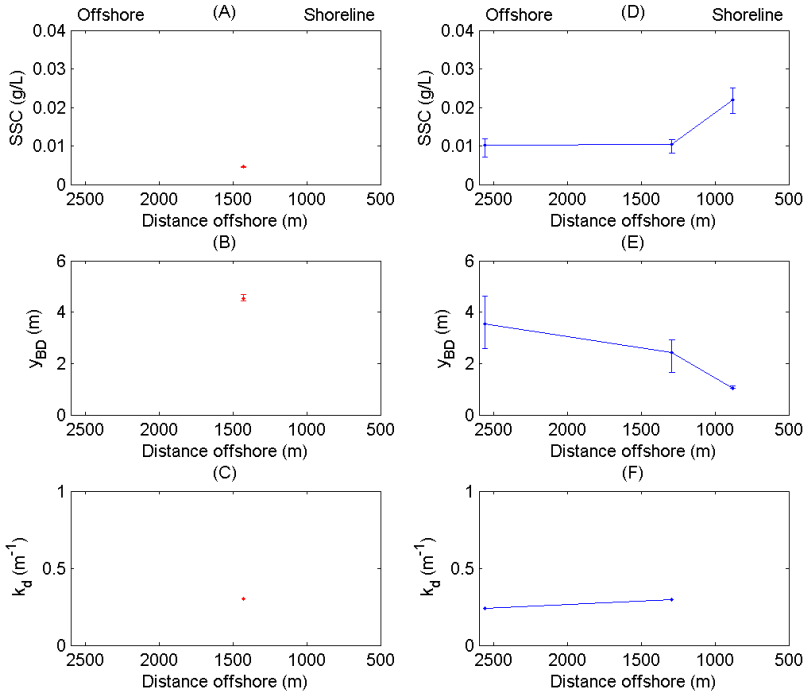

Figure B-18: Cross-shore variability in SSC, y_{BD} and k_d at SP1. Panels: A to C relate to S1 and D to F relate to S2. (A and D) SSC, (B and E) y_{BD} and (C and F) k_d.

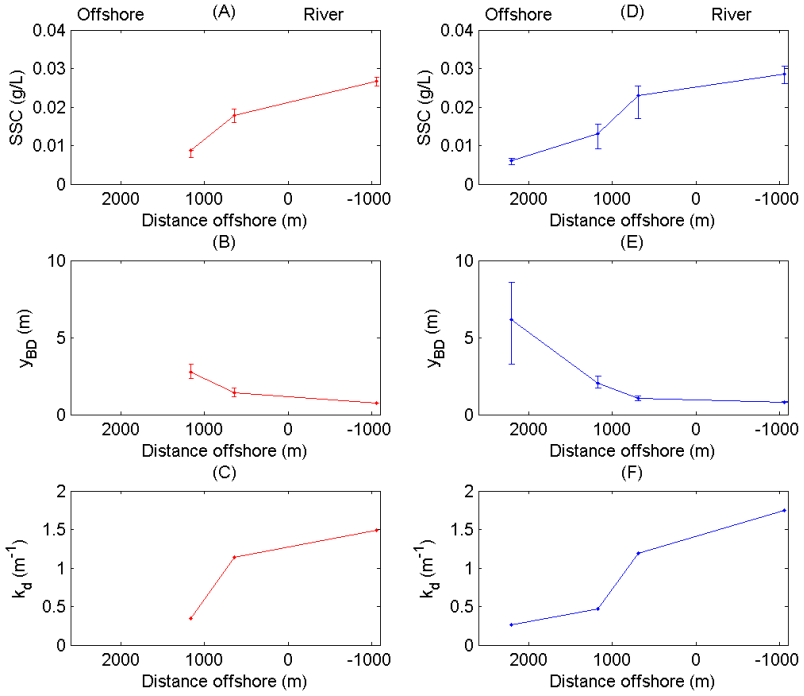

Figure B-19: Cross-shore variability in SSC, y_{BD} and k_d at SP2. Panels: A to C relate to S1 and D to F relate to S2. (A and D) SSC, (B and E) y_{BD} and (C and F) k_d. This plot has negative offshore distances, as these measurements were taken in Wanganui River at the wharf, which is "upstream" from the assumed shoreline position.

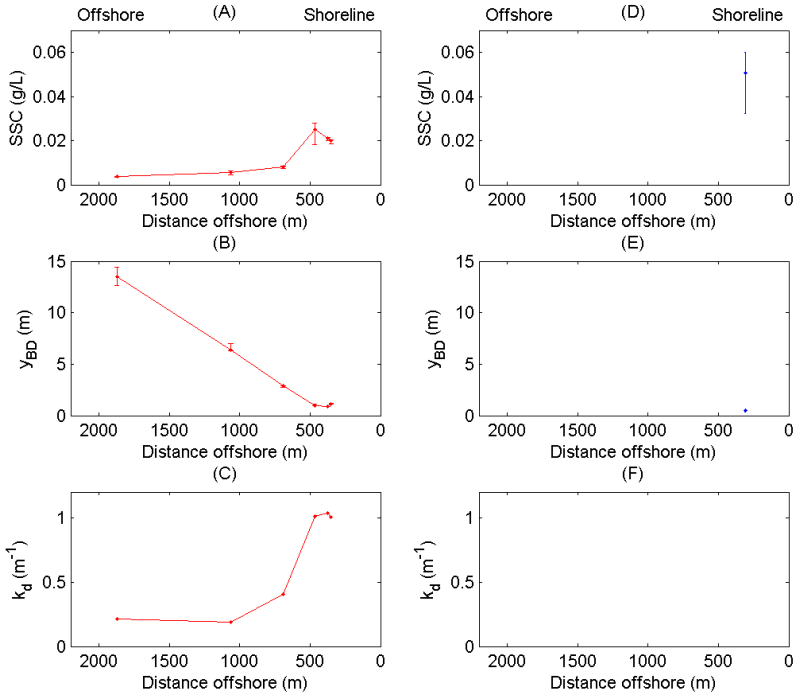

Figure B-20: Cross-shore variability in SSC, y_{BD} and k_d at SP4. Panels: A to C relate to S1 and D to F relate to S2. (A and D) SSC, (B and E) y_{BD} and (C and F) k_d.

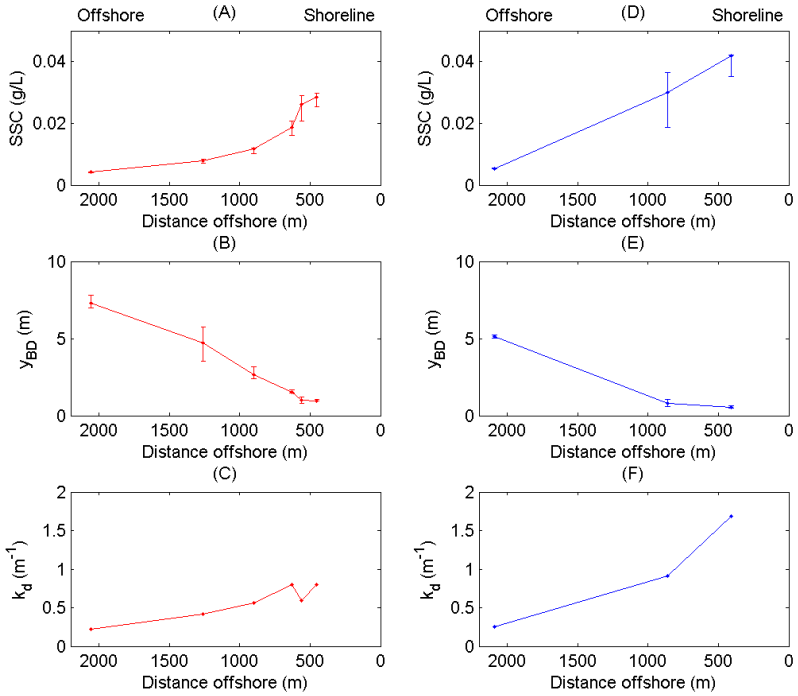

Figure B-21: Cross-shore variability in SSC, y_{BD} and k_d at SP5. Panels: A to C relate to S1 and D to F relate to S2. (A and D) SSC, (B and E) y_{BD} and (C and F) k_d.

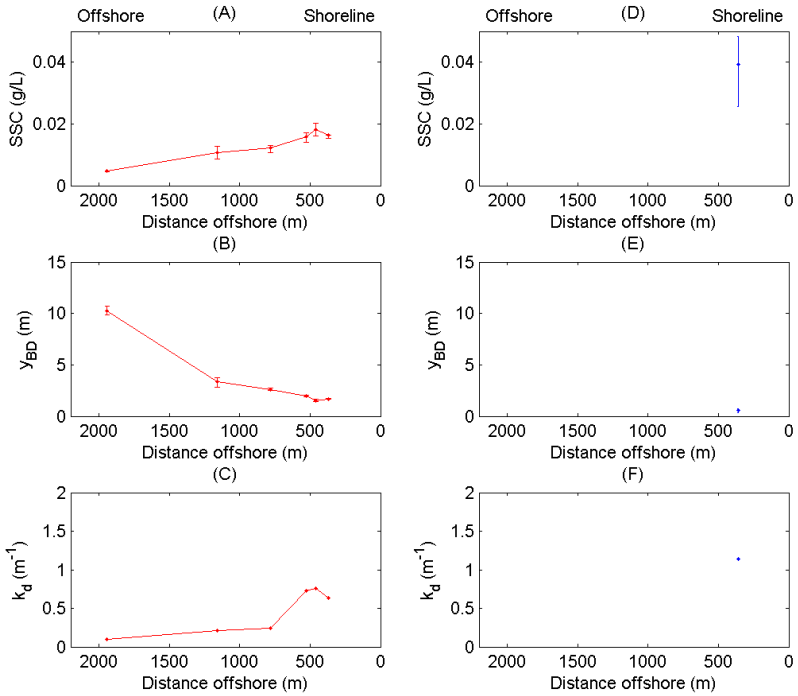

Figure B-22: Cross-shore variability in SSC, y_{BD} and k_d at SP6. Panels: A to C relate to S1 and D to F relate to S2. (A and D) SSC, (B and E) y_{BD} and (C and F) k_d.

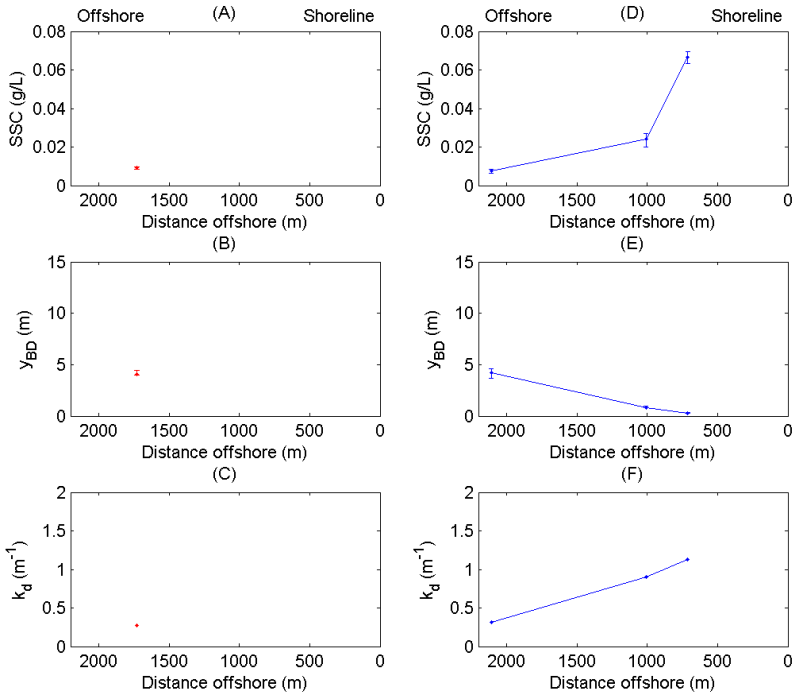

Figure B-23: Cross-shore variability in SSC, y_{BD} and k_d at SP7. Panels: A to C relate to S1 and D to F relate to S2. (A and D) SSC, (B and E) y_{BD} and (C and F) k_d.

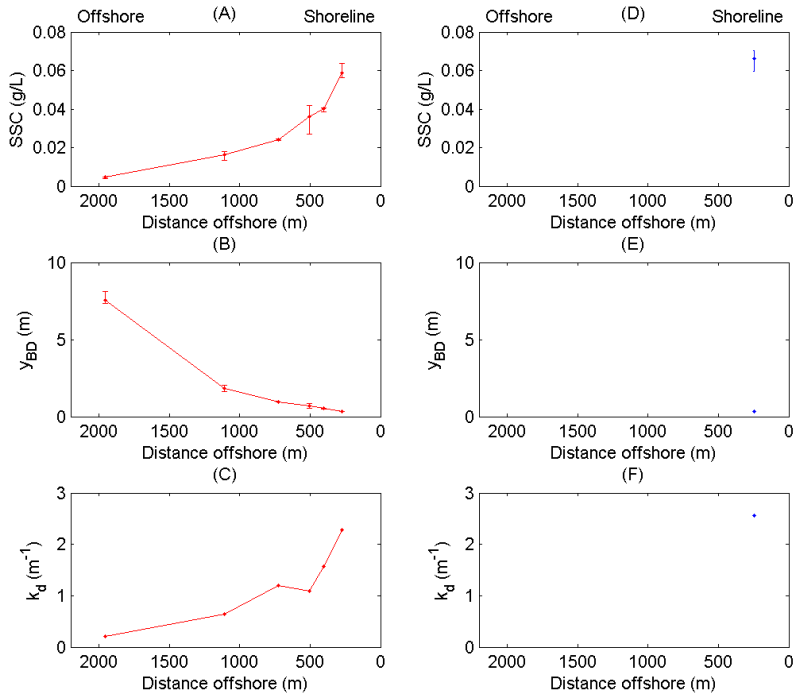

Figure B-24: Cross-shore variability in SSC, y_{BD} and k_d at SP9. Panels: A to C relate to S1 and D to F relate to S2. (A and D) SSC, (B and E) y_{BD} and (C and F) k_d.

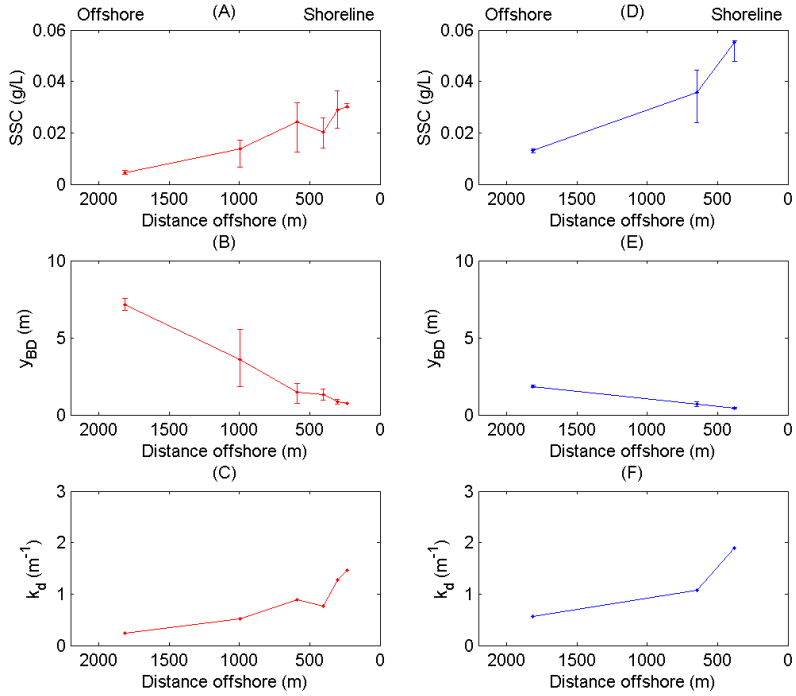

Figure B-25: Cross-shore variability in SSC, y_{BD} and k_d at SP10. Panels: A to C relate to S1 and D to F relate to S2. (A and D) SSC, (B and E) y_{BD} and (C and F) k_d.

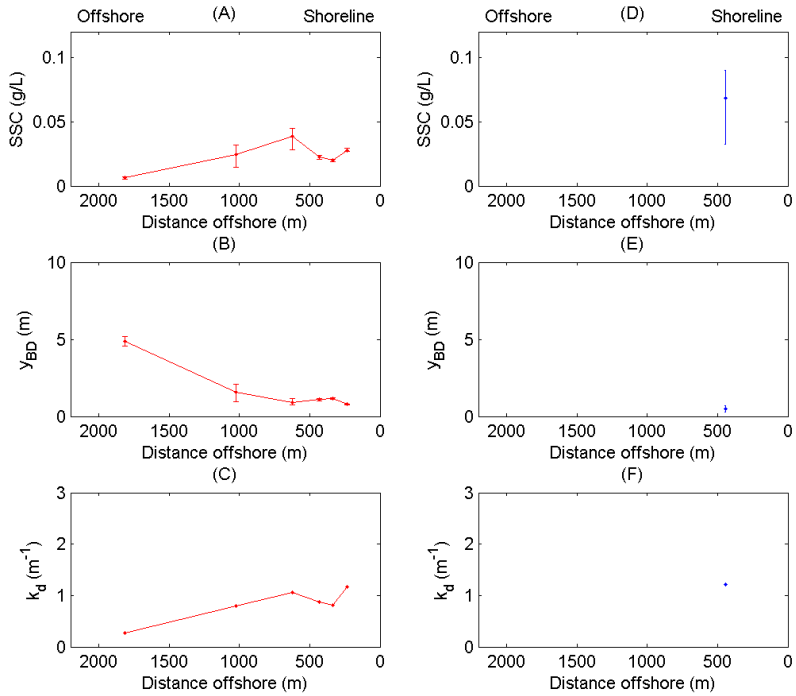

Figure B-26: Cross-shore variability in SSC, y_{BD} and k_d at SP11. Panels: A to C relate to S1 and D to F relate to S2. (A and D) SSC, (B and E) y_{BD} and (C and F) k_d.